Feasibility of a lightweight modular structure by allowing settlement

A case study on the use of short friction piles underneath different types of wall systems

by

P. de Leeuw

to obtain the degree of Master of Science
at the Delft University of Technology,
to be defended publicly on Friday March 13, 2025 at 15:30 PM.

Student number:	4719956	
Project duration:	June 17, 2024 – March 13, 2025	
Thesis committee:	Dr. ir. H. R. Schipper,	TU Delft, supervisor
	Dr. L. Flessati,	TU Delft, second supervisor
	Ir. G. Pagella,	TU Delft, third supervisor
	Ir. A. J. Robbemont,	Zonneveld Ingenieurs

This thesis is confidential and cannot be made public until March 13, 2025.

TU Delft

Preface

This thesis is the final part of my Master of Civil Engineering at the Technical University of Delft. It marks the end of my studies and will be the beginning of my future as an engineer.

First, I would like to thank all my supervisors from the university, Dr. ir. Roel Schipper, Dr. Luca Flessati, and Ir Giorgio Pagella, for all the guidance during this project. I could always come by if I had something to discuss and all the meetings were very helpful. It was a difficult road, finding the set up within of this interesting topic, but with your help I was able to create a research that I am proud of.

I would also like to thank Arnold Robbemont from Zonneveld Ingenieurs for helping me during this research. From my very first visit to your firm, you were very helpful with figuring out what my research would look like. Your enthusiasms on my findings really made it feel like I was researching something with great potential for future projects.

And finally, I would like to thank my family, friends, colleagues, and girlfriend, for supporting me all the way and helping me in difficult moments. I am lucky to have such great supporters in my life.

Thank you!

P. de Leeuw
Delft, Februari 2025

Abstract

The increasing demand for sustainable and easily constructible housing has led to the exploration of alternative foundation systems for lightweight modular structures. This research investigates the feasibility of using short helical piles to support a lightweight wooden building, assessing its settlement behaviour and structural integrity over time. Unlike traditional deep pile foundations, short helical piles are designed to be easily installed, removed, and reused, offering both environmental and economic advantages. However, their application in soft soils raises concerns regarding excessive and differential settlement.

The main research question for this thesis is:
"What is the structural feasibility of a lightweight, modular wooden building design on short, screwed foundation piles that is expected to have large amount of settlement?"

To answer this question, a literature study was done in combination with a case study. The literature established the boundary conditions for the use of helical foundation piles and explores the expected capacity and settlement behaviour in soft soil. Afterwards, it focusses on aspects such as decay and modular systems of timber construction elements.

With the knowledge obtained from the literature, a case study was developed. To investigate the behaviour of a lightweight structure that is expected to settle, a numerical modelling approach is used, combining PLAXIS 2D and SCIA Engineer. PLAXIS 2D was used for simulating the settlement behaviour of the structure at multiple stages in time, while the effect of these settlements on the superstructure was analysed in SCIA Engineer. Different wall systems were investigated, focusing on the influence of the wall stiffness, varying pile capacities, and the impact of uneven loading. Time-dependent settlement effects were evaluated at time stages just after the completion of the construction and at three additional points further in time. This provides insight on the short-term and long-term behaviour of the structure. To prove that a structure of this typology is sufficient for housing, it is tested on total settlement (U), differential rotations (β), tilt (ω), and element capacity (σ).

The results of the calculations indicate that for a lightweight, timber structure placed on short helical piles large amount of settlement can be expected when positioned in soft soil. However, the settlements will not lead to a significant stress increase that causes failure of structural elements. A stiffer wall system has the ability to redistribute more force to the foundation piles at the most outer position. This reduces the differential settlement between piles, but also reduces the maximum total settlement of the wall. The resistance to deformations of the outer foundation piles is therefore more impactful with a stiffer superstructure. In general, the findings suggest that with careful consideration of settlement behaviour, short helical piles can be a viable foundation solution for supporting lightweight houses.

Contents

List of Figures

List of Tables

1

Introduction

1.1. Context

Foundation design for buildings in the Netherlands is characterized by the diverse nature of the underground. In some areas, rock and sand are found close to the surface, allowing the use of shallow foundations. However, in more populated areas, thick layers of soft soils, such as clay and peat, cover the deeper Pleistocene sand layers. In these cases, deep pile foundations are often required to ensure adequate capacity and stiffness. Traditionally, deep pile foundations are used to mitigate excessive settlement, but these solutions come with high material costs and significant environmental impact. Research indicates that over 60% of a building's emissions stem from the materials used (Sandanayake et al., 2016), and minimizing the environmental impact of the foundation could significantly lower this figure.

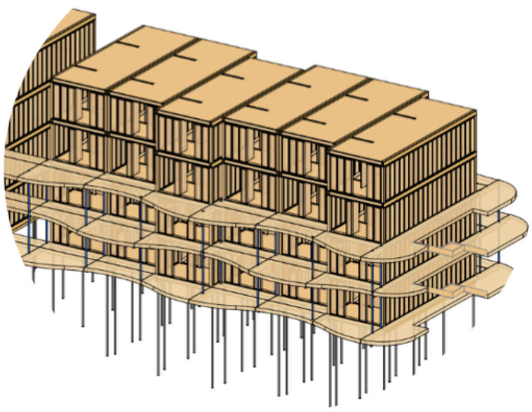

Figure 1.1: Early concept design

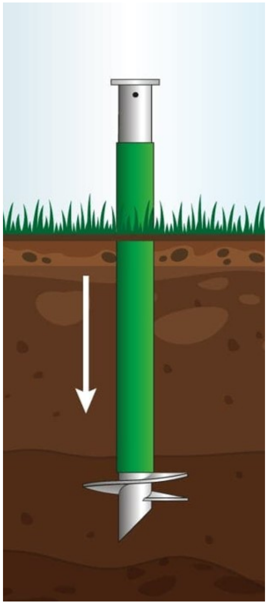

Figure 1.2: Helical pile

Besides reducing the environmental impact of buildings, the Netherlands is facing a severe housing shortage. The government is therefore planning to build 900,000 homes by 2030 (Rijksoverheid, 2024). However, the push for rapid construction is constrained by environmental ambitions of the same government, particularly the need to limit carbon dioxide and nitrogen emissions. This challenge has led to the search for more sustainable building solutions, including eco-friendly materials and designs.

An innovative design proposed by Zonneveld Ingenieurs involves the use of lightweight wooden elements supported by short foundation piles, specifically helical piles. These piles provide load-bearing capacity through a combination of shaft friction and end-bearing resistance. Their lightweight nature, ease of installation, and reusability make them a sustainable and practical choice for modular, environmentally friendly structures. However, some complications with this approach remain to be addressed.

1.2. Design Problem

Despite the benefits of short foundation piles, they also present notable design challenges. The main issue arises from the limited depth these piles can reach, often stopping in weaker soil layers rather than extending to a stable sand layer. As a result, short piles may have reduced load-bearing capacity and higher settlements compared to deeper foundations, making them less suitable for heavier structures. This limitation can lead to performance issues, especially in areas where the soil is highly compressible or where large loads are expected. While the use of lightweight materials like wood helps offset some of the load concerns, it does not fully eliminate the risk of instability in certain soil conditions.
The higher compressibility of such soils increases the risk of uneven settlement, potentially leading to structural issues such as tilting or misalignment over time. Regulations in the Netherlands generally impose strict limits on settlement to ensure building stability. However, an intriguing question arises: What if larger displacements do not compromise the superstructure, avoiding structural failure and significant differential displacements?

1.3. Design philosophy

The building is designed as a temporary solution to address the housing crisis. Its primary objective is to enable the rapid construction of homes without the use of heavy machinery at a given location, where they will remain for a period of five years. After this time frame, the structure will be dismantled and relocated for reuse at another site. This approach eliminates the need to accommodate long-term settlement effects and allows the site to be restored to its original condition. By providing temporary housing, this solution helps alleviate the housing shortage until larger, permanent projects can be developed. The compact apartments are particularly suited for young professionals, students, or first-time renters, offering a flexible and time-limited living arrangement.

1.4. Objective

This research will investigate the feasibility of a lightweight timber structure on short foundation piles by comparing a timber beam, a timber frame wall with OSB panels and a CLT wall placed on the foundation. The following aspects of the structural design will be investigated:

- The effect of not reaching a bearing sand layer on the load capacity and vertical displacement of a helical foundation pile;
- The effect of the stiffness of a wall system on the differential settlements of the structure;
- The effect of using smaller piles on the outer side of the wall;
- The effect of uneven loading on the differential displacement of the structure.

Comparing the different wall systems under different conditions to one another, will improve the knowledge of such a design and answer the question if such a design has potential for future buildings.

1.5. Research question

"What is the structural feasibility of a lightweight, modular wooden building design on short, screwed foundation piles that is expected to have large amount of settlement?"

This question will be answered by sub-questions tackled in different parts of the research.

- What are the implications of using short, screwed foundation piles in soft soil layers?
- What are the implications of using wooden elements for the superstructure?
- How does settlement affect the wall system of the superstructure?
- How can the stiffness of a wall systems influence the (differential) settlement of the structure?
- How does uneven loading affect the differential settlement?

1.6. Methodology

To answer the research questions, firstly information will be gathered from literature. This will provide a better understanding of all the processes at play underneath and within the structure. Key topics such as foundation typology, soil settlement, and their impact on structural performance will be thoroughly examined in Chapter 2. In Chapter 3, the structural components above ground-level will also be investigated on their properties and on how they obtain their stiffness.

The literature survey will form the basis for identifying potential design challenges of a timber wall system on short foundation piles. Three different wall systems with different stiffness properties will be investigated on their performance placed on top of helical piles. The wall structures will be tested on multiple design variables that impact the performance of the wall with respect to internal stresses (σ), deformations (ΔU), relative rotation (β) and tilt (ω). Chapter 4 goes into more detail on the design choices of this case study.

The case study will use Finite Element Software (FEM) to get insight into the structural performance. Two programs are used to get an accurate estimation of the behaviour of the settlement over time and the structural behaviour of the timber elements. For the settlement calculations, PLAXIS 2D is used and for the structural analysis SCIA Engineer is used. The displacements of the foundation piles will be translated to spring supports in the SCIA model. The obtained forces on top of the foundation piles will afterwards be used in PLAXIS. This will be repeated until a structural analysis can be done at the time steps T0, T10, T100 and T1000. The numbers representing the time passed after the construction process, so T10 meaning 10 days after the construction is finished. Chapter 5 explains this in more detail.

After the calculations are finished, the results will be presented in Chapter 6 with additional observations as discussion points. Due to the setup of this research, some simplifications must be done, which can influence the result of the calculations. These influences will be discussed in Chapter 7.

At the end of this research a conclusion will be given on the research questions based on the obtained results. A recommendation on the design concept will be presented and how future research can improve the validity of the design concept.

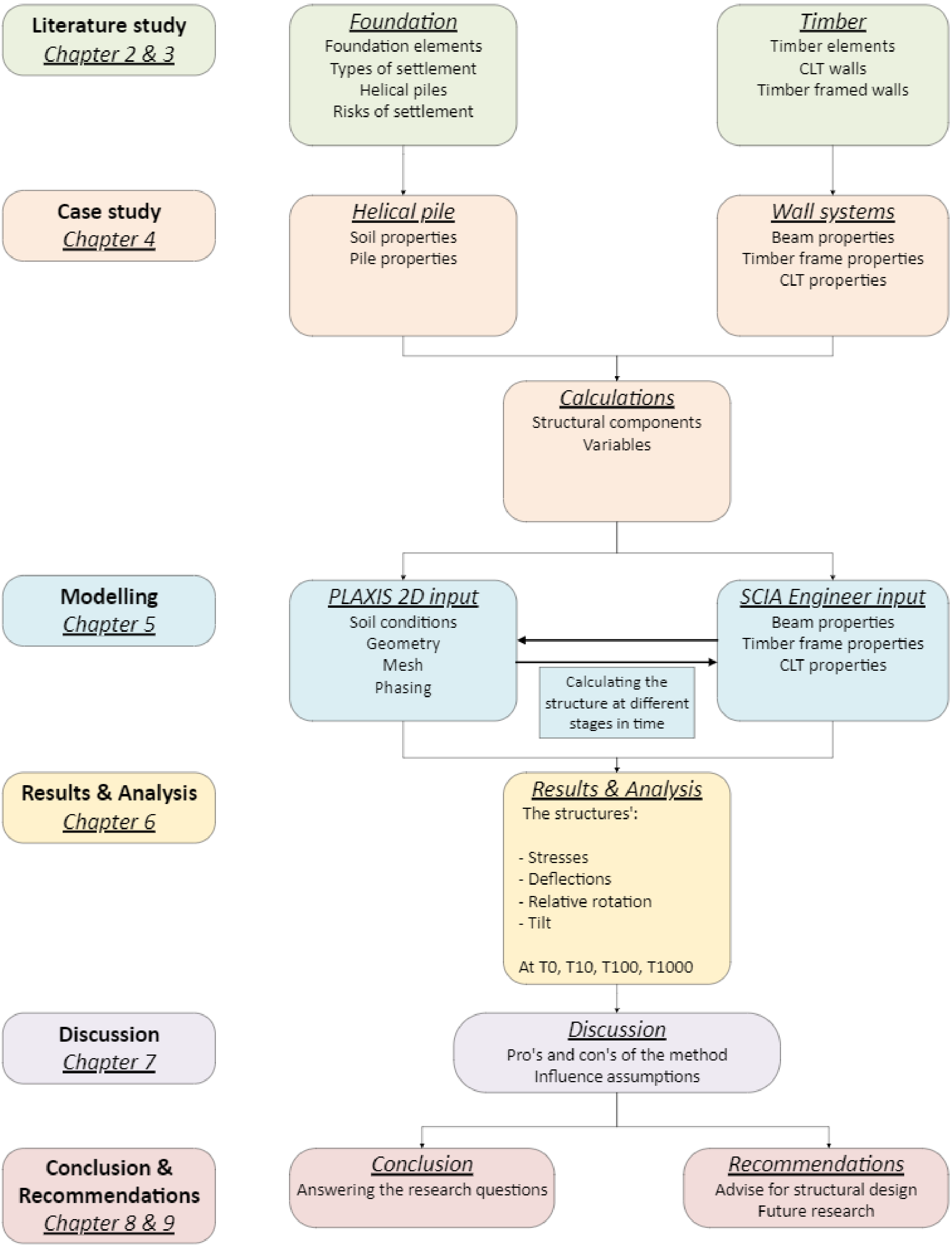

Figure 1.3: Methodology

2

Literature study - Foundations

In this chapter, the different aspects of using short foundation piles will be discussed. It will go into detail on the multiple foundation techniques in the Netherlands, the specifics of settlement, the specifics of using a helical pile, and the implications of allowing large amount of settlement of a construction.

2.1. Foundation in the Netherlands

The Netherlands is home to a variety of soil types, each playing a crucial role in determining suitable foundation types for construction. The country's soil primarily consists of sand, clay, peat, and silt, shaped by its geological history and water management practices. After the Pleistocene era ended around 10,000 years ago and the Holocene began, the melting glaciers left behind large amounts of sand, particularly in the eastern regions of the Netherlands. This part is above the seawater level and was untouched for millennia by the sea.

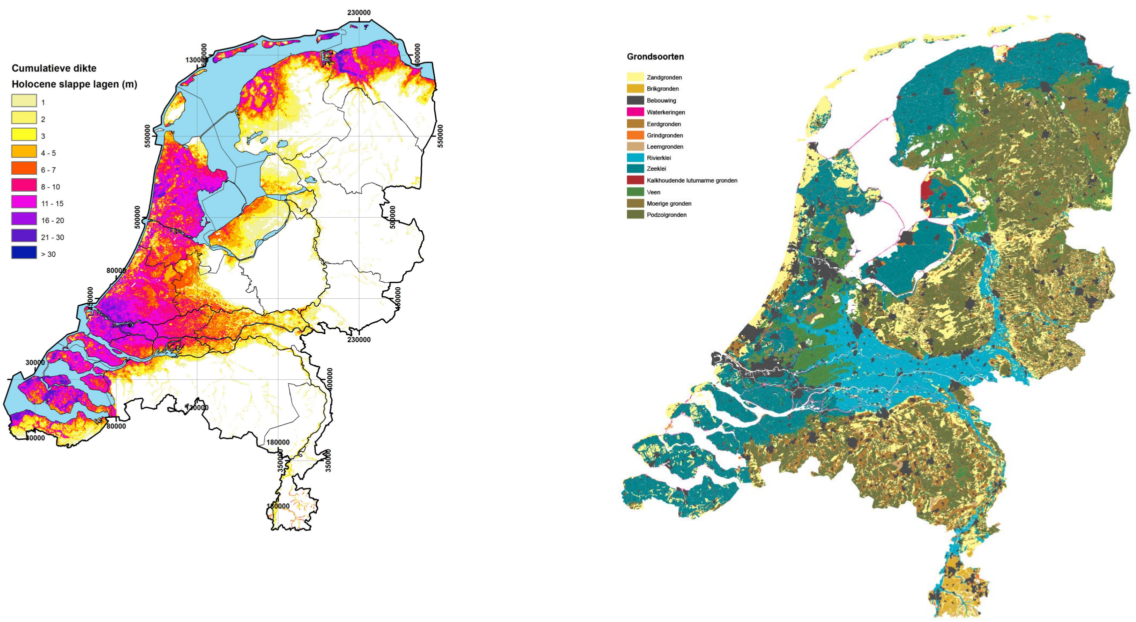

(a) Overview of the thickness of the Holocene soft soil in the Netherlands (TNO, 2016)

(b) Overview of the top layers of soil in the Netherlands ("Bodemkaart Nederland", 2014)

Figure 2.1: Overview of soil characteristics in the Netherlands

The more western part of the Netherlands is formed by the deposition of clay soil by rivers for thousands of years. The area is positioned below the seawater level and has been waterlogged for a long period of time. This resulted in the accumulation of organic material, leading to the formation of peat soil with a flat surface. A large area was reclaimed by drainage and water management for the purpose of agriculture. Now a large portion of the population lives in this area and there is a high demand for housing. An overview of the soil types in the Netherlands can be seen in figure 2.1.

Each soil type reacts differently to a constant applied load. So does sandy soil show a more immediate reaction to the load and do the clay and peat layers are more influenced with long term settlement (Huizinga, 1969). Understanding the properties of soil is crucial for predicting and managing the settlement behaviour of the ground. Soil properties such as grain size, composition, water content, and density directly influence how soil responds to stress increase. The three most important soil types are:

Sand
Sand soil consists of large to moderately fine grains. It has a high permeability and is a non-cohesive soil. This soil is mostly found at the coastal areas and in the east of the Netherlands. Sandy soil is generally stable, does not have large deformations and has a high strength. This makes it well suited for load-bearing purposes.

Clay
Clay soil consists of very small particles. It has a low permeability and a high cohesion. Clay soils are common in the area around rivers and in the polders of the Netherlands. The clay soil has less strength than sandy soil and tends to deform in case of changes in water content. This can happen due to environmental changes or due to a change in stress within the soil. This change in stress leads to the dissipation of water within the pores of the soil. This takes time and the soil is therefore susceptible to long term settlements, which is not desirable in structural designs.

Peat
Peat is an organic soil that is made up of fibrous remains of plants. The soil is formed by the compression of these particles which leads to its cohesion. While peat typically exhibits moderate permeability and high compressibility, its strength depends on the strain applied—requiring large strain to fully mobilize its strength. Due to these reasons, peat layers are generally avoided when designing a foundation.

With these properties, it becomes clear why the foundation of a building is almost always positioned in sandy soil. Unfortunately, in the western part of the Netherlands there are large layers of soft soil the foundation has to bypass.

2.1.1. Long foundation piles

To ensure a stable foundation in the western part of the Netherlands, where the soil primarily consists of soft clay, silt, and peat layers, long foundation piles are extensively utilized. These piles are driven deep into the ground to reach more stable soil layer, such as compacted sand or Pleistocene-era layers beneath the softer upper soils.

The long piles were initially made of wood during earlier construction practices. In recent decades, piles have been developed that consist out of materials such as concrete, steel, and composites. These modern materials provide greater strength and durability, which is needed for creating larger and heavier structures.

Long foundation piles need to resist large forces applied on them. Besides the forces applied by the structure, also the forces created by friction called downdrag or negative skin friction need to be taken into account. Negative skin friction arises when the pile stays in place vertically, but the surrounding soil deforms. The friction between the soil and the surface of the pile creates additional stresses within the pile, leading to the need for larger dimensions and stronger materials for the pile (Coduto et al., 2016).

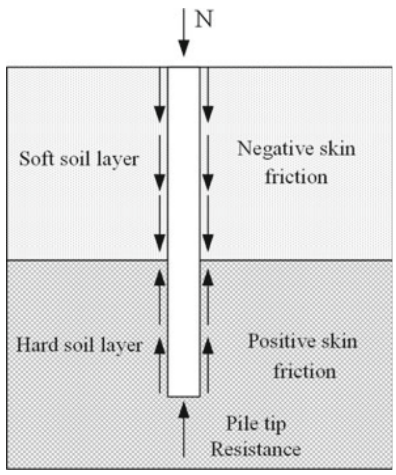

Figure 2.2: Negative skin friction (Lai et al., 2022)

The use of long foundation piles enables possibilities for construction in the western part of the Netherlands. However, this results in significantly higher material usage for construction in the west compared to similar projects in the east. Even lighter structures in the west necessitate the use of large foundation piles to ensure stability.

However, this results in a construction requiring a relatively larger amount of materials in the west compared to an identical structure in the east. Especially for lighter constructions, that still have to be placed on large foundation piles. The material used impacts a construction design economically, and sustainably. The materials used in these foundations have economic and sustainability implications, influencing both the cost and environmental impact of construction projects.

When a structure supported by foundation piles reaches the end of its lifespan and is deconstructed, retrieving the foundation piles is not feasible. The presence of skin friction generates forces that are so big that extracting the piles from the ground needs large machinery, and the pile staying intact is not guaranteed. As a result, the only viable way to reuse the materials is to design a new structure that incorporates the existing piles. This limits the design freedom for future structures at that location.

2.1.2. Wooden foundation piles

Before modern piles made out of concrete and steel were invented, constructions were supported by other materials. Amsterdam is an example of houses built on timber foundation piles that have been standing there for a long time. These wooden piles are more limited in their capacity compared to concrete and steel piles, but are also less expensive and more environmental friendly. Especially, if the trees that can be used for the timber piles are located near the building site. When designing a wooden foundation, one must take into account the water level.

To prevent exposure to air, the top of wooden foundation piles must always be positioned below the lowest expected groundwater table. This ensures that oxygen cannot reach the wood, thereby limiting the activity of aerobic bacteria and fungi responsible for most decay processes (Klaassen, 2007). However, even in waterlogged soils, wooden foundations remain susceptible to microbial degradation. In low-oxygen conditions, soft rot fungi may contribute to decay, while in fully anoxic environments, erosion bacteria can still degrade the wood. (Björdal, 2012) These bacteria, which erode the wood fiber cell walls, are responsible for wood degradation in various anaerobic terrestrial and marine environments worldwide. Although bacterial degradation occurs more slowly than fungal decay, it can still significantly reduce the load-carrying capacity of foundation piles over time, potentially leading to stability issues in supported buildings (Singh et al., 2016).

The capacity of wooden foundation piles is limited. The piles have to be produced out of wooden logs and the dimensions of the piles are limited to the available trees. Most timber piles are designed to carry axial loads of 100 to 400 kN (Prakash & Sharma, 1990), with the rule of thumb being 100 kN. At a certain depth, it becomes unfeasible to use the wooden piles. In Section 2.1.1 the concept of negative skin friction is explained. The thicker the soft soil layer surrounding a pile, the greater the negative skin friction it experiences when its end is embedded in less compressible soil. These force can become large enough that the pile has to use most of its capacity on resisting this friction, leaving no capacity left for the forces applied on top (Hogerheijde, 2023). In addition to this, other materials are often needed to improve the timber pile. The repeated blows during driving can cause splitting of the wood at the top and toe of the log. Steel toe points are often used to reduce this damage.

In present times, mostly concrete foundation piles are used. However, with the rise of circular construction, there is renewed interest in using timber foundation piles. An example is The Natural Pavilion in Almere, Netherlands, which was entirely built on timber piles in 2022 (“The Natural Pavilion”, 2022).

2.1.3. Shallow foundation

Shallow foundations are generally not preferred on soft soil due to the soil’s low load-bearing capacity, high compressibility, susceptibility to differential settlement. When the top soil consists of a stable sand layer, the shallow foundation becomes feasible. The sand layers ensures that the loads applied by the construction are spread out and the stresses become low enough to ensure no large settlements will occur. However, sometimes the choice is made to use shallow foundation on soft soil. For small, lightweight structures it is more cost effective to accept the deformations than to use foundation piles to reach lower sand layers.

The foundation is often placed just underneath ground level to obtain more resistance and have a higher stability of the soil. Sometimes ground improvement can help by realising a shallow foundation. The first meter(s) of the soil is removed and replaced by sandy soil. This improves the stability of the soil and makes heavy shallow foundation more feasible. It does require a lot of excavation works.

2.1.4. Short foundation piles

To support lightweight structures, a foundation consisting out of short piles can also be used. Although these piles do not reach deeper sand layers, they transfer vertical forces further into the ground. These deeper soil layers have been loaded by the layers on top for several years, which improves their settlement resistance. This method effectively utilizes the increased bearing capacity of these naturally consolidated layers, acting as a preloading technique without the need for additional soil placement. Due to the weak strength properties of the soil, the structure will settle, but to a lesser extent than with shallow foundation strips.

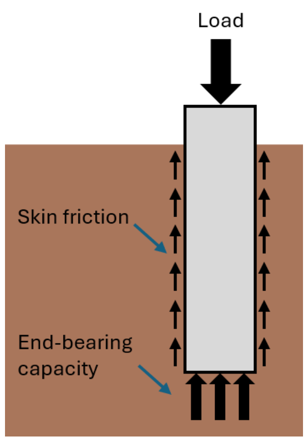

Figure 2.3: Friction piles

Short foundation piles behave differently from long ones because of how they interact with the soil around them. In long piles, the soil tends to settle while the pile remains stationary generation negative skin friction. With short piles, this negative friction doesn’t occur. Instead, as the short pile moves downward slightly under the load, it compresses the surrounding soil, creating an upward friction force on the sides of the pile. This upward force, combined with the pressure exerted by the soil beneath the base of the pile, provides the overall load-bearing capacity.

The piles have some benefits that make them potentially useful as the foundation of a sustainable lightweight construction. The piles use less material than longer foundation piles and they can be retrieved after the construction's lifetime. Furthermore, they do not require heavy equipment during installation in comparison to longer foundation piles. This makes them interesting for the case at hand (Engineersview, 2024) (Shuman et al., 2022).

This foundation type will be further expanded upon in Paragraph 2.3.

2.2. Soil settlement

Soil settlement is a critical aspect for building design. Settlement refers to the vertical displacement of the ground caused by the weight of the structure and other loads working on the structure. Knowing the settlement behaviour underneath the structure ensures proper design decisions can be made.

There are three stages of settlements: immediate settlement, primary consolidation settlement and secondary consolidation settlement. Each process is distinguished by their own relation with the imposed load (Verruijt, 1999).

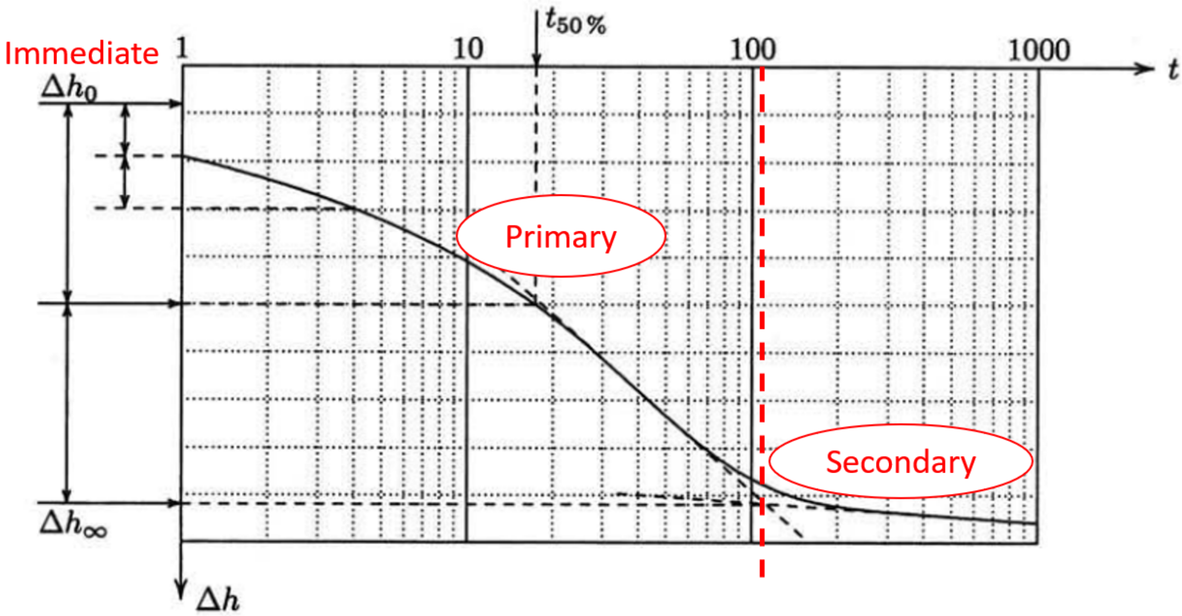

Figure 2.4: Vertical displacement over time

The settlement of the soil is influenced by multiple factors. Not only the soil itself, but also the loading and preloading of the soil are key factors in determining the settlement behaviour of the soil. Before the three settlement stages are investigated, the term *effective stress* will be explained.

2.2.1. Effective stress

The effective stress within the soil determines the settlement behaviour of the primary and secondary settlement of soil. It represents the portion of the total vertical soil stress, excluding the stress carried by water in the pores. The following equation describe the relation between the effective stress (σ'_{zz}), vertical soil stress (σ_{zz}) and pore water pressure (p).

The effective stress (σ') is expressed as:

$$\sigma'_{zz} = \sigma_{zz} - pwp \tag{2.1}$$

Where:

σ_{zz} Total vertical soil stress;
pwp Pore water pressure (or groundwater stress).

Vertical soil stress is the weight of the overlying soil per unit area at a given depth. The vertical soil stress (σ_{zz}) is expressed as:

$$\sigma_{zz} = \gamma \cdot z \tag{2.2}$$

Where:

γ Unit weight (density) of the soil;
z Depth of the soil layer being considered.

Groundwater stress depends on the depth to the water table and the unit weight of water (γ_w). Below the water table, the pore water pressure increases linearly with depth:

$$p = \gamma_w \cdot z_w \tag{2.3}$$

Where z_w is the depth below the water table. Note that the increase in pore water pressure can deviate from its linear behaviour depending on the subsurface soil conditions. However, this research will not go into detail on this phenomenon.

From the formulas it can be seen that effective stress is dependent on the depth and density of the soil. The deeper a soil layer, the greater the influence of overlying weight and water column pressure. Depth determines whether the soil is above or below the water table, affecting pore water pressure and, consequently, the effective stress. On its turn, the density or unit weight of soil influences both the total vertical stress and the soil's strength. Unsaturated soils above the water table exhibit effective stress due to the weight coming from only soil.

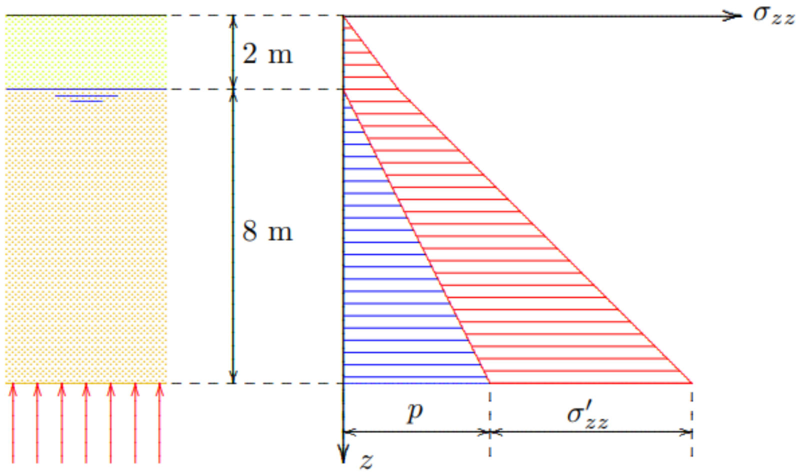

Figure 2.5: Example of stresses in a homogeneous soil layer (Verruijt, 1999)

In short, effective stress influences the strength and compressibility of the soil. The higher effective stress, the more stable soil and the less it will compress under an increase in load (Verruijt, 1999). The latter is explained in further detail in Sections 2.2.4 and 2.2.5.

2.2.2. Stress increase underneath a foundation pile

In Section 2.1.3 it is mentioned that sand is a desired soil type to position the bottom of the foundation element. The sand is more rigid and spreads out the load effectively. The spreading of the load results in a reduction of stress with depth, while the area over which the load acts increases, see Figure 2.6.

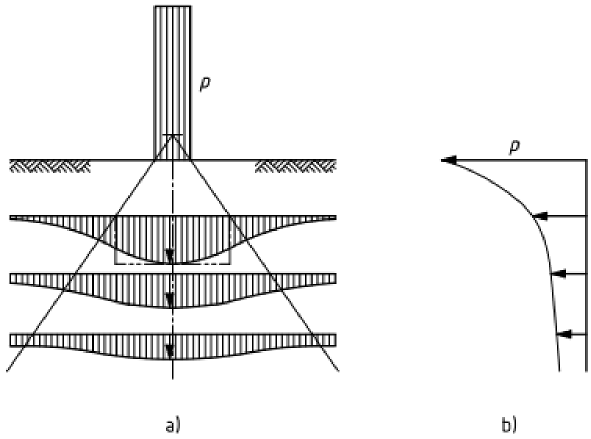

Figure 2.6: Redistribution of stress over depth 2 dimensional (a) and 1 Dimensional (b)

For circular footings, which relevancy will be explained in Section 2.3, the formula for calculating the stress underneath the center of the load is:

$$\Delta\sigma'_{v,z,d} = p_{\text{gem},d} \times \left(1 - \frac{1}{\sqrt{\left(1 + \frac{a^2}{z^2}\right)^3}}\right) \tag{2.4}$$

Where:

$\Delta\sigma'_{v,z,d}$: The calculated value of the effective stress increase at a depth z, in kPa;
$p_{\text{gem},d}$: The calculated value of the uniformly distributed load, in kPa;
a: Radius of the circular load, in m;
z: Depth, in m;

(Nederlands Normalisatie-instituut, 2017)

The deeper the stress is calculated, the lesser the increase in effective stress becomes. However, pile groups might influence the stresses underneath each other. Since the load spreads, closely positioned piles will also influence the stress increase underneath the other piles. This group effect will be further investigated in Section 2.3.4 (Nederlands Normalisatie-instituut, 2017).

2.2.3. Immediate settlement

First the immediate settlement occurs within a few hours to a few days after the load is applied. This is an elastic deformation where mostly the voids within the soil disappear and the pore water pressure stays the same. The formula for the immediate settlement is:

$$\Delta D = -\frac{(1+\nu)(1-2\nu)}{E(1-\nu)} * p * D \tag{2.5}$$

Where:

ΔD Compression of the soil layer;
ν The Poisson's ratio of the soil;
p The pressure or surface load that is applied;
D Thickness of the soil layer;
E The modulus of elasticity or Young's modulus of the soil.

(Verruijt, 1999)

The formula works for initial calculations, but assumes that the soil underneath the load is homogeneous and the soil is drained. This is often not the case and each layer should be looked at separately. It is a 1D calculation of immediate settlement and therefore does not take into account shear stresses and horizontal strains. The soil compression is also assumed to be fully reversible after the load is taken away, which also is not the case. The soil layer expands back to around 10 % of its original state. Reloading the soil will result in a lower change if the applied stress is lower than the earlier experienced stress, see Figure 2.7.

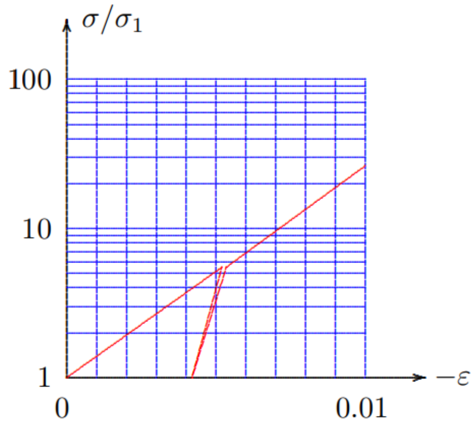

Figure 2.7: Stress-strain relation of soil applied to loading, unloading and reloading (Verruijt, 1999)

2.2.4. Primary consolidation

After a short while the primary settlement (or primary consolidation) takes place. This process is caused by the soil being compressed by a constant load, which leads to the water within the pores being applied to a constant stress, which leads to its expulsion over time. The so called hydrodynamic period leads to an increase of the effective stress. This process is most significant at locations with more fine grained soil, since this soil is weaker and the pores are smaller. The smaller pores make it more difficult for the water to dissipate. (Huizinga, 1969)

The primary vertical settlement of the ground can be determined by the following formula:

$$s_1 = \sum_{j=n}^{j=0} \frac{C_{c;j}}{1+e_j} * d_j * log(\frac{\sigma'_{v;z;0;d} + \Delta\sigma'_{v;z;d}}{\sigma'_{v;z;0;d}}) \tag{2.6}$$

Where:

s_1	is the primary settlement of the top of a layer, in meters;
$C_{c;j}$	is the value of the primary compression index of layer j;
e_j	is the void ratio of layer j;
d_j	is the thickness of layer j, in meters;
$\sigma'_{v;z;0;d}$	is the value of the vertical effective stress before loading for the middle of a layer at depth z, determined according to 6.6.2(f), in kPa;
$\Delta\sigma'_{v;z;d}$	is the value of the increase in vertical effective stress for the middle of a layer at depth z, determined according to 6.6.2(d), in kPa.

(Nederlands Normalisatie-instituut, 2017)

This formula determines the settlement at the top of one layer. (Nederlands Normalisatie-instituut, 2017)

In the Netherlands the method of Koppejan is often used. This method uses compression constants C'_p and C'_s for determining the settlement. The settlement formula of s_1 then changes to:

$$s_1 = \sum_{j=n}^{j=0} \frac{1}{C'_{p;j}} * d_j * log(\frac{\sigma'_{v;z;0;d} + \Delta\sigma'_{v;z;d}}{\sigma'_{v;z;0;d}}) \tag{2.7}$$

Where $C'_{p,j}$ is the value of the primary compression constant of layer j, valid for load increases from the yield stress, determined according to Chapter 3 of the NEN 9997. For normally consolidated soil, the yield stress is equal to the existing vertical effective stress.

Note that the primary settlement is time dependent. However, the formula does not show any time dependence. The value calculated with this formula is the final settlement due to the primary consolidation.

2.2.5. Secondary consolidation

In clay and peat soils, the settlement process does not end after primary consolidation, but continues at a slower rate. Most of the excess water has been consolidated and few water is left. Unlike primary consolidation, which is governed by pore water dissipation, secondary consolidation is driven by the gradual deformation and rearrangement of soil particles under sustained load. This process is however slower and linear on a logarithmic scale (Huizinga, 1969). The secondary consolidation can be calculated with the formula:

$$s_2 = \sum_{j=n}^{j=0} C_{a;j} * d_j * log(\frac{t_\infty}{t_1}) \tag{2.8}$$

Or in the Netherlands where the method of Koppejan is often used:

$$s_2 = \sum_{j=n}^{j=0} \frac{1}{C'_{s;j}} * d_j * log(\frac{t}{t_0}) * ln(\frac{\sigma'_{v;z;0;d} + \Delta\sigma'_{v;z;d}}{\sigma'_{v;z;0;d}}) \tag{2.9}$$

Where:

s_2	is the secondary settlement of the top of a layer, in meters;
$C'_{s;j}$	is the value of the secondary compression index of layer j;
d_j	is the thickness of layer j, in meters;
t	is the duration in days. For the final settlement, $t = 10,000$ days is used;
t_0	is the time unit, $t_0 = 1$ day;
$\sigma'_{v;z;0;d}$	is the value of the vertical effective stress before loading for the middle of a layer at depth z, determined according to 6.6.2(f), in kPa;
$\Delta\sigma'_{v;z;d}$	is the value of the increase in vertical effective stress for the middle of a layer at depth z, determined according to 6.6.2(d), in kPa.

(Nederlands Normalisatie-instituut, 2017)

2.2.6. Non-linearity of soil compression

Soil exhibits inherently non-linear and non-elastic behaviour under compressive loading. Unlike ideal elastic materials, where stress and strain follow a proportional relationship, soil deformation depends on various factors such as stress history, loading rate, and soil composition (Verruijt, 1999).

In naturally occurring soil deposits, pre-existing stresses from overlying layers influence the non-linear response. Since deeper soil layers experience higher initial stresses due to the weight of the overburden, their stiffness is typically higher. This relation can be seen in the formulas for primary and secondary consolidation, where the pre-existing effective stress plays a big part in the determination of the settlement.

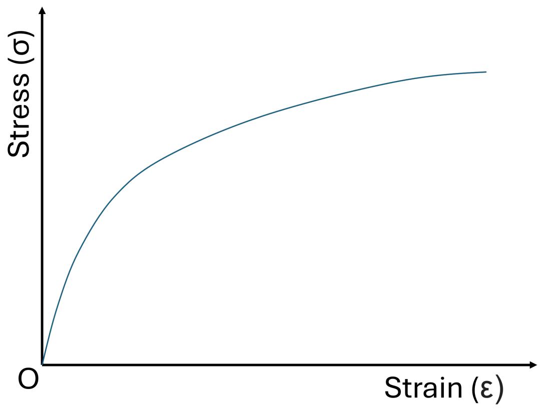

Figure 2.8: Non-linear stress-strain curve of soil

A stress-strain relationship for soil usually follows a non-linear curvature, as shown in Figure 2.8. At lower stress levels, the material exhibits relatively small strains, but as the applied stress increases, the corresponding strain grows at an accelerated rate. This means that the same increment in stress results in higher strains at larger stress levels compared to smaller levels. This behaviour shows that as deformation increases, the soil gradually loses stiffness. Which is especially relevant for foundations that need to deal with soil that is susceptible for settlement, since a foundation that has to deal with higher stresses also risks larger differential displacements between elements.

2.3. Helical piles

In chapter 2.1 short foundation piles are addressed. These piles combine the skin friction and the bearing surface to obtain their bearing capacity. Two types of helical pile designs are an isolated helical plate welded to a central shaft or continuous screw type piles. Each one focuses on one of the resistances while keeping the benefit of being an easy to install, retrievable pile.

2.3.1. Typology of short foundation piles

A short foundation pile can consist out of different materials like concrete, grout, wood, etc. For the pile to be retrievable and reusable it has to be made out of steel. For the steel foundation piles there are two options that can be used.

The first option is to focus fully on the friction between the shaft and the soil by using a screw shaped pile. The threaded surface of the pile improves the soil interaction surrounding the shaft. It creates additional areas of bearing pressure and more friction surface, see figure 2.9 (Karami et al., 2023).

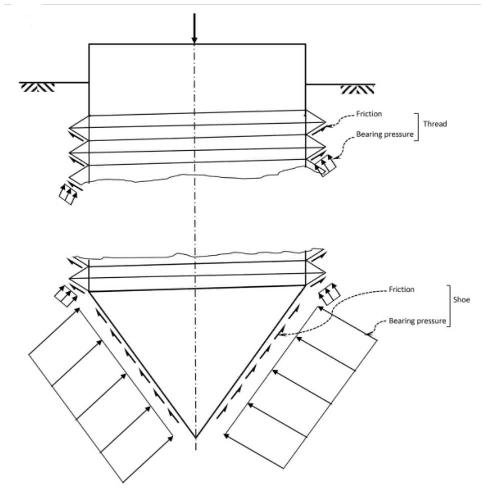

Figure 2.9: Mechanics of a screw type pile

The other pile type consist of a steel cylindrical element with a helix at the bottom that provides a surface for the vertical forces to spread out. With a smaller shaft diameter the friction force will be lower, but in return a higher end bearing capacity is obtained. The pile is more close to shallow foundation than to friction piles. It uses the existing effective stress at deeper soil layers to obtain a more stability and lesser settlement compared to a footing at the surface of the soil.

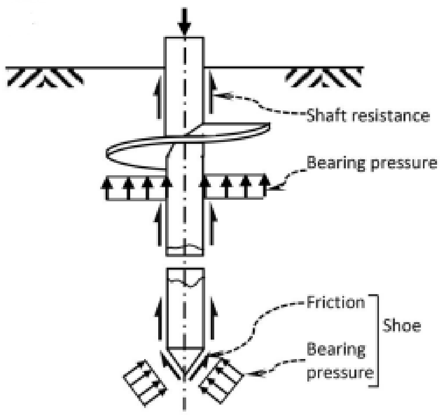

Figure 2.10: Attributes of a helical pile

Figure 2.11: Example of helical piles (Farhad Nabizadeh, 2017)

Both types are applicable for this research. However, the pile with the helical plate has some benefits over the screw shaped pile. Mainly, the simplicity, the fewer amount of steel needed and the ability to improve the pile by adding more helices, makes the helical pile more suited for this research. The last point will be expanded on in Paragraph 2.3.3. The main disadvantage of using these piles is the difficulty of installing them in stiff soils like sand. This study focuses on the placement of these piles in softer soils and therefore this will not be a problem (Karami et al., 2023).

2.3.2. Capacity of a helical pile

For this research, two capacities are important: The short term capacity (for load that occur over a short period of time) and the long term capacity (for loads that occur over a long time). The upcoming formulas will use the undrained shear strength Su to calculate the capacity. Depending on the duration of the load, this value changes. The value of c_u can be used for the short term capacity calculations, while for the long term capacity the drained shear strength T should be used. For the long term capacity, the pressure from the surplus of pore water pressure has dissipated and it has to rely on drained conditions. How to calculate the drained shear strength is shown in equation 2.28.

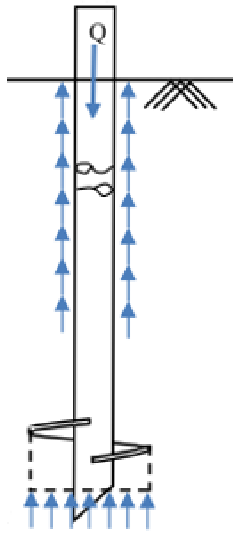

Figure 2.12: Short pile resistance (Prakash & Sharma, 1990)

The bearing capacity of a helical pile is obtained by the two earlier mentioned mechanisms. The surface area of the helix spreads out the load to a more desired stress level for the underlying soil. In literature the helix capacity in weaker soil can be obtained by the following formula:

$$q_h = 9,25 * s_u \tag{2.10}$$

Besides the resistance obtained from the helix, a resistance can be obtained by the shaft of the pile. When a pile is embedded in homogeneous soil, it tends to move downward under load, but the surrounding soil does not. This creates friction between the shaft and the surrounding soil, leading to an extra resistance of the pile. The shaft resistance can be obtained by using the following formula:

$$f_s = \alpha * s_u \tag{2.11}$$

Where s_u is the undrained shear strength of the soil and α is a factor for drilled shaft foundations:

$$\alpha = 0,4 * [1 - 0,12 * ln(s_u/P_A)] \tag{2.12}$$

With P_A being the atmospheric pressure (Shuman et al., 2022).
The capacity of an individual helix is confirmed in the practical guide for helical piles (Perko, 2009). The resistance is determined with the following steps:

$$P_u = \sum_n q_{ult} * A_n \tag{2.13}$$

Where q_{ult} is a modified version of the bearing capacity formula by Terzaghi. The updated formula includes the shape factor of the bearing element and the depth. The formula for can be written as follows:

$$q_{ult} = cN_c s_c d_c + q' * (N_q s_q d_q - 1) + 0.5\gamma D N_\gamma s_\gamma d_\gamma \tag{2.14}$$

Where:

q_{ult}	is the ultimate bearing pressure;
c	is the cohesion c_u for short term and drained shear strength T for long term;
q'	is the effective overburden stress at the bearing depth;
γ	is the soil unit weight;
D	is the diameter of the helical plate;
N_c, N_q and N_γ	are the bearing capacity factors;
s_c, s_q and s_γ	are the shape factors;
d_c, d_q and d_γ	are the depth factors.

The bearing capacity, shape and depth factors are determined by the following formulas:

$$N_q = e^{\pi \tan(\phi)} * \tan^2\left(45 + \frac{\phi}{2}\right) \tag{2.15}$$

$$N_c = (N_q - 1)\cot\phi \tag{2.16}$$

$$N_\gamma = (N_q - 1)\tan(1.4\phi) \tag{2.17}$$

$$s_c = 1 + \frac{N_q}{N_c}\frac{B}{L} \tag{2.18}$$

$$s_q = 1 + \frac{B}{L}\tan\phi \tag{2.19}$$

$$s_\gamma = - + 0.4\frac{B}{L} \tag{2.20}$$

$$d_c = 1 + 0.4K \tag{2.21}$$

$$d_q = 1 + 0.2K\tan\phi * (1 - \sin\phi)^2 \tag{2.22}$$

$$d_\gamma = 1 \tag{2.23}$$

$$K = \arctan(\frac{H}{B}) \tag{2.24}$$

Where:

B	is the width of the bearing element (in this case $B = D$);
L	is the Length of the foundation element;
K	is a scaling parameter;
ϕ	is the angle of internal friction of the soil.

When the piles are placed in fine-grain soil for a short period of time, the value of ϕ is equal to 0. The equation can be simplified to:

$$q_{ult} = 9s_u \tag{2.25}$$

A similar equation as equation 2.10.

The book gives a simplified equation for the shaft resistance.

$$f_s = \alpha H(\pi d) \tag{2.26}$$

Where:

α	is the adhesion between the soil and the shaft;
H	is the length of the helical pile above the helix;
d	is the diameter of the shaft;

The adhesion is determined as followed:

$$\alpha = 2/3T \tag{2.27}$$

$$T = c' + \sigma_n' \tan\phi \tag{2.28}$$

Where:
T is the drained shear strength;
c' is the effective cohesion;
σ_n' effective confining stress;

According to Bowles (Perko, 2009), a conservative value for the T of a helical pile in in undrained fine-grain soils, can be given by Formula 2.29.

$$T = s_u \tag{2.29}$$

When comparing the helix and shaft resistance to one another, a significant difference can be seen. The dimensions of the pile consist of a small shaft diameter and a large helix diameter at the bottom. This leads to the shaft surface of the pile being relatively small, which leads in turn to the shaft resistance having little influence on the total capacity of the pile. However, for smaller loads the shaft resistance might be beneficial for the final design, since it reduces the loads used for calculating settlements.

2.3.3. Improvements of a helical pile

Different design changes can be made to the pile for improving its capacity. Options of changing the shaft or helix diameter are obvious adjustments. The same counts for making longer piles to reach deeper layers.

Adding helices can also be used to improve the piles capacity. How the pile will act, is related to the spacing between the helices. If the ratio S_h/D (Spacing of helix / Helix diameter) is higher than 1.5, the helices can be seen as an individual bearing failure mechanism. If the spacing is smaller than this ratio, the soil between the helices will act as a cylinder that shears with the surrounding soil (Türedi & Örnek, 2020). It basically acts as a large shaft. Figure 2.13 demonstrates this effect.

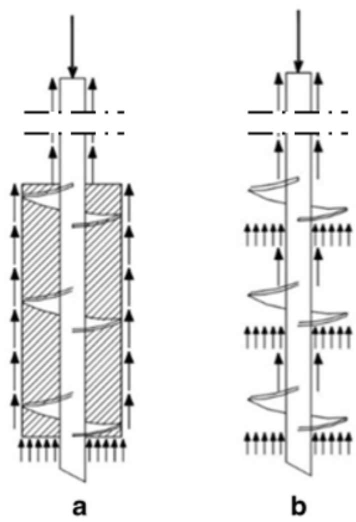

Figure 2.13: Two failure mechanisms of a multi-helix piles: (a) cylindrical shear failure; (b) individual bearing failure (Jahanshahi-nowkandeh & Choobbasti, 2021)

Despite increasing the capacity of the pile, the improvements come at a cost of using more material, increasing the weight and creating more torsional resistance. The latter makes the piles make it more difficult to install the piles and more heavy equipment might be needed. Decisions of increasing the capacity should take this into account.

2.3.4. Group effect of a helical pile

Placing piles near to each other can cause an interaction between them where the stress fields intercept. An example of this can be seen with pile driving. When a long foundation pile is driven into the ground, the soil surrounding the pile has an increase in stress. Placing another pile next to it will not be as easy. The helical piles are screwed into the ground. This minimizes the increase in pressure and the piles do not influence the construction phase.

The efficiency of a foundation can either increase or decrease by grouping the foundation piles. The grouping of piles will increase the soil stress underneath the pile group. In sandy soil this is a benefit. The bearing capacity of the soil increases while the deformations stay minimal due to the properties of the sandy soil. However, in clayey soils the increases soil stress becomes a problem. A higher stress will lead to higher deformations than with individual piles. Another mechanism that can occur is called block failure. This happens when the stress in the soil between the helical piles becomes too high and fails. Figure 2.14 shows a schematising of this mechanism.

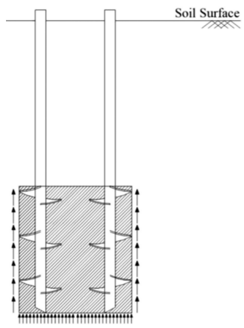

Figure 2.14: Short pile resistance (Jahanshahinowkandeh & Choobbasti, 2021)

To make sure the helical piles have individual failure mechanisms, an appropriate distance should be used between them. Research shows that in clayey soil the spacing ratio should be $S_h = 2D$ for the individual pile failure mechanism to be critical. Figure 2.15 shows the displacement of three different pile groups with each a different S_p/D_p ratio.

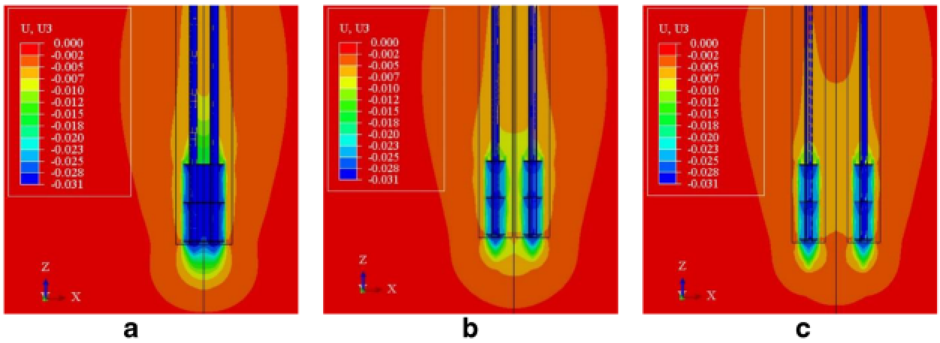

Figure 2.15: Vertical displacement contours of helical piles subjected to axial compressive loading in clayey soil for inter-helix spacing ratios of $(a) S/D_p = 1.05, (b) S/D_p = 2$, and $(c) S/D_p = 3$ (Jahanshahinowkandeh & Choobbasti, 2021)

.

The figure shows a distinct difference in behaviour between situation a and b. Other research also shows similar settlement ratio with a spacing ratio of 2D and 3D (Elsherbiny & Naggar, 2013). Note that the results from these researches are based on piles with multiple helices. If the helices are located in sandy soil, the ratio also changes to $S/D_p = 3$.

Beyond the effect of multiple helical piles on the bearing capacity, the settlement behaviour also changes. Underneath the bearing plate the eads out through the soil, see Figure 2.6. When piles are positioned close to each other, their stress fields overlap, leading to a greater stress increase in the soil compared to an isolated pile. In sandy soils, increased confinement from adjacent piles enhances stiffness and reduces settlement. In contrast, in clayey soils, closely spaced piles may result in increased settlement due to higher stress-induced pore water pressures and subsequent consolidation.

2.4. Risks of allowing settlement

In construction design, the avoidance of settlement is for good reason. While minor settlement is natural over time, excessive or uneven settlement can cause problems for the construction. Avoiding significant settlement is a normally top priority in construction design because it ensures the safety, functionality, and durability of buildings. This part will go deeper into of the risks of allowing settlements.

2.4.1. Total settlement

The total settlement of a structure (δ) is defined as "the change in foundation elevation from the original unloaded position to the final loaded position" (Prakash & Sharma, 1990). See Figure 2.16.

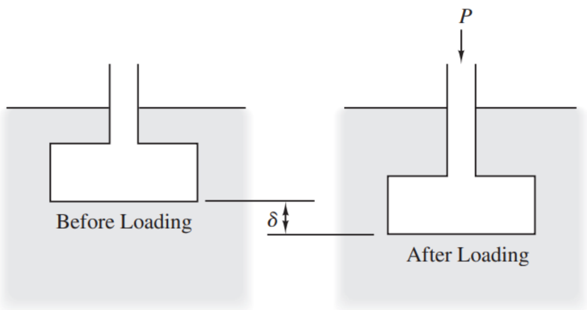

Figure 2.16: Total settlement in a spread footing foundation (Prakash & Sharma, 1990)

When a structure start to settle evenly, it does not mean that structural problems will occur. However, the structure might experience other challenges such as:

- **Connections to other structures**: When structures settle at a different rate, the connections between the two structures can be damaged. Another example is when an existing structure is extended, the newly added part can settle at a different rate. At the start, the floors of beams will be at the same height, but after some time passes they can be misaligned.
- **Utility problems**: Utility lines such as electronic cables or water pipes are installed at the beginning of the structures lifetime, often underneath the ground surface. When a structure starts to settle at a large rate, the connections can be distorted. This issue is particularly problematic for gravity-driven systems like sewers.
- **Surface water**: To prevent rainwater from entering, the ground floor of a building should be slightly elevated compared to the surrounding terrain. After settlement, a former good building design, might not fulfil this requirement anymore.
- **Aesthetics**: Even if the structural integrity or functionality of the building remains unaffected, noticeable settlement can create unsightly appearances, impacting the structure's overall aesthetics. A window just above the ground level, might not be as one imagined before investing in the building.

(Prakash & Sharma, 1990)

All these issues can be avoided with a proper design. Several buildings are still in service even after experiencing large total settlements. However, most of the time extensive settlements are avoided. The Eurocode gives the following guideline on total settlement to ensure the safety and quality of constructions:

"The total settlement of a construction cannot be more than 50 mm unless the relative rotations are still acceptable afterwards in addition to the settlements not causing problems for the pipes and electronic failures." (Nederlands Normalisatie-instituut, 2017)

2.4.2. Differential settlement

A structure that moves down perfectly vertical, will not cause structural problems. There are no additional stresses that occur due to the total settlement. Differential settlement do cause extra stresses to occur. Differential settlement is when different parts of a structure settle at varying rates or to different extents, leading to uneven support of the building. This uneven settling is influenced by several factors, such as:

- **Variations in soil composition**: If a building is constructed on a site with multiple soil types—such as sand in one area and clay in another—the different compressibility and load-bearing capacities of these soils will cause sections of the building to settle at different rates.
- **Uneven load distribution**: When the building's weight is not evenly distributed across the foundation. For instance, if one part of the building carries heavier loads—such as machinery or a taller section of the structure—this area may exert more pressure on the soil, causing it to settle more compared to the lighter sections.
- **Difference in foundation elements**: One support can be stiffer than another one, which leads to a lesser deformation of the rigid support. This mostly occurs with building expansions.
- **Construction rigidity**: A rigid superstructure can spread out the load better than a less rigid one.
- **Position**: The position of the structure in relation to other structures.

(Arapakou & Papadopoulos, 2012)

These differential settlements are mostly avoided. Constructions are calculated with fixed supports and the foundation is designed to not exceed the norm. When excessive settlement take place, these supports can displace vertically at different rates, which in turn can lead to tilt within the structure. In regulations the differential settlement are measurable by looking at tilt and the relative rotation of the structure elements.

- **Relative rotation (β)**: The angular displacement between different parts of a structure, indicating that one part of the structure has rotated relative to another.
- **Tilt (ω)**: The overall inclination of the structure from its original vertical or horizontal alignment. It represents the movement of the entire structure as it leans or inclines to one side.

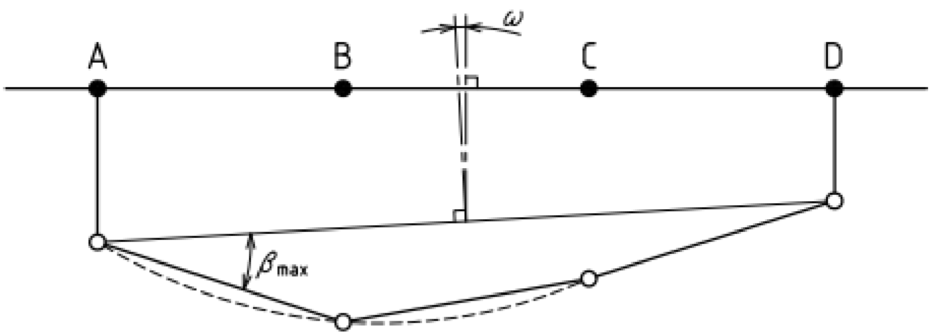

Figure 2.17: Definition of relative rotation (β) and tilt (ω)

For these settlements different requirements have been constructed by the Netherlands Standardization Institute (NEN). The limit for ultimate limit state (ULS) type B is often set to a maximum relative rotation (β) of 1:100. For residential buildings, in general, the limit for the serviceability limit state (SLS) is that the tilt (ω) and/or relative rotation (βx) should not exceed a value of 1:300. The standardization helps to ensure the quality and safety of constructions.

The standardized regulations make sure that a building is comfortable to live in and that the stress build up will not become too large.

Finally, the NEN also proposes another solution for the construction grant safety and not needing to keep the relative rotations in mind. The rule states:

"If it has been shown from the calculation based on the applied mechanics and the properties of the materials used that, when one pile or group of piles of the cooperating piles under a rigid part of the building structure (beam, wall, etc.) is removed, the settlement (for piles under compression) or the uplift (for piles under tension) of the building structure at the location of the removed pile or pile group, relative to the adjacent pile or pile group, is less than or equal to 5 mm under the influence of the prescribed load combinations in the serviceability limit state according to 2.4.2, then a building or part thereof may be considered rigid."

This rule comes down to the building being really stiff and therefore assumes large relative rotations cannot occur (Nederlands Normalisatie-instituut, 2017).

2.4.3. Settlements in relation to the superstructure

In the last section, the influence of rigidity is said to influence the differential settlement of a structure. This can best be explained by an example.

A beam supported at three locations is loaded equally by q. The middle support fails and the system changes to a beam on two supports. The higher the stiffness of the beam, the less impact the failed support has on the deformations of the beam.

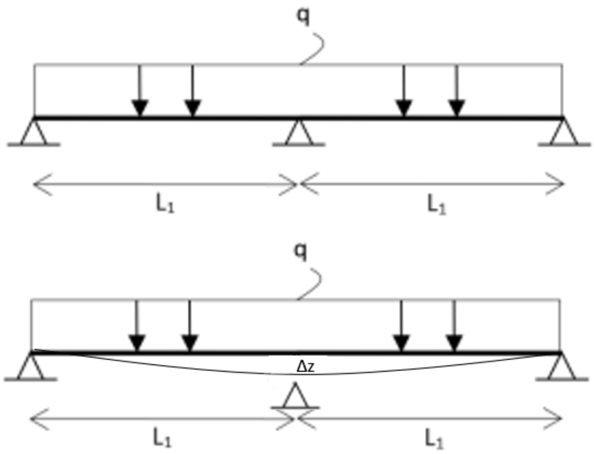

Figure 2.18: Beam undergoing failure of the middle support

Improving the stiffness of the construction elements comes at the cost of minimal usage of materials. Larger dimensions or stiffer materials have to be used to achieve a rigid structure. Proper design does also play a big role.

A study from Angeliki E. Arapakou and Vasileios P. Papadopoulos researched the influence of rigidity on differential settlements in a structure. A typical five-span frame building with varying stiffness was analysed in 2D using the finite element numerical method. Some conclusions can be obtained from this research:

- A more rigid superstructure leads not only to less differential settlement, but also to less settlement overall in compressible soil.
- Critical stress values within the structure could be reached due to differential settlements, even when the value of differential displacement is below the limiting value of 1/150.

- Reduced rigidity leads to lower bending moments within the structure.

(Arapakou & Papadopoulos, 2012)

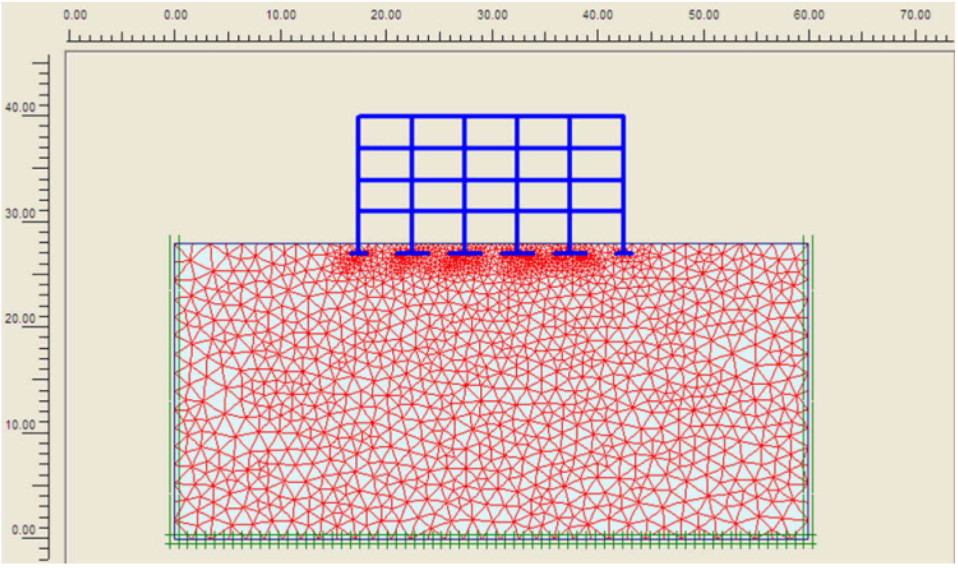

Figure 2.19: Finite element model of a typical multi-story building (Arapakou & Papadopoulos, 2012)

2.5. Conclusion foundation design

There is a large variety of foundation designs in the Netherlands. The use of long piles ensures stability, but comes with higher material costs and sustainability considerations. Shallow foundations and preloading techniques offer alternative solutions for certain lightweight projects, but are not suitable for locations large layers of soft soil. Short helical piles offer a balanced solution, providing greater environmental and economic benefits compared to traditional deep foundations, while still experiencing significant settlement.

The helical pile takes the vertical load from the superstructure to a deeper layer in the soil that has a higher existing effective stress. This will reduce the settlement and obtains a capacity the deeper the footing is positioned underneath the surface. The piles can be improved by adding multiple helical plates that can act in two different ways depending on the spacing between them. The piles have to be placed at minimal distance of 2 times the diameter in clay soil for minimizing pile interaction and maximizing the load-bearing efficiency.

Applying these foundation piles in clay soil will cause large settlements in comparison to placing placing them in sandy soil. The settlements of a pile can differ due to a difference in loading, variation in soil composition, difference in foundation elements, construction rigidity and position. These total- and differential settlements can cause not only cause functional problems, but structural problems as well. Norms have been created to regulate settlements of a building ensure these problems are avoided. Total settlement of a construction cannot be more than 50 mm unless the relative rotations are acceptable and the settlement do not cause any problems with pipes and electronics. Furthermore, the relative rotation and tilt of a structure should not exceed 1:300 in the serviceability limit state (SLS).

The structural feasibility of this structure is therefore dependent on the differential settlements between the supports. The design of the superstructure can influence these differential settlements. A stiffer structure is able to redistribute the loads more evenly to the foundation compared to a less stiff structure. In addition does a more rigid superstructure reduce the overall settlement of a structure since the maximum support load is decreased. This will however increase the stresses within the structural elements and increase the material needed.

3

Literature study - Timber structures

Wood is unique construction material with its own properties and limitations. While steel and concrete are celebrated for their uniformity, strength, and durability, wood stands out for its natural origin and environmental benefits. This chapter explores the history of timber structures, their unique properties, the different design aspects that should be taken into account in a timber structure, and how different, modular wall systems can be implemented to resist differential displacements.

3.1. History

Wood has been a fundamental building material for thousands of years. It has shaped the built environment from ancient civilizations and is still used widely in modern constructions. Its workability, and versatility made it a natural choice for early builders, enabling the creation of a wide range of structures from simple shelters to complex temples and fortresses. With the rise of concrete and steel in structures, wood was less necessary in constructions. These materials were stronger and stiffer than wood, so larger and more efficient buildings could be realised.

In recent times, the unique advantages of wood are being recognized once again. As a renewable resource, sustainable forestry practices ensure a continuous supply of wood. Additionally, wood absorbs carbon dioxide during its growth, making it a climate-friendly building material. Its high strength-to-weight ratio makes it an ideal choice for structures where weight reduction is essential. Consequently, wood is re-emerging as a vital material in contemporary architecture and construction, valued for its environmental benefits and structural capabilities.

This does not mean all aspects of using wood as a construction material are positive. Unlike steel and concrete, wood is composed out of fibres. This leads to its mechanical properties depend on the direction of the load relative to the fibre. The directions of the fibres play therefore a big role in the capacity of the element which makes it harder to calculate with. Furthermore wood can vary a lot in its properties. Since it is an organic material the properties are influenced by the species, growing conditions, and processing methods. Natural defects such as knots, splits, and checks can weaken wood and let the capacity vary between two elements that are designed with the same dimensions. The durability of wood must be carefully considered, as it is susceptible to biodegradation by fungi, bacteria, or insect attacks. Moreover, its mechanical properties are influenced by moisture content, which can affect its performance (Forest Products Laboratory, 2021).

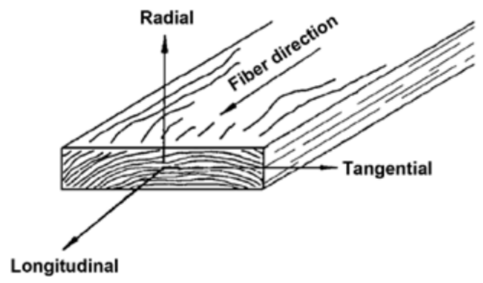

Figure 3.1: Fiber direction in wood (Forest Products Laboratory, 2021)

3.2. Design considerations of solid sawn, glulam, and hardwood

As stated in the last section, wood is one of the oldest building materials. Over time, a wide range of wood products have been developed, each with their own advantages and disadvantages. This section explores three key wood typologies: solid sawn wood, Glued laminated timber (Glulam), and hardwood. Each one having their own properties on strength, resistance to humidity, size options, sustainability, and cost.

3.2.1. Solid Sawn Wood

Solid sawn wood is derived from directly sawing logs into specific dimensions. Its natural strength and widespread availability make it a popular choice in construction (Forest Products Laboratory, 2021).

- **Strength**: The *Timber Engineering book* (Blaß, H. J., & Görlacher, R., 2017) notes that the mechanical properties of solid wood are highly variable, depending on natural factors like knots, grain orientation, and density. This variability can lead to less predictable performance compared to engineered wood products.

- **Humidity Resistance**: The *Wood Handbook* (Forest Products Laboratory, 2021) highlights that solid wood is hygroscopic, meaning it absorbs and releases moisture based on environmental conditions. This often results in warping, twisting, or shrinking unless the wood is properly protected.

- **Size Options**: The size of solid sawn wood is limited by the dimensions of the source tree, making it less suitable for large-span or heavy-load applications(Blaß, H. J., & Görlacher, R., 2017).

- **Sustainability**: The *Wood Handbook* emphasizes that while solid wood is a renewable resource, harvesting large-diameter logs can lead to deforestation and ecological harm. Smaller diameter beams are mostly sustainable.

- **Cost**: Solid sawn wood is typically the most affordable option due to its straightforward processing. However, prices can vary significantly based on species and grade. High-quality or large-dimension lumber can be costly due to limited availability (Forest Products Laboratory, 2021).

3.2.2. Glulam (Glued Laminated Timber)

Glulam is an engineered wood product made by bonding multiple layers of timber with high-strength adhesives. It is specifically designed to overcome the limitations of solid sawn wood in structural applications.

- **Strength**: Glulam achieves superior strength and stiffness by distributing imperfections across laminated layers. This results in higher load-carrying capacity and greater resistance to bending compared to solid wood (Blaß, H. J., & Görlacher, R., 2017).

- **Humidity Resistance**: The *Wood Handbook* notes that glulam exhibits improved dimensional stability, making it less prone to warping or shrinking in humid environments. Proper sealing and treatment further enhance its performance.

- **Size Options**: Glulam can be manufactured in a wide range of sizes and shapes, including long spans and curved forms, making it highly versatile for architectural and structural applications (Blaß, H. J., & Görlacher, R., 2017).

- **Sustainability**: According to the *Wood Handbook*, glulam makes efficient use of wood by utilizing smaller, fast-growing trees. However, the adhesives used in its production may contribute to environmental impacts, which should be considered.

- **Cost**: Glulam is more expensive than solid sawn wood due to its manufacturing complexity and the use of adhesives. However, its ability to span longer distances and its structural efficiency can reduce the overall material needed, potentially lowering total project costs (Forest Products Laboratory, 2021).

3.2.3. Hardwood

Hardwoods are derived from broadleaf trees and are highly valued for their strength, durability, and natural resistance to humidity. The hardwood species are more suited for structures in challenging environments.

- **Strength**: Hardwoods are exceptionally strong and durable. The *Timber Engineering book* (Blaß, H. J., & Görlacher, R., 2017) highlight that their dense grain structure allows for high load-bearing capacity, making them ideal for structural and demanding applications.
- **Humidity Resistance**: The *Wood Handbook* points out that many hardwood species, such as Teak and Iroko, are naturally resistant to moisture and decay due to their dense grain and high oil or tannin content. This makes them suitable for humid environments, including outdoor and marine applications.
- **Size Options**: Hardwoods are often available in moderate dimensions, limited by the size of the source tree. However, their inherent strength allows for smaller cross-sections in structural applications while maintaining performance (Blaß, H. J., & Görlacher, R., 2017).
- **Sustainability**: The *Wood Handbook* underscores the importance of sustainable sourcing for hardwoods, as their slower growth rates and high demand can lead to overharvesting. Deforestation is shown to be a large problem in southern continents such as Africa and South America, due to the larger amount of trees being cut in comparison to the amount of trees planted (Blaß, H. J., & Görlacher, R., 2017).
- **Cost**: Hardwoods are generally the most expensive option due to their density, durability, and slower growth rates. Exotic species like Teak and Ipe are particularly costly but offer unparalleled performance in humid environments (Forest Products Laboratory, 2021).

3.2.4. Summary

Solid Sawn Wood

- **Strength**: Variable, depends on natural defects.
- **Humidity Resistance**: Prone to warping and shrinking.
- **Size Options**: Limited by tree size.
- **Sustainability**: Renewable but needs responsible sourcing.
- **Cost**: Most affordable option.

Glulam (Glued Laminated Timber)

- **Strength**: High, due to engineered structure.
- **Humidity Resistance**: Stable and resistant with proper treatment.
- **Size Options**: Customizable, large spans possible.
- **Sustainability**: Efficient use of wood resources, can be manufactured with small trees.
- **Cost**: Moderate to high.

Hardwood

- **Strength**: Very strong and durable.
- **Humidity Resistance**: Naturally resistant.
- **Size Options**: Moderate, but strong in small sections.
- **Sustainability**: Requires responsible sourcing.
- **Cost**: High, especially exotic species.

3.3. Structural implications of timber elements

As mentioned in the section before, the strength of wood depends on the direction of the load making it a heterogeneous material. In addition to this can wood samples with similar physical characteristics differ in their mechanical properties. The Eurocode accounts for this variability through safety factors and design measures.

3.3.1. Design factors

The safety measures taken by implementing different factors and considerations can be characterised as followed:

- **Characteristic strength**: The characteristic strength, f_k, is defined as the 5th percentile of the tested strength values for timber. This conservative approach ensures that only 5% of the material is expected to have a lower strength than the given value:
- **Partial safety factor**: The Eurocode applies partial safety factors to reduce the characteristic strength of wood to a design value. For timber elements, γ_M accounts for uncertainties in material properties, such as variability in strength and the effects of defects.
- **Service Classes and Environmental Conditions**: The Eurocode accounts for the influence of environmental conditions on wood properties. t defines service classes based on expected conditions of use, which influence the strength modification factors applied in design. For example:
  - *Service Class 1:* Dry environments (e.g., indoors).
  - *Service Class 2:* Moderately humid environments.
  - *Service Class 3:* Wet or outdoor environments.
- **Modification factor**: Wood strength varies with the duration of the applied load and the moisture content. The Eurocode introduces the modification factor, k_{mod}, to adjust for this.

The design value X_d of a strength property must be calculated with the following equation:

$$X_d = \frac{k_{\text{mod}} \cdot X_k}{\gamma_M} \tag{3.1}$$

Where X_d is the characteristic value of a chosen strength property (Nederlands Normalisatie-instituut, 2011).

3.3.2. Decay prevention

Wood being an organic material, makes it vulnerable to various forms of decay. It is susceptible to decay from fungi, insects, moisture and more.

Fungal decay is caused the development of fungi. The most common fungal decay are brown rot and white rot, based on the colour of the rotten wood. These fungi break down the cell structures of wood to grow which leads to the loss of structural capacity of the wood. These fungi thrive in moist environments and can lead to rapid decay under the right conditions.

To prevent fungal decay there are several options. Structural wood should be dried beforehand and kept dry. This means preventing the wood from getting in contact with rain, condensation or wet ground. Elevating the foundation to a proper level above the ground, implementing design features such as overhangs and the use of protective coating, are all design measures that can achieve this.

In Figure 3.2 four common types of fungal growth on wood are shown: (a) mold discolouration; (b) brown rot in pine (characterized by dark colour and cubical cracking); (c) white rot in maple (distinguished by its bleached appearance); (d) soft rot in a preservative-treated pine utility pole (showing shallow surface decay).

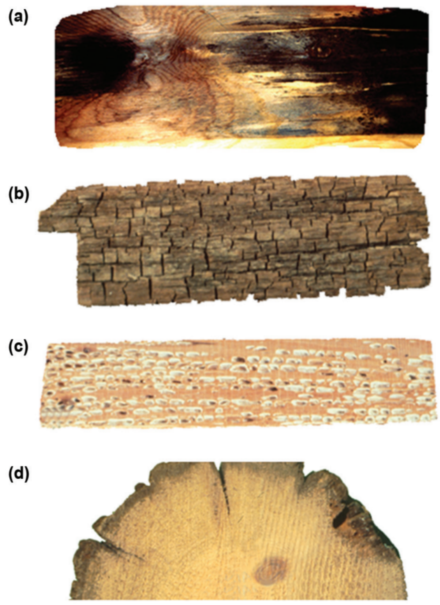

Figure 3.2: Representative examples of four common types of fungal growth on wood: (a) mold discolouration; (b) brown rot in pine; (c) white rot in maple; (d) soft rot in a preservative-treated pine utility pole. (Forest Products Laboratory, 2021)

Elevating the foundation helps with more than just fungi, it also prevents insects from reaching the foundation. Termites and other insects are also a challenge for wooden structures. Termites consume wood, while beetles and ants bore into wood, creating tunnels and weakening its structure. The wood can also be treated chemically to prevent an insect infestation.

Like said earlier, water infiltration can make the wood susceptible to fungal decay, but it also influences other degradation processes. Repeated cycles of wetting and drying cause wood to expand and contract, leading to warping, cracking, and splitting. Extreme temperatures can exacerbate issues related to degradation processes due to moisture. The best way of treating the wood is preventing the exposure to excessive moisture content. Ensure that wood components are adequately ventilated to allow moisture to escape. If this does happen, water will infiltrate the wood and start degradation processes. Figure 3.3 shows examples of this mechanism and the solution.

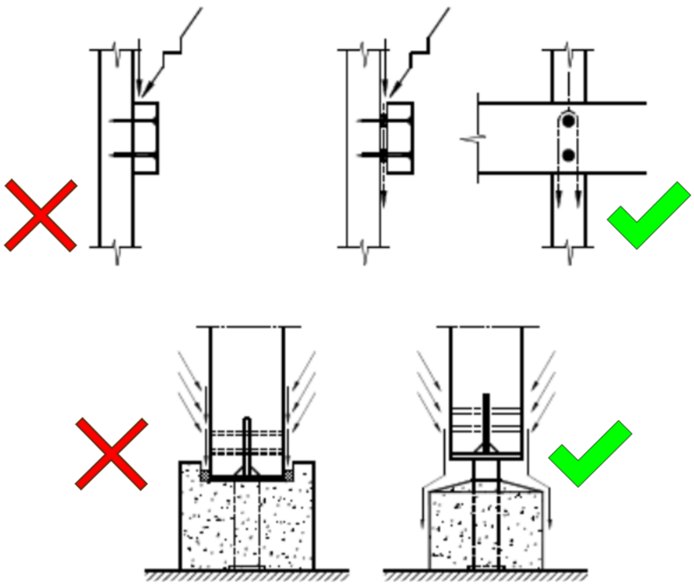

Figure 3.3: Wooden element design implementations preventing water locking (Trutalli, 2017)

Finally, wood being water-logged can also be the solution to degradation. Wood decays at a slower rate when there is a lack of oxygen, so when wood does not get exposed to air and stays underneath the ground water level, it is protected to fungi and bacteria. This is the reason why the wooden foundation piles in cities like Amsterdam are still functional (Forest Products Laboratory, 2021).

3.4. Wall systems

The construction of modular timber buildings partly depends on the selection of an appropriate wall system, which plays a critical role in meeting structural, thermal, and regulatory requirements. The wall guides the vertical loads to the foundation, but can also help in achieving a higher stiffness of the structure. Two primary types of wall systems commonly used in modular buildings are timber frame panels and Cross-Laminated Timber (CLT) walls. Each has its own characteristics and advantages that make them suitable for different modular building applications.

3.4.1. Modular wooden buildings

Using the wooden panels as a wall makes it resistant to more than only vertical loads. The mechanisms that contribute for deformations of a wall are bending, shear, sliding and rocking, see Figure 3.4.

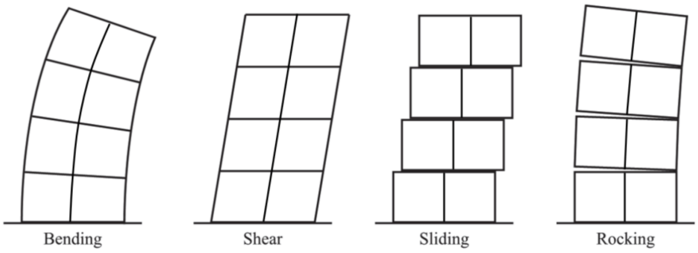

Figure 3.4: Four mechanisms of wall deflections (Mol, 2023)

The effects of these for mechanisms can be treated independently. Although they interact with each other, the additional deflections are too small to play a significant part in the total deflection.

$$\Delta_{\text{Total}} = \Delta_{\text{Bending}} + \Delta_{\text{Shear}} + \Delta_{\text{Sliding}} + \Delta_{\text{Rocking}} \tag{3.2}$$

The stiffness of the wall can be schematized as four springs in series.

$$k_{\text{Total}} = \frac{1}{\frac{1}{k_{\text{Bending}}} + \frac{1}{k_{\text{Shear}}} + \frac{1}{k_{\text{Sliding}}} + \frac{1}{k_{\text{Rocking}}}} \tag{3.3}$$

The stiffnesses for sliding and rocking are more difficult to predict due to their dependence on the connections between the panels. However, they can play a large part in the total displacements in systems with multiple elements (Brandner et al., 2018). In the case of differential settlement, these mechanisms are important. The schemes stay the same, but sideways. With the mechanisms it is important to take into account the connections between the panels. Dowels and bolts are common practice for connecting wooden elements with the capacity depending on the wooden properties, and the properties and positioning of the connecting elements. The connections between wall panels make up the sliding and rocking stiffness of the wall by preventing the panels to move independently.

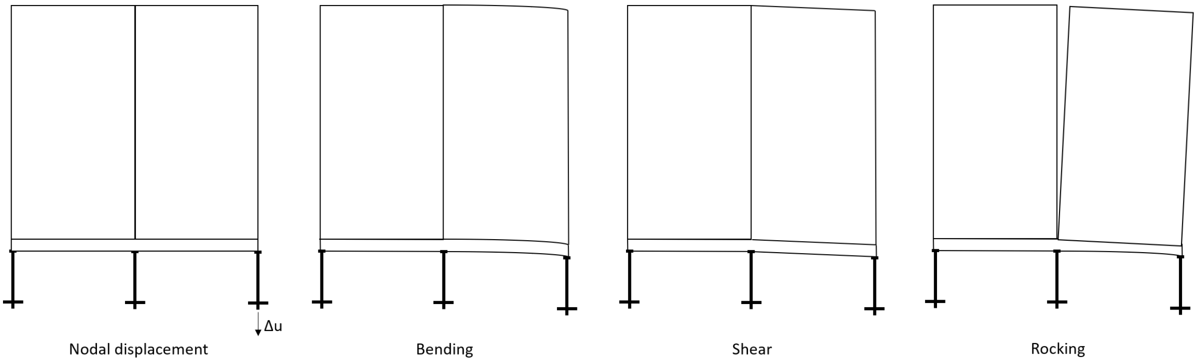

Figure 3.5: Mechanisms on a wall system imposed to differential settlement

3.4.2. CLT wall panels

Cross-laminated timber (CLT) is a construction material, consisting of layered wooden planks glued at right angles to create high-strength panels, see Figures 3.6 and 3.7. The distinctive quality of CLT lies in its capacity to form large, rigid surface panels with significant load-bearing and stabilizing properties. These panels, often used in walls and floors, provide essential structural support and improve thermal and fire safety in building designs. (*The CLT Handbook*, 2019)

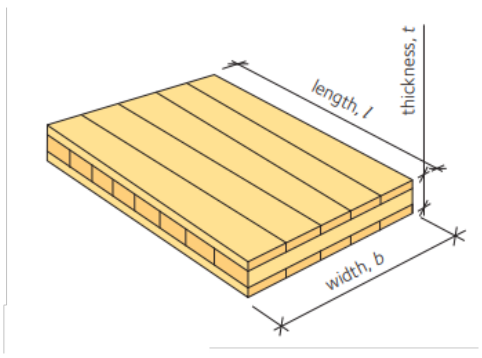

Figure 3.6: CLT panel

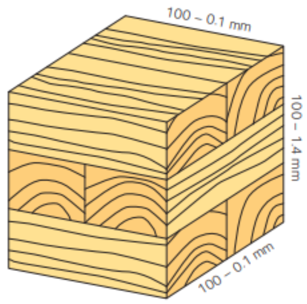

Figure 3.7: CLT fibres

Mechanics CLT wall

The different directions of the fibres in the CLT plate makes it have orthotropic properties. The panels consist of uneven amounts of layers, this makes the panel symmetric in its plane. However, one direction therefore has more strength than the other and is calculated differently. Figure 3.9 gives a schematisation of the different axes that are important for calculations in CLT.

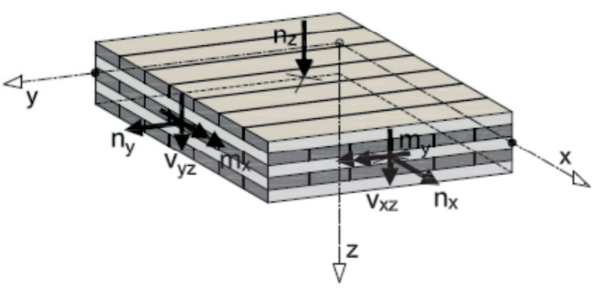

Figure 3.8: Definition of aces and denomination of forces

Figure 3.9 explains the multiple stresses that can occur within a CLT plate and which stresses need to be calculated in each direction (Brandner et al., 2018).

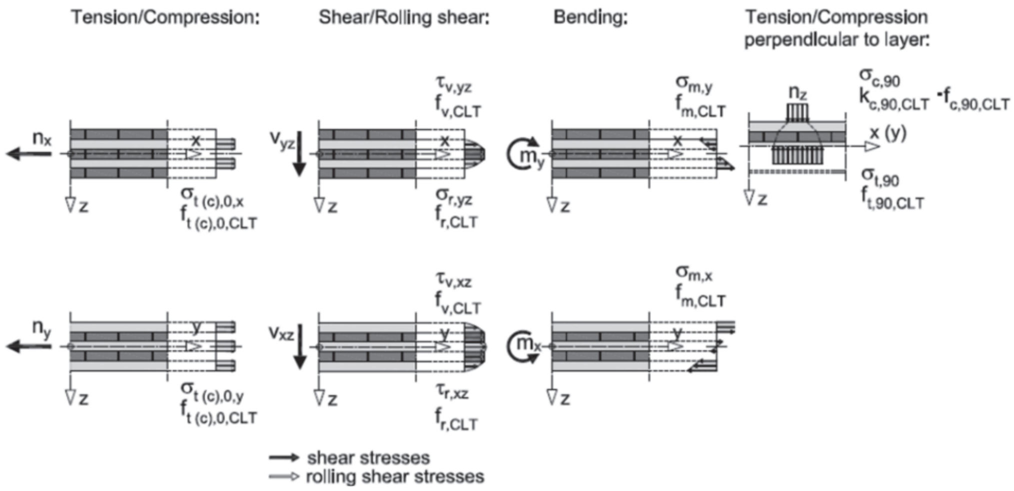

Figure 3.9: Definition of aces and denomination of forces

Properties CLT panel

The CLT panels will be modelled in SCIA Engineer. This software recommends using the properties of strength class CL24 that can be found in Table N.1 of the Eurocode 1995-1-1. The values are based on strength class C24, which is commonly used for the production of CLT panels.

Table 3.1: Mechanical properties of CLT frames with wood class C24 (Nederlands Normalisatie-instituut, 2011)

Property	Symbol	Unit	Strength Class C24
Bending strength (Out of plane loading)	$f_{m,k}$	N/mm^2	24
Tensile strength (In-plane loading)	$f_{t,0,k}$	N/mm^2	14
Tensile strength (Perpendicular to plane)	$f_{t,90,k}$	N/mm^2	0.1
Compressive strength (In-plane)	$f_{c,0,k}$	N/mm^2	21
Compressive strength (Perpendicular to plane)	$f_{c,90,k}$	N/mm^2	2.5
Shear strength (Out of plane loading)	$f_{v,k}$	N/mm^2	3.5
Rolling shear strength	$f_{r,k}$	N/mm^2	0.7
Modulus of elasticity (In and out of plane)	$E_{0.05}$	N/mm^2	11000
Modulus of elasticity (Perpendicular to plane)	$E_{90,\mathrm{mean}}$	N/mm^2	370
Shear modulus (Out of plane loading)	G_{mean}	N/mm^2	650
Rolling shear modulus	$G_{90,\mathrm{mean}}$	N/mm^2	50

3.4.3. Timber frame wall

Timber Frame Panels are lightweight, versatile wall assemblies that typically consist of a wooden framework filled with insulation and covered with sheathing materials. These panels offer flexibility in design and are relatively easy to manufacture, transport, and assemble, making them ideal for modular construction. Their lightweight nature allows for quicker installation and reduces the need for heavy-duty lifting equipment on site (D'Amicoa et al., 2016).

Mechanics timber frame wall

The main difference between a CLT wall and a timber framed wall is the stability mechanisms. The framework of the wall is not able to resist large amount of deformations. The timber frame is used to with stand the vertical loads and will struggle with other types of load, due to the horizontal stability depending on the connections between the slabs.

This horizontal resistance is obtained by the plate attached to the timber frame. This frame acts the same as the CLT elements that resist the bending and shear within the panel, but to a smaller degree.

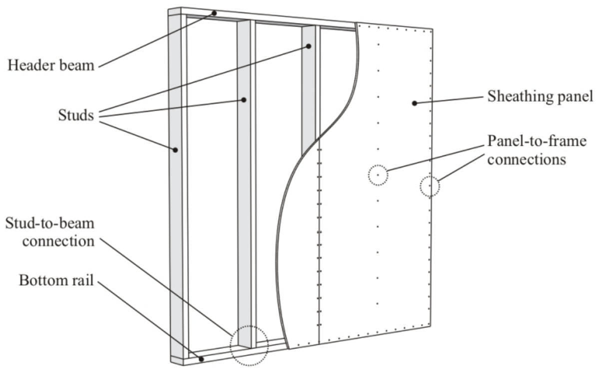

Figure 3.10: Schematisation timber framed wall (D'Amicoa et al., 2016)

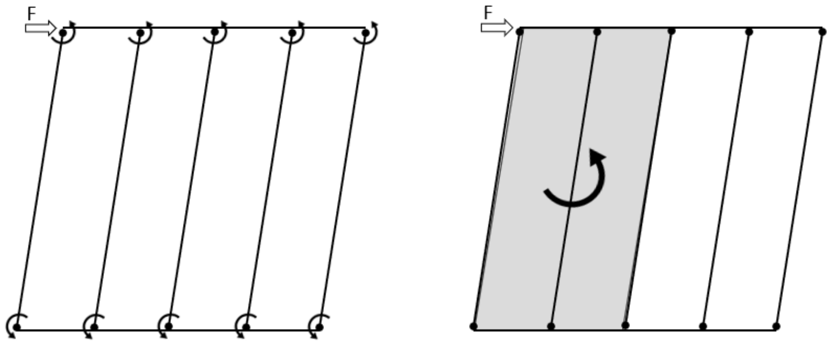

Figure 3.11: Stability timber frame vs timber frame with OSB plate

The most economical panels consist out of Oriented Strand Board (OSB), an engineered wood product made from strands of wood that are oriented in specific directions and then bonded together. There are several types of OSB available, each designed for different applications based on their load-bearing capacity and resistance to moisture. The types of OSB are classified as follows:

- **OSB/1:** For use in dry conditions, typically for interior applications such as furniture or interior non-structural elements.
- **OSB/2:** Designed for load-bearing applications in dry conditions. Commonly used for interior wall sheathing or roofing.
- **OSB/3:** Suitable for load-bearing applications in humid conditions. Typically used in external applications such as external wall sheathing, flooring, and roofing in areas where moisture exposure is likely.
- **OSB/4:** A higher-strength version designed for demanding load-bearing applications in humid conditions. It is often used in heavy-duty applications like industrial flooring or exterior cladding.

Depending on the humidity, a OSB type has to be chosen (Nederlands Normalisatie-instituut, 2011).

Properties OSB/3 panel

In this research, the OSB plate is assumed to be positioned at a place where moisture exposure is likely and works as a stability element. The OSB/3 is there chosen.

Orientation of face strands		∥ span direction			⊥ span direction		
Nominal thickness in mm		**>6 - 10**	**>10 - 18**	**>18 - 25**	**>6 - 10**	**>10 - 18**	**>18 - 25**
Characteristic strength values in N/mm²:							
Load ⊥ panel face:							
Bending	$f_{m,k}$	18,0	16,4	14,8	9,0	8,2	7,4
Compression	$f_{c,90,k}$	-					
Shear	$f_{v,k}$	1,0					
Load ∥ panel face:							
Bending	$f_{m,k}$	-	-	-	-	-	-
Tension	$f_{t,k}$	9,9	9,4	9,0	7,2	7,0	6,8
Compression	$f_{c,k}$	15,9	15,4	14,8	12,9	12,7	12,4
Shear	$f_{v,k}$	6,8					
Characteristic mean stiffness values in N/mm²:							
Load ⊥ panel face:							
Modulus of elasticity	E_{mean}	4 930			1 980		
Shear modulus	G_{mean}	50					
Load ∥ panel face:							
Modulus of elasticity	E_{mean}	3 800			3 000		
Shear modulus	G_{mean}	1 080					
Characteristic densities in kg/m³:							
Density	ρ_k	550					

Figure 3.12: OSB/3 properties based on the NEN 1995 Table C.9 (Nederlands Normalisatie-instituut, 2011)

3.5. Conclusion structural timber design

Wood has played an integral role in the evolution of construction, moving from use in ancient craftsmanship to its renewed importance in modern sustainable building designs. Although the introduction of steel and concrete, which are stronger and stiffer, reduced wood's use in large-scale projects, its environmental benefits and versatility resparked the interest in the material. Certain design aspects must be taken into account for a proper timber structure design. The material has a high variability in its strength and is susceptible to decay by fungi, insects and bacteria. By following the Eurocode's safety factors, the safety of a timber structure can be designed on a proper level. For ensuring the wood is not impacted by decaying processes, proper elemental design choices should be made. The following design aspects should be taken into account for this case study:

- The timber elements should not get in touch with the ground to prevent rotting of the material.
- Between the ground surface and the timber elements there should be a sufficient distance that prevents the humidity level from becoming too high.
- The connections between the structural elements should allow the water to flow, preventing the accumulation of water.
- Protection measurements should be taken to prevent water to get in direct contact with the wood, for example, at the roof. This will prevent a decline in the strength of the wooden elements. If there is no other option, the wood can be chemically enhanced, but it will become less reusable and sustainable.

To investigate the relation between the stiffness of the superstructure and the differential settlements, different wall systems can be used. CLT panels can be used as elements that increase the stiffness of the wall by a large amount, while timber framed elements with OSB panels increase the stiffness by a smaller amount. The use of CLT panels comes at the cost of an increase of the self weight of the structure and the use of more material, making the structure more expensive.

Mechanisms such as rocking between the modular panels should be avoided. The stresses created by rocking will be redistributed entirely by the connections, increasing their dimension and therefore the materials needed for a proper design.

4

Case study

With the literature on settlement and timber constructions, a case study can be formed around the research questions given in the introduction. For this, multiple decisions have to be made on the properties used in the case study.

- A suitable location has to be chosen, that represents the aim for this construction typology.
- A choice must be made on the type of foundation piles.
- A superstructure or multiple superstructures must be chosen, that allows the investigation of the impact of stiffness on the differential settlement of a structure.
- Differentiations must be applied to the standard model that investigate varies causes of differential settlement.

This chapter will list these considerations taken into account for designing the case study and give the considered soil profile, pile foundation, elements of the wall system, and model differentiations.

4.1. Location of choice

As seen in Figure 2.1 there is a large variety of soil types in the Netherlands. In the eastern part, the thickness of weak soil layers is mostly 2 meters or less. For a research based on settlements, these parts are not interesting. The low compressibility of sand will make the deformations negligible and a light weight structure is assumed to not be influenced by differential settlement.

In the western part, large amount of compressible soil is present. To investigate of the design is suitable for this part of the Netherlands, two locations will be researched. These locations will be picked with the following aspects in mind.

- The placement of the helix should be in a soil layer that is not peat. This soil has the worst stiffness of the possible soil layers and will not be able to provide enough stiffness for reasonable vertical forces;
- The location should be picked conform the design philosophy. This means that the locations like grasslands will be considered and not locations the building won't end up anyway;
- The locations should be distinctive and differ in the thickness of compressible layers. This way the influence of the soil layers can be researched;
- Multiple boreholes should be available at each location. This way differential settlement due to varying soil composition can be investigated.

With all these considerations in mind, the location of choice is positioned in a grassland between Delft and Rotterdam near the "Oude Leedenweg". This location contains large layers of weak soil that is a mixture of sea clay and peat, see Figure 2.1. Its placement is in an area where there is a demand for more houses and with the university being nearby, a suitable location for smaller houses like student homes. A CPT test of the chosen location can be found in Appendix A.

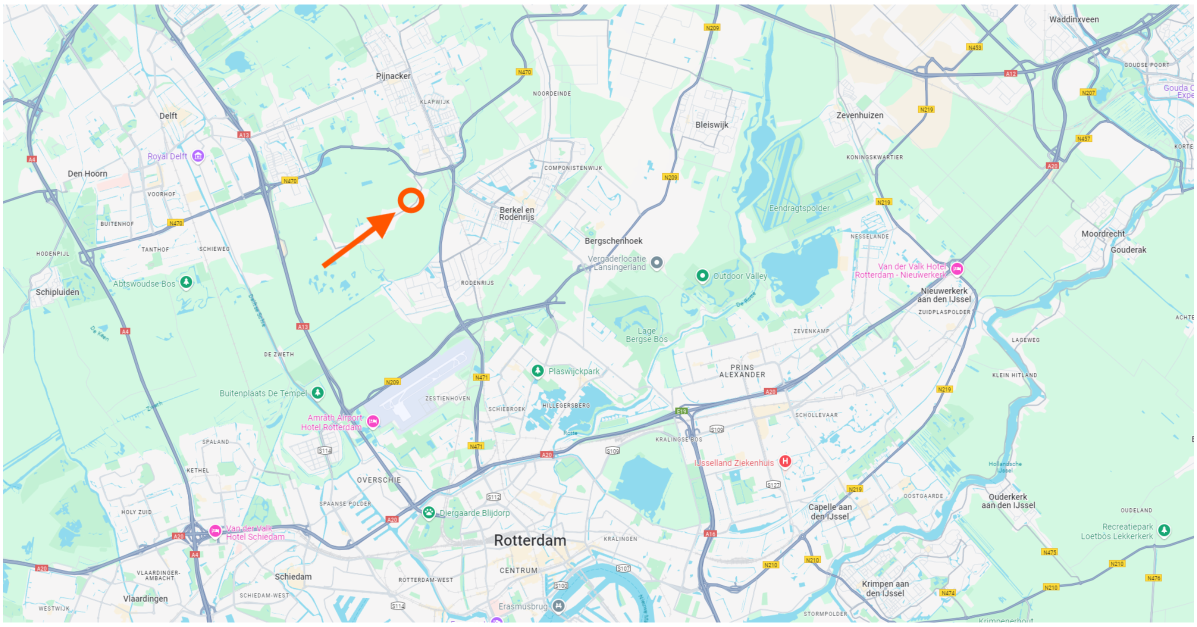

Figure 4.1: Location of choice in google maps

An estimation of the type of soil can be determined by looking at height of the friction ratio and cone-resistance at each depth. Appendix A goes into more detail on the exact method used.

This results in the soil profile shown in Table 4.1.

Table 4.1: Soil profile Oude Leedenweg

Top Layer (m)	Bottom Layer (m)	Soil Type
0.0	-0.5	Peat weak
-0.5	-0.6	Clay weak mod
-0.6	-1.8	Peat mod
-1.8	-5.0	Clay sandy mod
-5.0	-10.6	Clay clean mod
-10.6	-11.3	Peat mod
-11.3	-12.2	Clay clean weak
-12.2	-12.7	Clay sandy mod
-12.7	-16.0	Sand clean mod

The groundwater level will be assumed to be at 4.6 meters underneath NAP. This value is estimated by available information in Dinoloket. From the database the Groundwater level graph of a nearby location is obtained and after 2004 the groundwater has exceeded -4.6 m NAP once, see Figure A.4. With ground level being at -4 m NAP, the phreatic level in the model will be at -0.6.

Each soil type has its own properties. The properties used in this section are given in Table 5.3. In the model calculations more properties will be added. The values are based on the NEN 9997-1 Table 2b, which is put in the Appendix A.

4.2. Pile of choice

The foundation pile used in this research will be a screwed, steel, helical pile with a helical plate at the bottom that provides a surface area. The pile should fulfil the following aspects:

- The pile should have a sufficient bearing capacity for the possible loads applied on top;
- The pile should be able to be placed and reobtained without the use of heavy machinery. This means that the pile cannot be too large, since the larger the pile is, the more torsional resistance it has during installation;
- The dimensions of the pile have to be realistic and based on literature;
- The distance between the centres of the helical piles has to be at least two times the diameter of the helical plate ($2D$).

The choice for the depth helical plate of the piles will be $3m$ underneath the ground surface. This depth obtains the goals of this research to position the foundation in soil that is less deep than the sand and being able to retrieve the piles after the lifetime of the structure has expired. The piles bypass the peat layers that have little to no bearing capacity and reaches a clay layer. Clay soil, due to its higher density compared to peat soil, plays a more substantial role in increasing the effective stress. Consequently, the 1.2 m layer of sandy clay above the helical plate is crucial in reducing settlement. In the calculations, it is assume that the helical plate is flat and not curved. The influence of this shape is not within the scope of this research. The properties of a standard pile are:

$Unitweight$	$78,5kN/m^3$;
E_{ref}	$2,0 * 10^5 N/mm^2$;
d	$0,1m$;
D	$0,6m$.

The values used are based on the parameters used in the research done at Jackson State University (Shuman et al., 2022) and on hand calculations on the maximum bearing capacity. The maximum applied load on a pile in an ultimate limit state is expected to not exceed a value of $50kN$ with a minimum spacing between the piles of $2D$. In Appendix D a hand calculation of the bearing capacity of the helical pile is found. In the Appendix, it is shown that the helical pile has a higher bearing capacity than needed, but that the diameter of 600 mm is chosen to account for the uncertainty in soil capacity and to minimize the settlements.

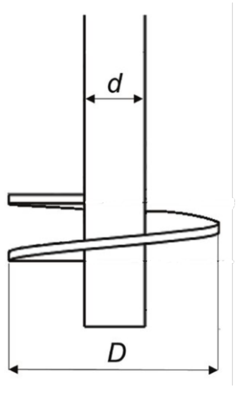

Figure 4.2: Schematisation of the diameters

4.3. Super structure choice

In Figure 4.3 the preliminary design of the building is shown. The first thing to note is that the building consists of multiple floors stacked on top of each other. In this research, the amount of floors will be reduced to 2 floors, which is more reasonable for this case study where the loads should be reduced to a minimum. A schematization of the structural model is shown in Figure 4.4.

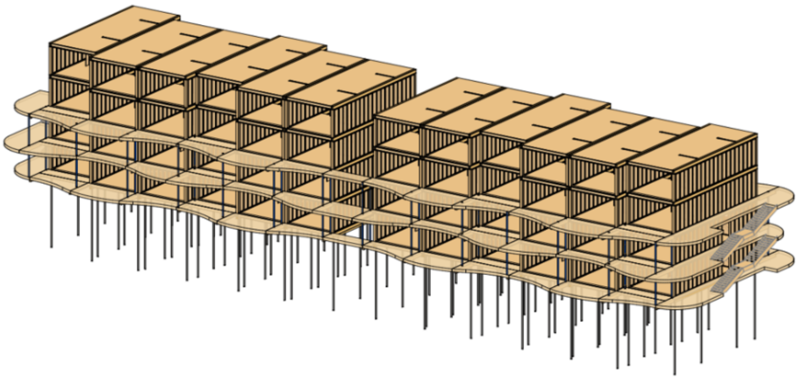

Figure 4.3: Preliminary design

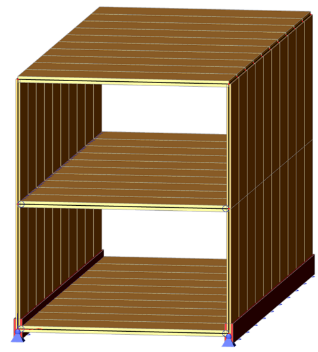

Figure 4.4: Schematization of the structural model

4.3.1. Structural elements

The structural model is divided in several elements: The supports, a continuous beam, the walls and the floor slabs.

The supports
The supports underneath the walls consist of the earlier chosen helical piles. They will be implemented as spring supports that represent the settlements of the piles. This will be further explained in the Section Methodology 5.1.2.

Continuous beam
On top of the supports a continuous beam is placed. This continuous beam will help with redistributing the loads of the structure and work as a connection point between the piles, floor and walls.

Walls
Positioned above the continuous beam are the wall elements. Three different variations are researched: no stability wall, a timber framed wall with OSB plates and a CLT wall. Each wall has its own purpose in this research:

- The continuous beam without a stability wall will investigate the possibility of relying fully on a single construction element. This can be beneficial since the only connections that should be taken into account, are the connection to the foundation piles.
- A timber framed wall represents a stability wall that is cheaper, easier to build, less heavy. The frame itself will not help redistributing the forces, however the attached OSB panel will.
- The CLT wall investigates the settlements underneath a stiff wall, minimising the relative rotations between piles. The wall typology is however more costly and heavier than the timber frame wall.

These variations will give inside on the influence of stiffness of the superstructure on the feasibility of the system.

Floor
The floor elements will not be researched in this thesis, but their self weight and the surface loads

applied to them, must be taken into account. A CLT floor with 5 layers is chosen, because of its slenderness and simplicity.

Until this point three variations have been made. These will be characterized as Calculation A, Calculation B and Calculation C. With the standard loading scheme discussed in the upcoming Section 4.3.3, the first calculations in this research can be summarized with the flowchart given in Figure 4.5.

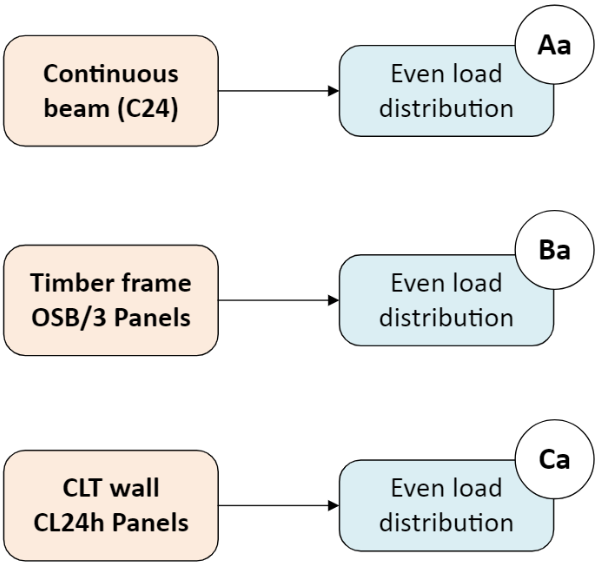

Figure 4.5: Flowchart of the first calculations

4.3.2. Simplifications

For this research, recreating a building complex is ambitious for the given time frame. Therefore, one wall location will be zoomed in on. This simplifies the calculation from a 3D to 2D. Furthermore, only one wall will be investigated. In reality, there are two walls positioned on top of the continuous beam, but to simplify the model, only one is used in the calculations, see Figure 4.6.

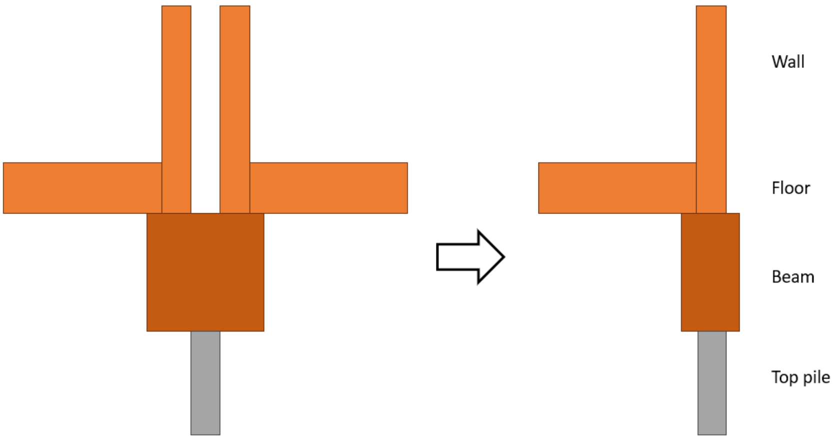

Figure 4.6: Sketch of the cross section above the pile, *left* how it is supposed to be, *right* how its simplified in the model

Keep in mind that this also halves the loads applied on the foundation. However, the last simplification increases the load on a single pile. Instead of all eleven piles being positioned underneath the continuous beam distance of 1,2 m from one another, only 6 piles will be modelled. This simplification will decrease the computation time, while still providing information on the behaviour of the structure supported by multiple helical piles. Figure 4.7 gives a schematisation of the simplification. Note that the removed piles in the structural model are still taken into account in the calculations for the soil settlement.

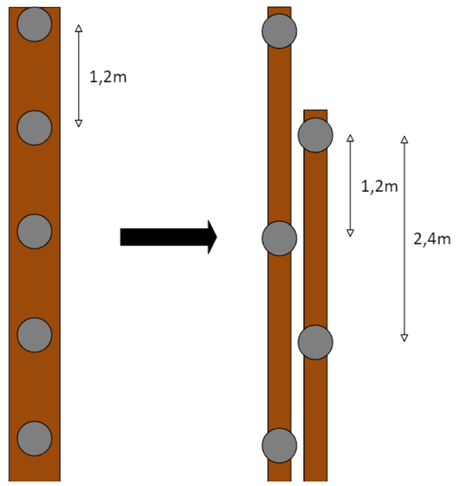

Figure 4.7: Schematisation of the assumed pile placement

4.3.3. Load combinations

The vertical loads applied on the structure are determined by the NEN 1990 and 1991. The loads in the 2D plain have to represent the loads that are present in a 3D model. For the 3D structure the loads that would be applicable are:

The permanent load (G):

- *Self weight*: The weight of the structural elements itself.
- *Weight of the finishing layer at the floors*: 0,2 kN/m^2

The variable load (Q):

- *Living loads*: 1,5 to 2,0 kN/m^2
- *Snow load*: 0,56 kN/m^2

(Nederlands Normalisatie-instituut, 2019b)

Two different load combinations are relevant for this research. The Ultimate Limit State (ULS) is used to determine if the maximum bearing capacity of a foundation pile. The ULS calculation the combinations factors shown in Table 4.2.

Table 4.2: Load combinations for the ULS (Nederlands Normalisatie-instituut, 2019a)

Design Situations	Permanent Load	Dominant Variable Load	Other Variable Loads
(by 6.10a)	$1.35 \cdot G_{Kj,sup}$	$1.5 \cdot \psi_{0;i} Q_{j,1}$	$1.5 \cdot \psi_{0;i} Q_{j,i}$
(by. 6.10b)	$1.20 \cdot G_{Kj,sup}$	$1.5 \cdot Q_{k,1}$	$1.5 \cdot \psi_{0;i} Q_{j,i}$

The Ultimate Limit State capacity will have higher values of load compared to the loads applied over a longer period of time. The latter being relevant for the settlement calculations. The factors for Quasi-permanent loads are used in combination with the Service Limit State (SLS) for these calculations. These loads do fluctuate but are assumed to be present most of the time.

Table 4.3: Load combinations for the SLS(Nederlands Normalisatie-instituut, 2019a)

Design Situations	Permanent Load	Dominant Variable Load	Other Variable Loads
SLS	$1.0 \cdot G_{Kj,sup}$	$1.0 \cdot \psi_{0;i}Q_{j,1}$	$1.0 \cdot \psi_{0;i}Q_{j,i}$

The factor $\psi_{0;i}$ will become a value of 0.3 that is then multiplied by a variable load of 1,5 kN/m^2. This represents the loads besides the self weight of the construction, for instance the furniture in the building. In this calculation the loads on the roof of the building are not taken into account.

4.3.4. Model variation: Lower strength outer piles

The research is focused on 3 wall variants. With the calculations described in the last paragraphs, the structure can be research on normal conditions. One of the criteria of the design is that the relative rotations (β) are within the boundaries of the Eurocode. Looking at the settlement of the structure, this value is mostly dependent on the difference between the outer piles and the pile next to them, see Figure 4.8.

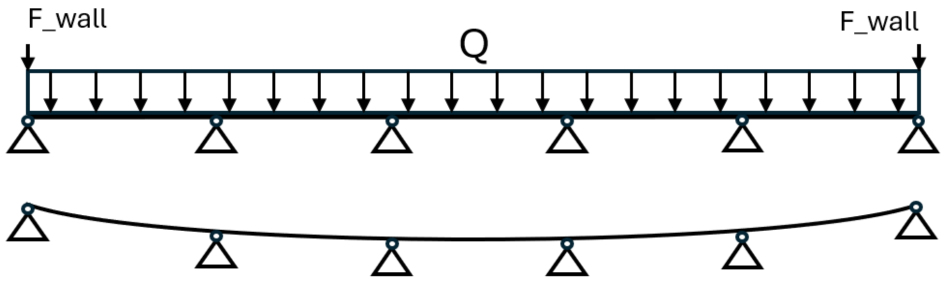

Figure 4.8: Schematisation of the settlement for normal system

To make the validity of the structure less dependent on the settlement of the outer pile, a pile with lesser strength can be used. This will make overall capacity of the building less, but decreases the dependence on the relative rotations. This is especially significant for walls with a lesser stiffness.

To research the impact of using piles with lesser strength, a pile is used with a smaller diameter for the helical plate. The reduction of the amount of steel used is minimal, but this method can also reduce the amount of wood that is needed.

$Unitweight$	$78,5kN/m^3$;
E_{ref}	$2,1 * 10^5 N/mm^2$;
d	$0,1m$;
D	$0,5m$.

In addition to the potential benefits, this modification researches the impact of the outer piles underperforming. A pile at this position is the most susceptible to being influenced by increased loads in the surroundings. This modification will give more inside on the performance of the structure imposed to large differential settlement.

4.3.5. Model variation: Uneven loading

In the most ideal situation, the load is equally distributed over the whole surface area of the building. This will most likely not be the case and therefore a sensitivity analysis will be run on the different wall systems.

In the analysis there will be looked at the impact of a constant increase in load at one side of the building impacts the stability. The variable load is increased from 1,5 kN/m^2 to 2,0 kN/m^2.

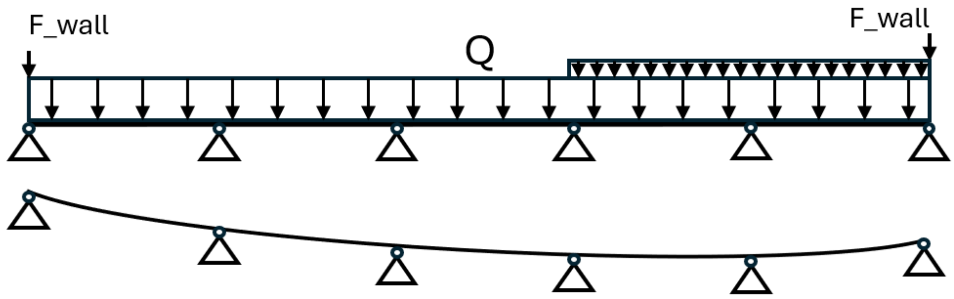

Figure 4.9: Schematisation of the settlement with uneven loading

This variant investigates what happens to the construction when it is imposed to tilting by differential settlement. The calculations will also be done for the variations with less stiff outer foundation piles.

4.3.6. Boundary conditions

To determine the dimensions of each calculation the values for Relative rotation (β) and tilt (ω) found in Section 2.4 cannot be exceeded with a unity check (U.C.) of 0,8 at the first time step (T0). The same applies for the maximum allowable stress (σ).

Throughout the calculation process, the displacement and reaction force of the supports will be measured. However, the stresses within the structural elements will be measured at the timestep with the largest differential displacements. This timestep is expected to generate the most stress.

4.4. Summary

In this research the different wall systems that will be investigated are a continuous beam, a beam with on top a timber frame including OSB panels, and a beam with CLT panels on top. The dimensions of each wall system adjusted until they fulfil the requirements for Relative rotation (β), tilt (ω) and maximum allowable stress (σ) at $T0$ with a U.C. less than $0,8$ at time step T0.

The impact of using outer piles with less strength and the impact of uneven loading will be investigated for each wall system as well. A flowchart of the calculations can be seen in Figure 4.10 with the matching mechanical schemes in Figure 4.11.

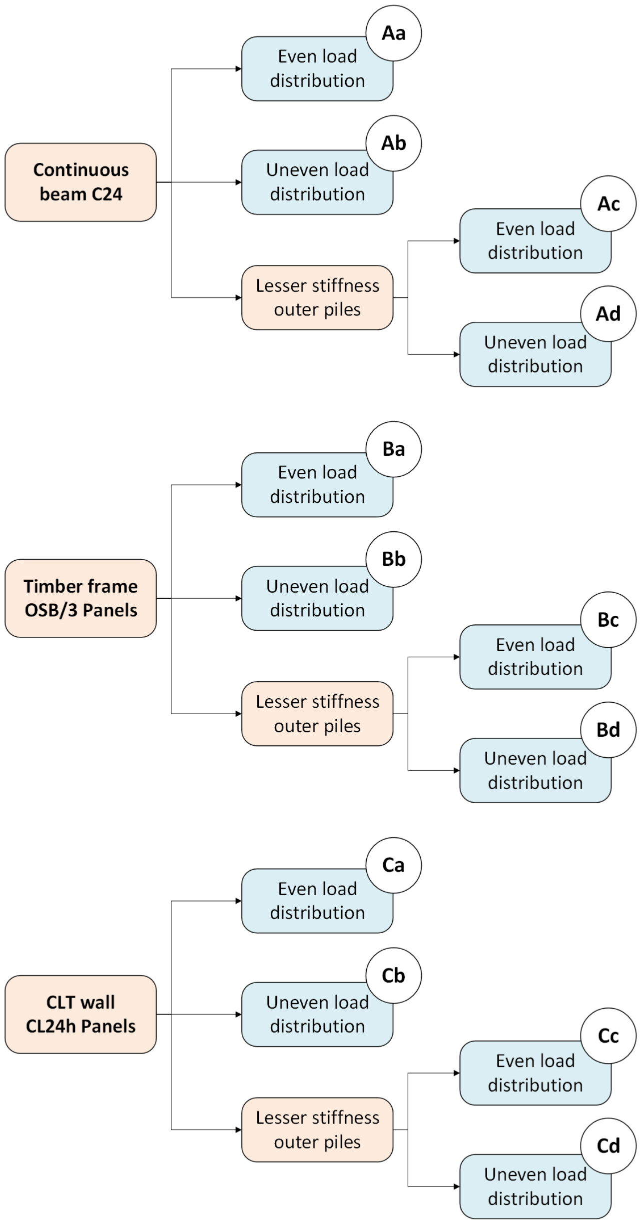

Figure 4.10: Flowchart of the calculations done in this research

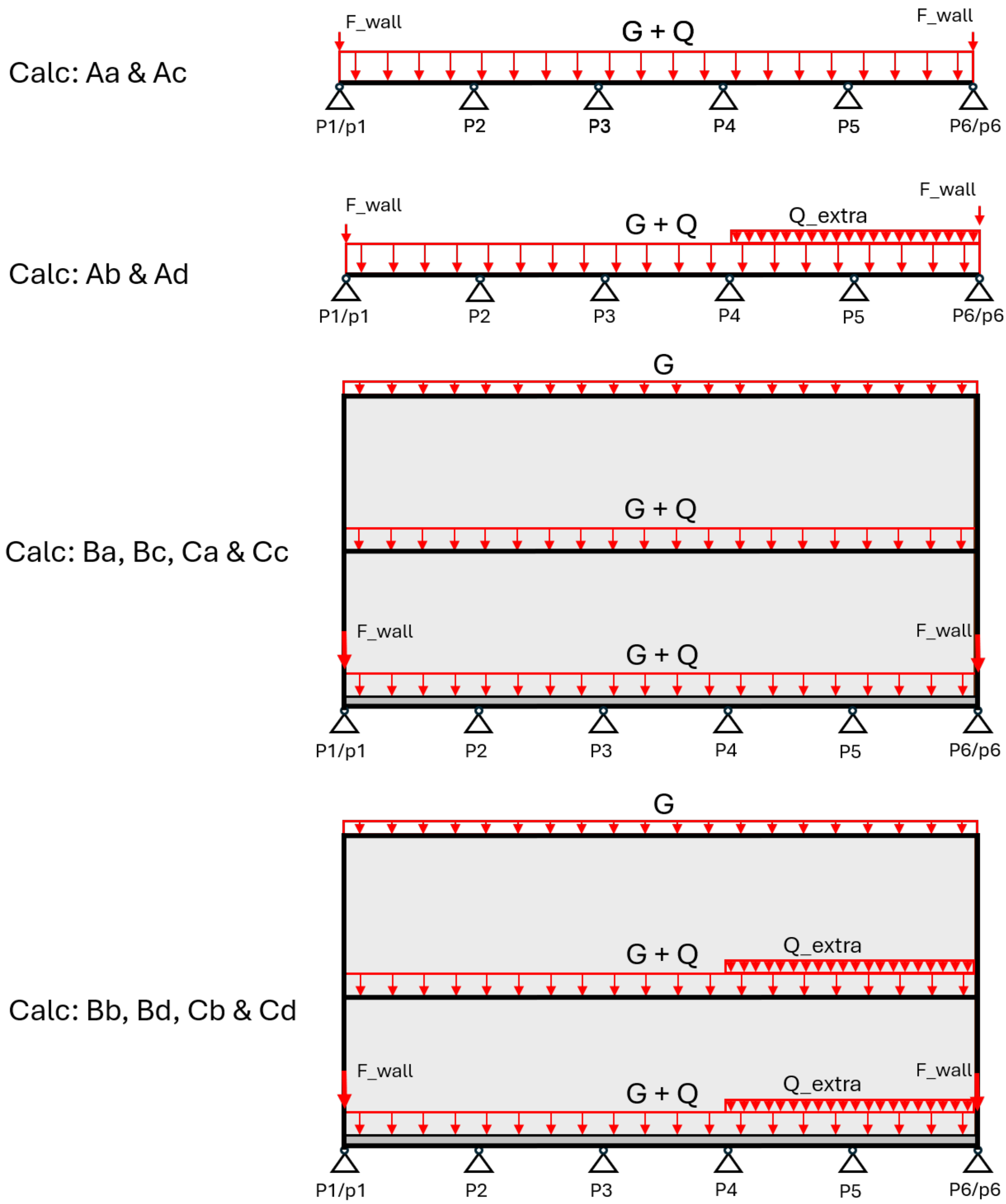

Figure 4.11: Overview calculations case study

5
Model

This chapter outlines the model setup for the case study. It begins by introducing the chosen software used for calculating settlement and structural performance, detailing how they are integrated to analyse the long-term effects of settlement. Athe chapter describes the foundation pile model in PLAXIS 2D and the timber structure in SCIA Engineer, explaining their configurations. The used properties will be given, along with a discussion of the assumptions and simplifications made in the modelling process.

5.1. Calculation set up

With the boundary conditions of this case study determined, the model can be constructed. This will be done with two different Finite Element (FEM) software: PLAXIS 2D and SCIA Engineer. The results from one application will be used in the other by following several steps.

5.1.1. Choice of calculation software

Due to the nature of this project, software has to be chosen that can investigate the long term settlement of a structure on soft soil, and the response of timber structural elements. To achieve both, there is chosen to use two different programs: PLAXIS 2D and SCIA Engineer.

PLAXIS is a finite element software widely used in geotechnical engineering. It allows researchers to investigate the behaviour of soil, structural elements and their interactions. A singular pile can be modelled in PLAXIS 2D to investigate its behaviour in soft soil. The software takes into account all three types of settlement discussed in Section 2.2. The downside of the software is that it does not provide a solution for a 3D structure and only simple structural elements can be modelled. For the latter, SCIA Engineer is used.

In SCIA Engineer the 2D wall system of the structure will be modelled. The program will look at the consequences of the settlement on the structure. SCIA is able to implement the helical piles in soft soil as non-linear spring supports, to simulate the displacement displacement of the foundation at different stages in time. In the end the model will provide information on the internal forces, bending moments, stresses and displacements.

5.1.2. Methodology of the case study

In this section, each step of the calculation process will be explained. The calculation will start with the foundation elements. The results in the settlement calculations will be used as input in the structural model, which in turn will give information on the support reactions back to PLAXIS. This will iterate for a four time steps to predict the behaviour over of the long term settlement. Each step is described in more detail in this section. Figure 5.1 schematizes the workflow. In Appendix E.1 a fully worked out calculation is given as an example.

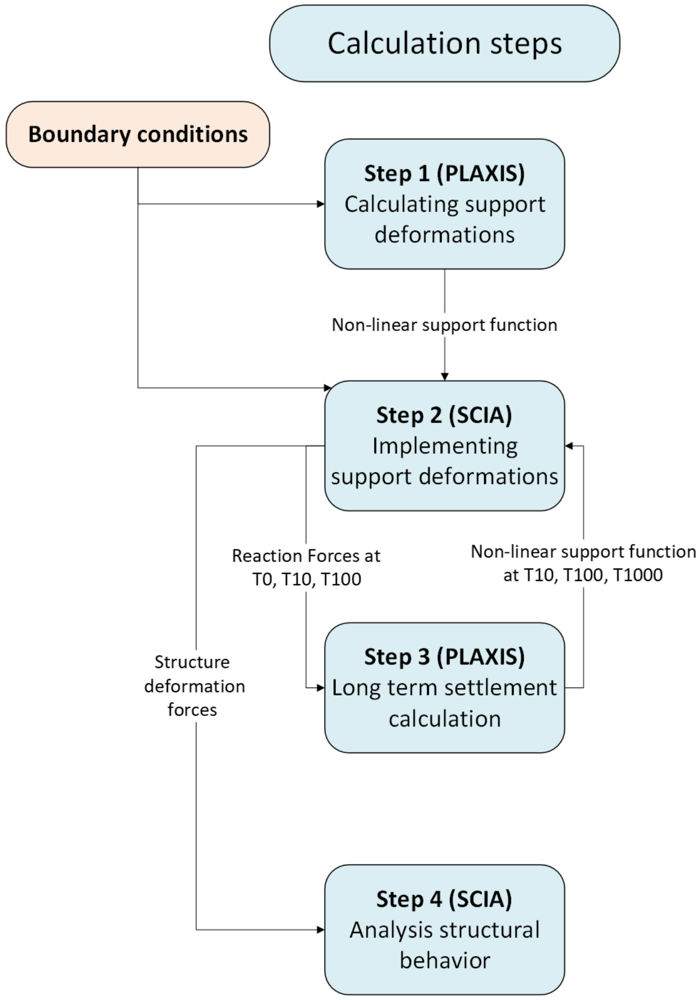

Figure 5.1: Flowchart of the calculation steps within the case study

Step 1: Calculating the support deformations at T0

A helical pile will be modelled in PLAXIS 2D with the parameters of the corresponding calculation as illustrated in Chapter 4. The chosen soil profile is constructed and a helical pile is implemented. Different forces between the 5 and 35 kN are applied on top of the pile to investigate the settlement response of the pile. The forces will increase from $F = 0$ at day 0 until the input force $F = F_{input}$ is reached at day 30. Day 30 represents the end of the construction phase and will be referred to in this research as T0 (day 0 after construction). The process is schematised in Figures 5.2 and 5.3. The obtained information can now be used as input for SCIA engineer.

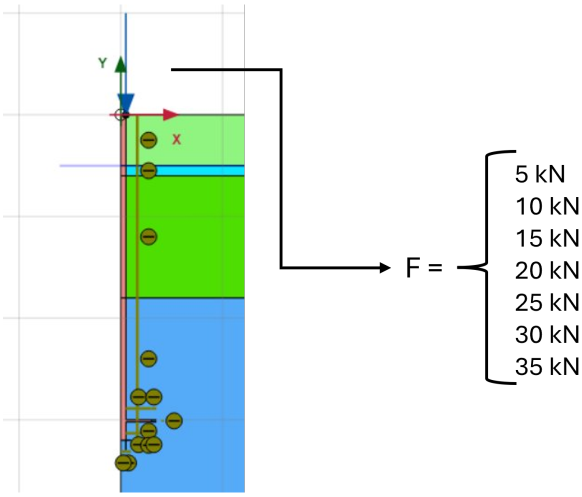

Figure 5.2: Pile model in PLAXIS 2D with the different applied forces on top

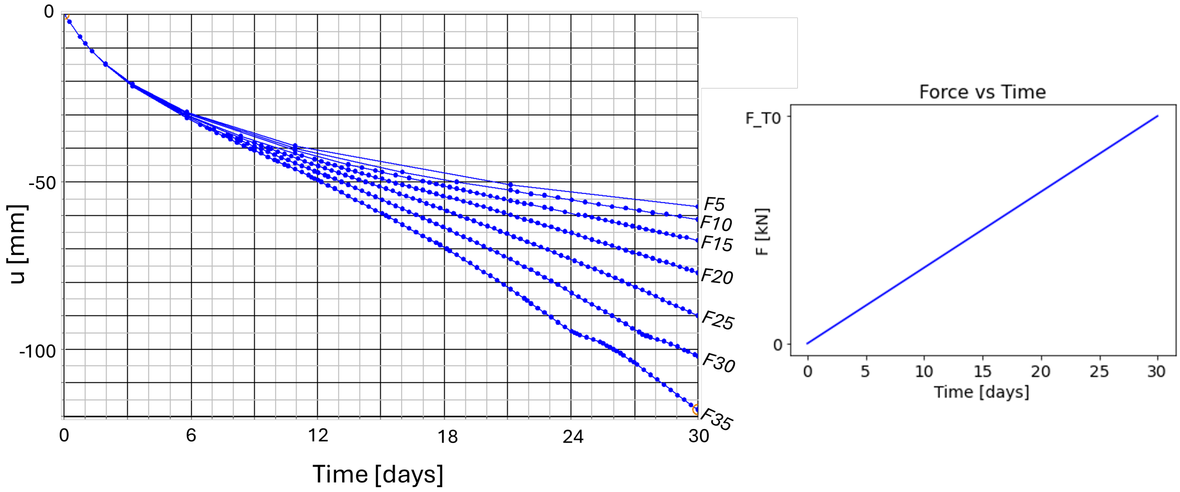

Figure 5.3: Pile displacement over time for different applied forces (left), Force input (right)

The settlement of an individual pile is now obtained. It should now be converted to a model capable of investigating the response of the whole superstructure.

Step 2: Implementing the deformations in SCIA Engineer
In SCIA Engineer, the construction is modelled. In this model, the supports underneath the structure need to represent the deformations of a helical pile obtained from PLAXIS.

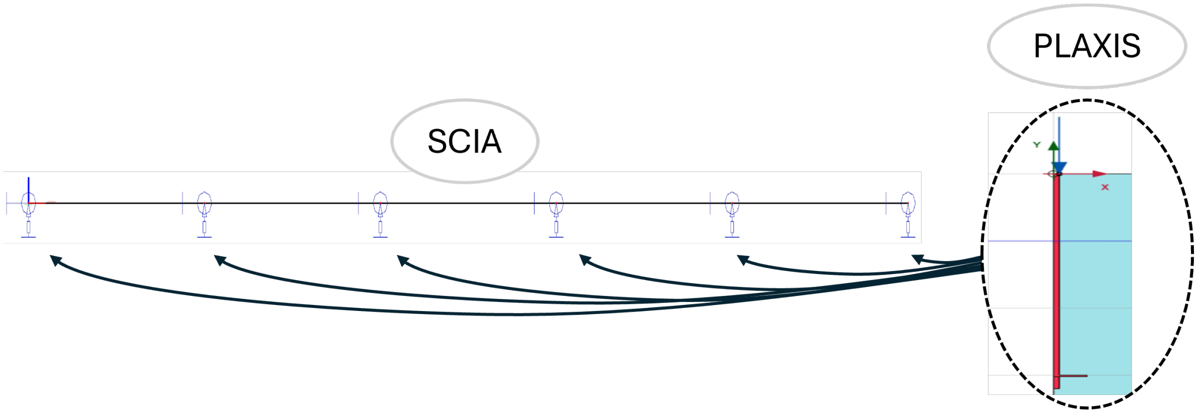

Figure 5.4: Pile model in PLAXIS translated to spring support in SCIA Engineer.

The calculated deformations from step 1 are translated to a non-linear, displacement-force function in SCIA. This function makes sure that support reaction after the calculation, meets the level of settlement that corresponds with that force. The deformation of each support will than be calculated iteratively by the software and end up at an equilibrium where the final value for the displacement and support reactions can be obtained. Figure 5.5 shows the translation of the deformations from PLAXIS to SCIA.

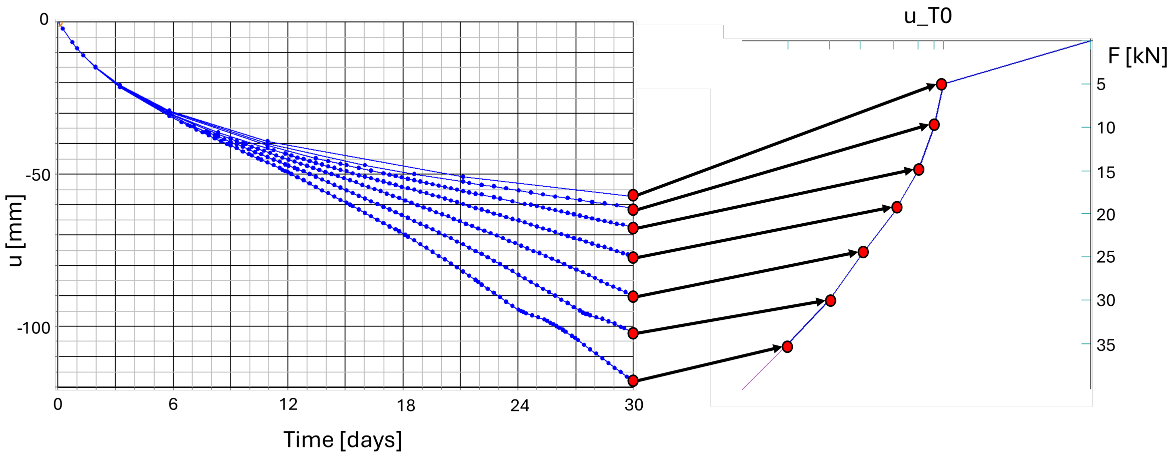

Figure 5.5: Translation of settlement at T0 (30 days after the start of construction) to a non-linear spring support

The newly obtained function represents the settlement of an individual pile at T0. However, neighbouring piles will also have an impact on the settlement. The stress applied to the soil spreads out and leads to settlements for the surrounding soil, see Section **??**. The degree in which the settlement of each pile is influenced by others depends on the position and the height of the load. A pile that is positioned in the middle of a group, has more closely positioned piles than a pile at the border and will be influenced more. The calculated values are worked out in Appendix C, where calculations for the group effect are presented for various forces at different stages over time.

The results of this calculation can be used to add displacements to earlier found load-deformation function in SCIA. For calculations A and C, the expected reaction forces are between 20 kN and 25 kN. The additional settlement will therefore be based on the group effect of piles loaded with 25 kN. This assumption leads to more differential settlement and impacts the results therefore more negatively. The additional settlement is 1,6 mm for the outer piles and 3,2 mm for the inner piles at T0. For calculation B, the expected reaction forces will be between 15 kN and 20 kN. Here, the additional settlement is 1,3 mm for the outer piles and 2,6 mm for the inner piles at T0.

The values for the additional settlement are added to the calculated deformations from PLAXIS, resulting in a shift in the non-linear function. This is illustrated in Figure 5.6.

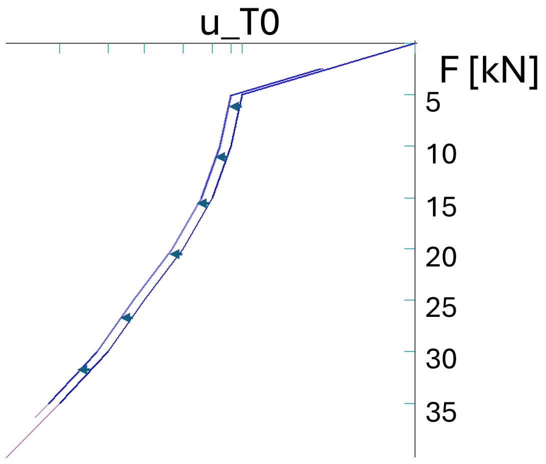

Figure 5.6: Group effect on a load-deformation graph, illustration

The non-linear functions used for the calculations at T0 in calculation $A\alpha$ is shown in Figure 5.7 as an illustration.

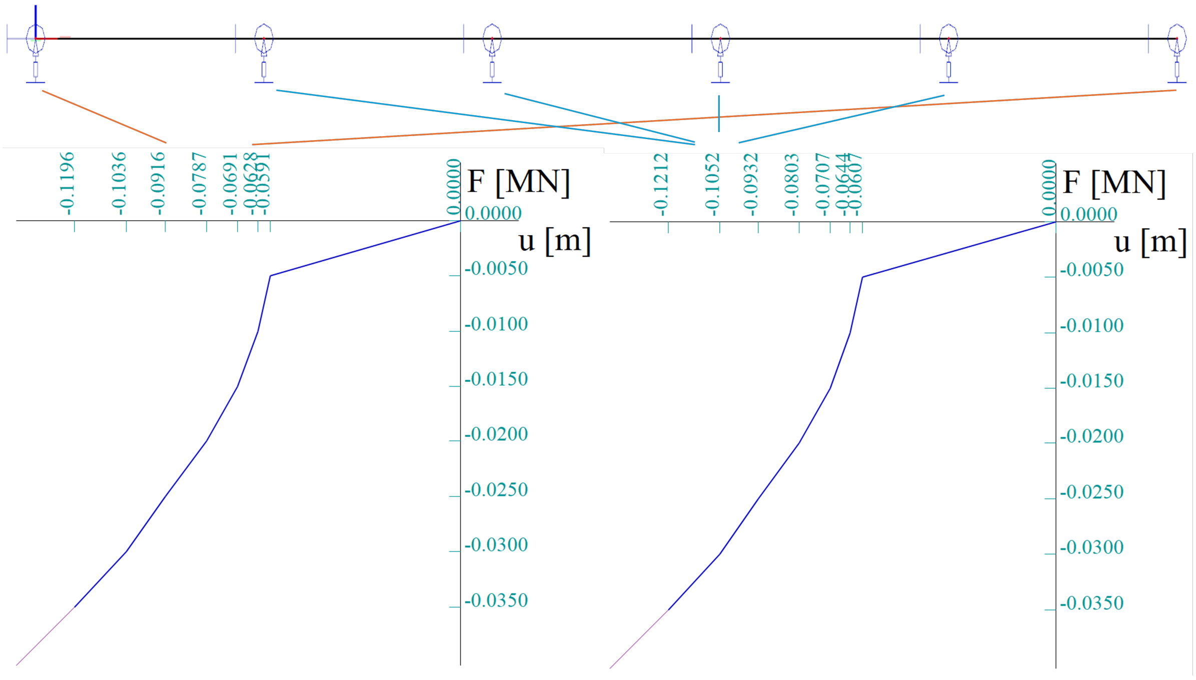

Figure 5.7: Support functions for the outer supports (left) and Inner supports (right)

The final load-deformation values for the non-linear supports are given in Table 5.1 and 5.2.

Table 5.1: Load-deformation values for piles including the group effect for non-linear supports in calculation A and C at T0

Applied Force at T0 [kN]	**F5**	**F10**	**F15**	**F20**	**F25**	**F30**	**F35**
(u_{T0}) D600 inner piles [mm]	-59.1	-62.8	-69.1	-78.7	-91.6	-103.6	-119.6
(u_{T0}) D600 outer piles [mm]	-60.7	-64.4	-70.7	-80.3	-93.2	-105.2	-121.2
(u_{T0}) D500 outer piles [mm]	-60.1	-67.0	-80.3	-97.2	-118.0	-140.2	-162.9

Table 5.2: Load-deformation values for piles including the group effect for non-linear supports in calculation B at T0

Applied Force at T0 [kN]	**F5**	**F10**	**F15**	**F20**	**F25**	**F30**	**F35**
(u_{T0}) D600 inner piles [mm]	-58.8	-62.5	-68.8	-78.4	-91.3	-103.3	-119.3
(u_{T0}) D600 outer piles [mm]	-60.1	-63.8	-70.1	-79.7	-92.6	-104.6	-120.6
(u_{T0}) D500 outer piles [mm]	-59.8	-66.7	-80.0	-96.9	-117.7	-139.9	-162.6

With the supports modelled, the load on top of each support can be calculated with a non-linear calculation. From this calculation the deformations, support reactions and stresses in the construction at T0 can be obtained.

Step 3: Long term settlement calculations
Now that the support reactions are determined at T0, they can be used for calculating the long term settlement. This will be done with the following method:

The support settlement of each pile will be run for a second time between 0 and 30 days, so until T0, but with the obtained support reaction in step 2. This will simulate the estimated settlement for that time period. Afterwards, the next 10 days for the pile will be simulated. This has to be done for multiple forces to create a range in the function that represents the settlement correctly. If only one force is ran, the function would become linear and would not be accurate.

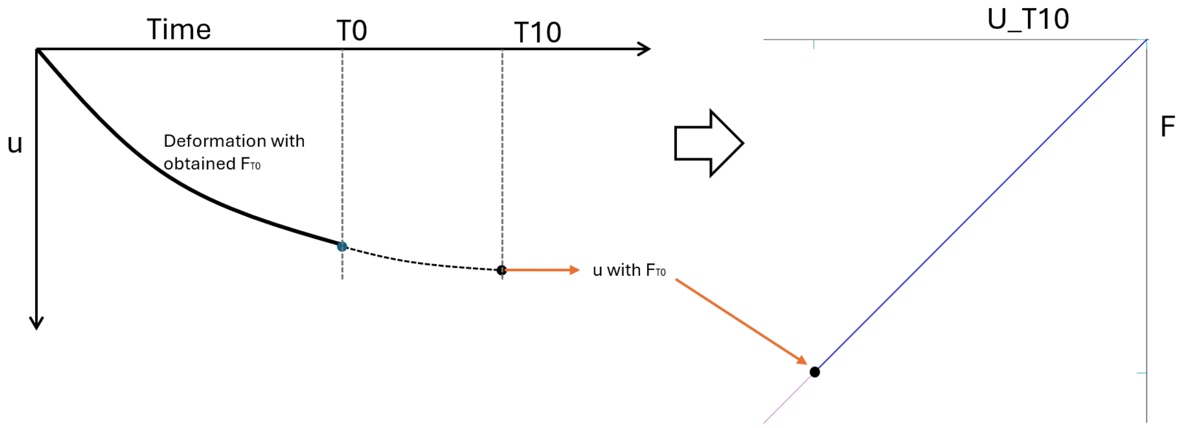

Figure 5.8: Illustration for settlement calculation of 1 pile at T10 with only the earlier obtained F_{T0} (Incorrect)

This will be done by running the simulation with three different loads on top of the pile: $0.9F_{T0}$, F_{T0}, and $1.1F_{T0}$ (10% less load, the obtained load, and 10% more load). The load at T10 is assumed to be within this load region and the results are only accurate if this is the case. The three different forces are chosen to create a new non-linear function with a region that accurately represents each foundation pile and their settlement history.

The newly obtained settlement for each pile can be implemented in SCIA as a new non-linear function. The additional settlements caused by neighbouring piles are added and each pile has their own load deformation function based on position and previous settlement.

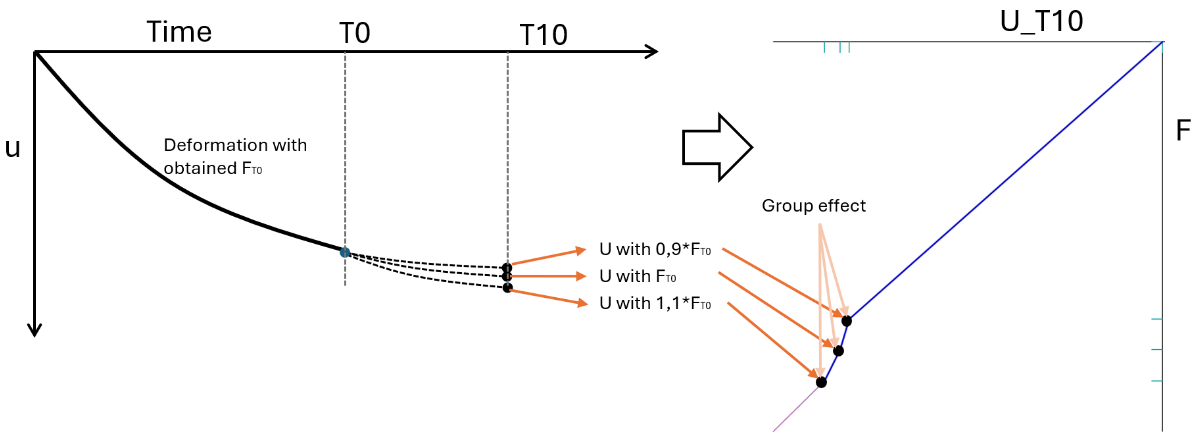

Figure 5.9: Illustration for settlement calculation of 1 pile at T10 (correct)

With a new non-linear calculation the deformations, support reactions and stresses at T10 can be obtained. This process will be repeated iteratively, so the life time of each pile is reconstructed with the new force obtained at T10 and the process will be repeated for the next 90 days. In the end, results on support reactions and displacements are obtained at T0 (immediately after the construction of the building is finished), T10 (10 days after construction), T100 (100 days after construction), and T1000 (1000 days after construction).

Step 4: Structural analysis
After each calculation, the wall construction can be analysed with respect to internal stresses (σ), deformations (ΔU), relative rotation (β) and tilt (ω), see Chapter 4, at the time steps T0, T10, T100, and T1000. This will give intel on how the structure behaves over time and if the values for these boundary conditions drastically change. With the knowledge of how the structure behaves on long term settlement, a conclusion can be drawn on the feasibility of each wall system for a modular, lightweight structure that is expected to have large amount settlement.

Due to the set up of this calculation method, some assumptions have to be made. The next sections will discuss the input of each software and what the simplifications are in the model set up.

5.2. PLAXIS

The PLAXIS 2D model is split into different sections. First, the input of the soil will be explored. The location used in this project will be discussed and the input properties of the soil are researched. The next section discusses the model type with the structural set up used to accurately simulate a helical pile. Then the mesh size is chosen and the different structural improvements that will be used, are discussed.

5.2.1. Soil conditions

In Chapter 4.1 the boundary conditions of the location are given. The result can be seen in Figure 5.10.

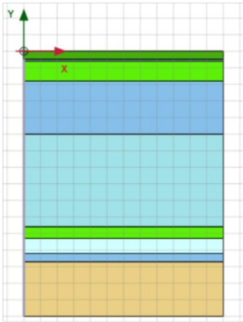

Top Layer (m)	Bottom Layer (m)	Soil Type
0.0	-0.5	Peat weak
-0.5	-0.6	Clay weak mod
-0.6	-1.8	Peat mod
-1.8	-5.0	Clay sandy mod
-5.0	-10.6	Clay clean mod
-10.6	-11.3	Peat mod
-11.3	-12.2	Clay clean weak
-12.2	-12.7	Clay sandy mod
-12.7	-16.0	Sand clean mod

Figure 5.10: Soil profile Oude Leedeweg

Each soil type has its own properties. These properties will be implemented in PLAXIS 2D to accurately simulate the pile settlement. In the table 5.3 below all the parameters used, are given. These are based on the values given in the NEN 9997-1 Table 2b which is put in the Appendix A.

Soil	γ'_{unsat} $[kN/m^3]$	γ'_{sat} $[kN/m^3]$	E_{ref} $[MPa]$	ν	c'_{ref} $[kPa]$	ϕ $[Degrees]$	ψ	C_c	C_s	C_α
Sand clean mod	18	20	45	0.3	0	32.5	0	-	-	-
Clay clean weak	14	14	1	0.3	0	17.5	0	0.493	0.049	0.013
Clay clean mod	17	17	2	0.3	5	17.5	0	0.230	0.023	0.006
Clay sandy mod	18	18	3	0.3	5	22.5	0	0.173	0.017	0.004
Peat weak	11	11	0.3	0.3	1.5	15	0	0.691	0.069	0.023
Peat mod	12	12	0.5	0.3	2.5	15	0	0.461	0.046	0.015

Table 5.3: Soil properties for the used ground profiles.

Where:

γ'_{unsat}	Volumetric weight of unsaturated soil;
γ'_{sat}	Volumetric weight of saturated soil;
E_{ref}	Elasticity modulus of the soil;
ν	Poisson's ratio;
c'_{ref}	Effective cohesion;
ϕ	Effective angle of internal friction;
Ψ	Suction;
C_c	Primary compression index;
C_s	Secondary compression coefficient for stresses below the upper stress limit;
C_α	Secondary compression index.

For this research, the time-dependent settlements of compressible soils will be investigated. To capture a realistic behaviour of the soil, the layers will be constructed in a soft soil creep model. This will take into account the immediate, primary and secondary settlement of the structure, which other models lack.

5.2.2. Implications soil set up

Homogeneous soil profile

For this research the soil at each location of the foundation pile is assumed to the same. This might not be a good reflection of the reality since changes in layer thickness can also change the settlement curve of the pile. Because the location has large layers of weak soil, it is assumed that small changes in thickness that can occur over a distance of 12 meter, are not substantial enough to influence the outcome of the calculation drastically.

Soft soil creep

The way the secondary settlement is implemented in a soft soil creep model, is dependent on the effective stress and not the increase in effective stress. Wherefor, the soil will settle without additional loading. This does not match the earlier found behaviour of secondary settlement given in table 2.8 and 2.9, where the deformations become 0 without an increase in stress.

To avoid unrealistic creep strain rates, it is recommended the PLAXIS material manual to the set initial OCR higher than 1.0, typically around 1.2-1.4, making the material lightly overconsolidated. This adjustment changes the pre-consolidation pressure and decreases the consolidation settlement at the start.

However, the higher OCR also impacts the trajectory of the settlement curve over time. After the primary consolidation period has ended, the expected trajectory of the settlement is linear on a logarithmic scale. The pile settlement is tested in a large clay layer with 2 different values of the OCR: 1 and $1,4$. The difference in settlement rate can be observed and a decrease in settlement over 10000 days of more than 50 percent.

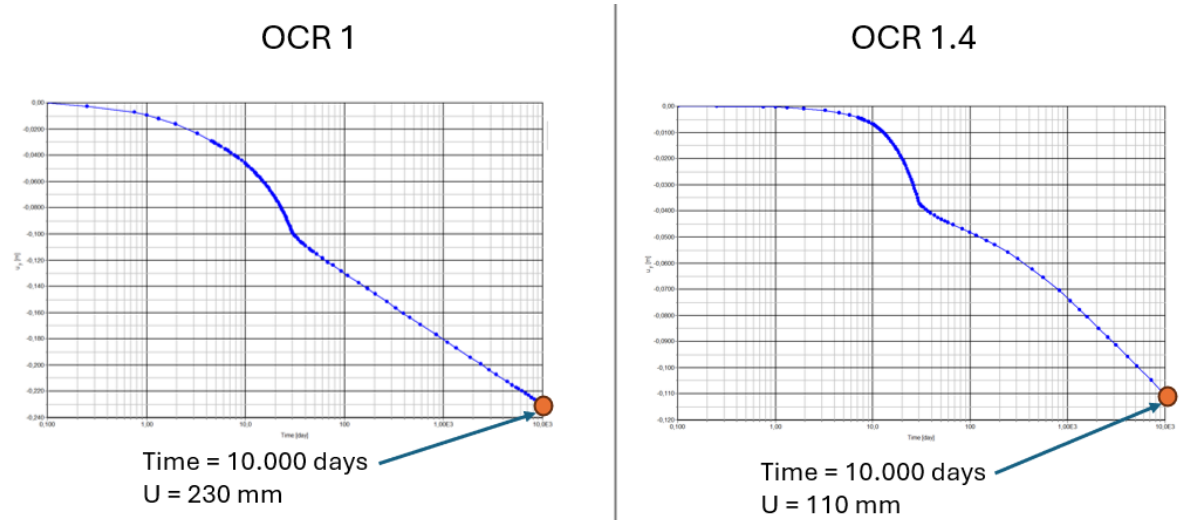

Figure 5.11: Comparison OCR value 1 to 1.4

For this research the OCR is set at a value of 1. This value is chosen because of the unpredictability of the soil. The soil properties are an estimation and therefore changing values for a more favourable result, has to be based on specific research.

5.2.3. Structural setup

At the start of a project, PLAXIS 2D give the engineer the option between two types of models: A plain strain model or an Axisymmetry model. The plain strain model assumes that the 2D plain is infinitely large in the z-direction. This model is used for projects with a large surface area like constructing an embankment. For this research the model of choice is an Axisymmetry model. The 2D input in this model will have rotational symmetry around a vertical axis.

The main reason this model choice is the shape of the foundation pile. It consists of a shaft and a helix

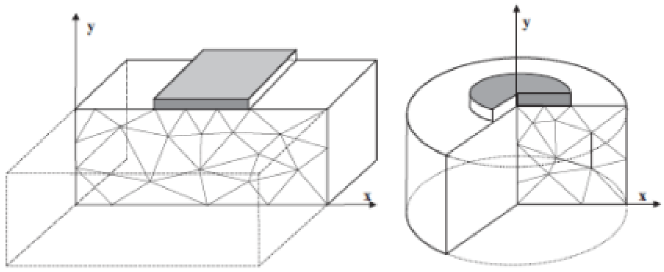

Figure 5.12: Difference between a plane strain (left) and axisymmetrical model (right) (*Reference Manual 2D*, 2024)

which both have a circular shape. The helices will be modelled as a horizontal plate. This is not their true shape, but do represent the surface area of the helix working on the soil. The shaft is modelled to investigate the friction between the shaft and the soil.

An example of the created steel polygon can be seen in Figure 5.13. The steel elements is modelled with the following properties:

$Soilmodel$	Linear Elastic;
$Drainagetype$	Non-porous;
$Unitweight$	$78,5kN/m^3$;
E_{ref}	$2,1*10^5N/mm^2$;
d	$0,05m$;
D	$0,3m$;
ν	0;
R_{inter}	$0,5$ (The interface shear factor);

Between the soil and the foundation piles, interfaces are applied. These interfaces simulate the interaction between the surface of the structure and the soil. The pile is screwed into the ground and made out of steel. Compared to a driven concrete pile the roughness of the steel pile is low and the installation method also results in a weaker interface connection. A value of 0,5 is chosen because of these negative effects.

Figure 5.13: Helical pile model in PLAXIS 2D

Finally, the vertical force on top of the pile is not placed in the centre, but on the side of the shaft. A force placed in an axisymmetrical model will be rotated around the y axis and the input value therefore has to be divided by the circumference. If the force is placed in the middle of the model, it will be divided by 0, which is not possible. The input force will therefore be a value of $F/(2r/\pi)$ kN/m. When translated to a point-load, it would equal F.

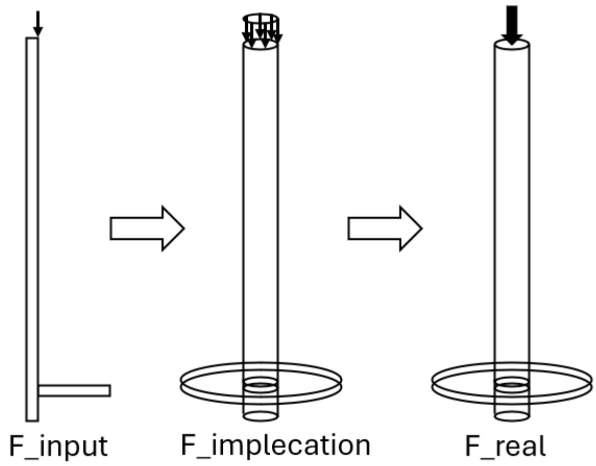

Figure 5.14: Sketch of the implications of modelled force on top of the pile

5.2.4. Implications structural set up

Single pile model

Due to the model being axisymmetrical, it is not possible to model multiple piles. How a group of piles react under certain conditions, can therefore only be estimated. Previous Section 5.1.2 goes into more detail on how this is implemented.

Group effect: pore excess water pressure

The same modelling choices affect the dissipation of the water under an increase in stress. The primary consolidation is caused by the expulsion of the water within the pores. The positioning of the piles leads to the water being able to effectively dissipate to a side, see Figure 5.15.

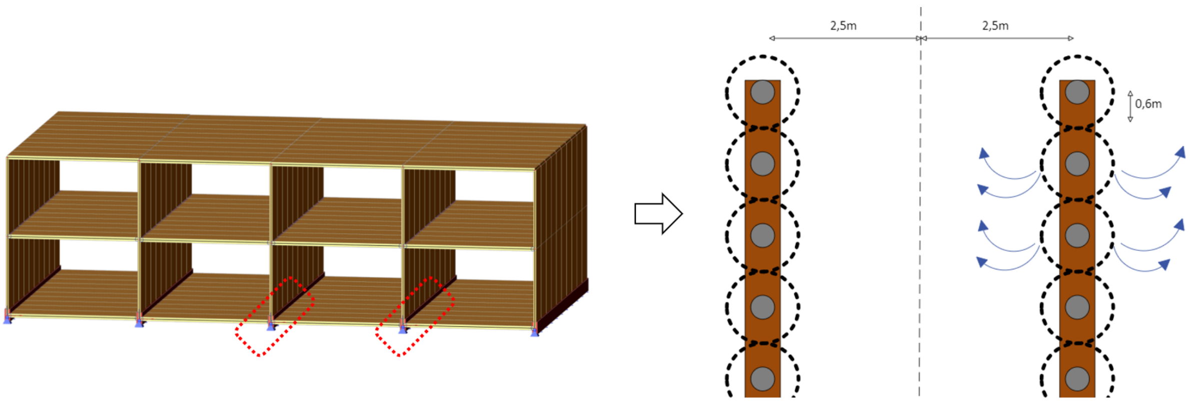

Figure 5.15: Schematization of water expulsion influenced due to group effect

This group effect cannot be modelled in an axisymmetrical model and the primary settlement will therefore occur faster than in reality.

5.2.5. Mesh size

When performing finite element analysis in PLAXIS 2D, the mesh size you choose for your model plays a critical role in the accuracy and efficiency of the simulation. The mesh divides the geometry into smaller elements, and the size of these elements affects how well the model can capture the behaviour of the soil. The choice of the mesh size comes down to accuracy vs computational time. A finer mesh size will give better results, but takes longer to produce. Whereas a coarser mesh is faster, but might not capture critical behaviours accurately.

The best choice for this research is to find a balance between the two. The long term calculations of the secondary settlement takes a relatively long time to compute and therefore the most fine mesh is not efficient. A medium mesh size comes close to the value of a very fine mesh and is chosen to make the progress less time consuming and still keep an fairly accurate estimations. These comparisons can be found in Appendix D.4. The mesh generated is more fine near the helical pile to more accurately predict the stresses and deformations in this area, see Figure 5.16

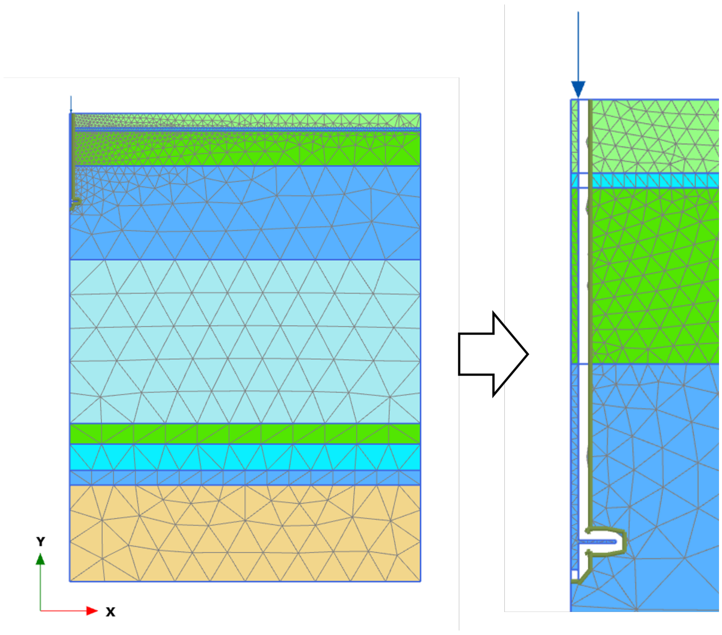

Figure 5.16: Generated mesh for a helical pile calculation

5.3. SCIA Engineer

This paragraph will discuss the different modelling choices made in SCIA. Setting up a model for a small wooden building involves defining the building's structural elements, materials, and boundary conditions.

5.3.1. Structural elements

Different models have been constructed for the calculations A, B and C. For the calculations from group A a continuous beam is modelled, and for groups B and C, a wall is modelled on top of a continuous beam. Underneath each system 6 supports are positioned that represent the helical foundation piles. A schematisation is given in Figure 5.17. The piles are named P1 to P6 with the size of the outer piles depending on the calculation. A lower case 'p' representing a pile with less capacity.

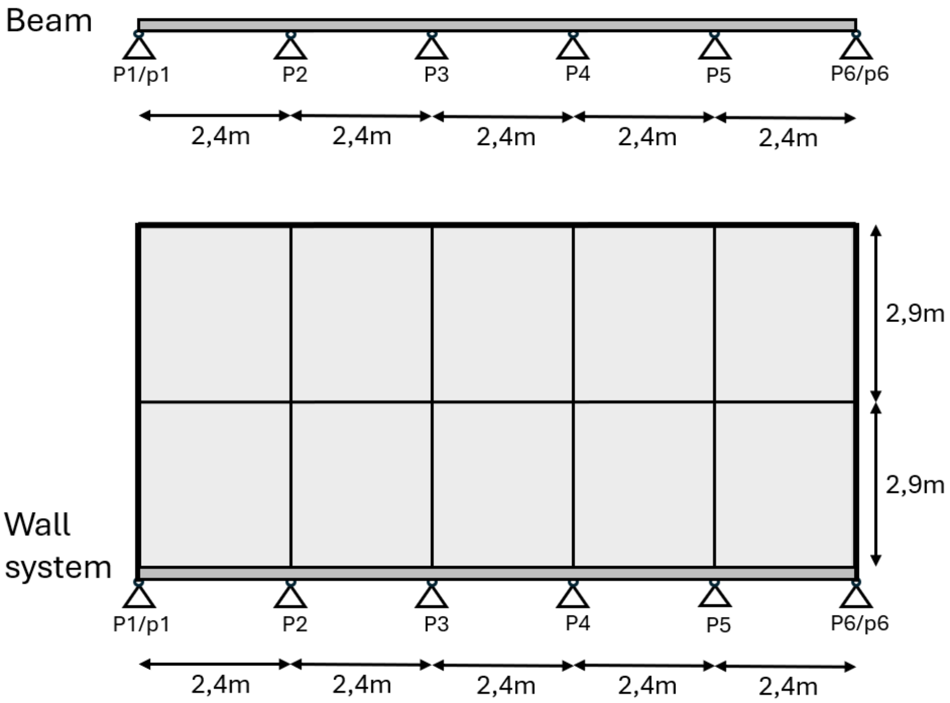

Figure 5.17: Schematisation of calculation model A (Beam) and Models B and C (Wall system)

Table 5.4: Overview of beams, walls, and piles with their respective types and dimensions.

	Beam type	BxH [mm x mm]	Wall Type	d [mm]	Pile Type	r_helix [mm]
Calc Aa	GL24h	200x560	-	-	P	300
Calc Ab	GL24h	200x560	-	-	P	300
Calc Ac	GL24h	200x200	-	-	P & p	300 & 250
Calc Ad	GL24h	200x200	-	-	P & p	300 & 250
Calc Ba	GL24h	200x200	OSB/3	10	P	300
Calc Bb	GL24h	200x200	OSB/3	10	P	300
Calc Bc	GL24h	200x200	OSB/3	10	P & p	300 & 250
Calc Bd	GL24h	200x200	OSB/3	10	P & p	300 & 250
Calc Ca	GL24h	200x200	CLT	100	P	300
Calc Cb	GL24h	200x200	CLT	100	P	300
Calc Cc	GL24h	200x200	CLT	100	P & p	300 & 250
Calc Cd	GL24h	200x200	CLT	100	P & p	300 & 250

The properties of the used materials are given in the following tables:

Table 5.5: Mechanical Properties of GL24h Timber (NEN-EN 14080)

Properties GL24h	Symbol	Value
Bending strength	$f_{m,k}$	24 MPa
Characteristic density	ρ_k	385 kg/m^3
Mean density	ρ_{mean}	420 kg/m^3
Mean modulus of elasticity parallel to the grain	$E_{0,mean}$	11,500 MPa
Characteristic modulus of elasticity parallel to the grain	$E_{0.05}$	9,600 MPa
Mean modulus of elasticity perpendicular to the grain	$E_{90,mean}$	300 MPa
Tensile strength parallel to the grain	$f_{t,0,k}$	19.2 MPa
Tensile strength perpendicular to the grain	$f_{t,90,k}$	0.5 MPa
Compressive strength parallel to the grain	$f_{c,0,k}$	24 MPa
Compressive strength perpendicular to the grain	$f_{c,90,k}$	2.5 MPa
Shear strength	$f_{v,k}$	3.5 MPa
Mean shear modulus	G_{mean}	650 MPa

Table 5.6: Mechanical Properties of OSB/2 Timber panels in dry conditions or OSB/3 Timber panels in humid conditions (NEN-EN 12369-1)

Properties OSB/3	Symbol	Value
Mean density	ρ_{mean}	550 kg/m^3
Bending strength	$f_{m,k}$	16,4 MPa
Tensile strength parallel to the grain	$f_{t,0,k}$	9,4 MPa
Tensile strength perpendicular to the grain	$f_{t,90,k}$	7,0 MPa
Compressive strength parallel to the grain	$f_{c,0,k}$	15,4 MPa
Compressive strength perpendicular to the grain	$f_{c,90,k}$	12,7 MPa
Shear strength	$f_{v,k}$	6,8 MPa
Mean modulus of elasticity parallel to the grain	E_{mean}	3800 MPa
Mean modulus of elasticity perpendicular to the grain	$E_{mean,90}$	4930 MPa
Mean shear modulus	G_{mean}	1080 MPa

Table 5.7: Mechanical Properties of C24 Timber used in the timber frame and CLT panels (NEN-EN 338)

Properties C24	Symbol	Value
Mean density	ρ_{mean}	420 kg/m^3
Bending strength	$f_{m,k}$	24 MPa
Tensile strength parallel to the grain	$f_{t,0,k}$	14 MPa
Tensile strength perpendicular to the grain	$f_{t,90,k}$	0.4 MPa
Compressive strength parallel to the grain	$f_{c,0,k}$	21 MPa
Compressive strength perpendicular to the grain	$f_{c,90,k}$	2.5 MPa
Shear strength	$f_{v,k}$	4.0 MPa
Mean modulus of elasticity parallel to the grain	E_{mean}	11,000 MPa
Mean modulus of elasticity perpendicular to the grain	$E_{mean,90}$	370 MPa
Mean shear modulus	G_{mean}	690 MPa

The CLT panels exhibit orthotropic properties due to their composition. Each panel consists of five layers of C24-grade lamellas, with each lamella having a width of 80 mm and a height of 20 mm. Consequently, the total thickness of the panel is 100 mm. The orientation of the lamellas alternates between layers, with three layers aligned along the x-axis and two layers aligned along the y-axis. This alternating configuration enhances the structural performance of the panel by improving its strength and stiffness in multiple directions. Figure 5.18 shows a CLT panel for the input in SCIA.

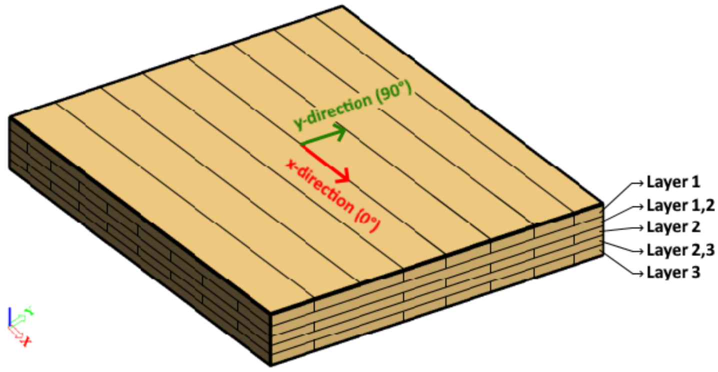

Figure 5.18: CLT panel

5.3.2. Applied loads

The vertical loads applied on the structure are determined by the NEN 1990 and 1991. The loads in the 2D plain have to represent the loads that are present in a 3D model. For the 3D structure the loads that would be applicable are:

The permanent load (G):

- *Self weight*: The weight of the structural elements itself.
- *Weight of the finishing layer at the floors*: 0,2 kN/m^2

The variable load (Q):

- *Living loads*: 1,5 to 2,0 kN/m^2
- *Snow load*: 0,56 kN/m^2

(Nederlands Normalisatie-instituut, 2019b)

Translating these loads to a line/point load results in the values given in Table 5.8:

Table 5.8: Overview of values and calculations for walls, floors, and loads.

Self weight floors		
Density (ρ)	4.2	kN/m^3
Floor height (h)	0.1	m
Floor width (b)	2.5	m
q_{fl}	**1.05**	**kN/m**
Weight floor finishings		
Floor load	0.2	kN/m^2
Floor width (b)	2.5	m
q_{fin}	**0.5**	**kN/m**
Variable load on floors		
Living loads	1.5	kN/m^2
Floor width (b)	2.5	m
q_{var}	**3.75**	**kN/m**
Self weight outer walls		
Density (ρ)	4.2	kN/m^3
Wall height (h)	6	m
Wall length (L)	2.5	m
Wall thickness (d)	0.1	m
F_{wall}	**6.3**	**kN**
Self weight walls		
Only for Calc. A		
Density (ρ)	4.2	kN/m^3
Wall height (h)	6	m
Wall thickness (d)	0.1	m
q_{wall}	**2.52**	**kN/m**

Load schemes
From Table 5.8 the load schemes for calculation can be constructed.

Load scheme calculation Aa & Ac

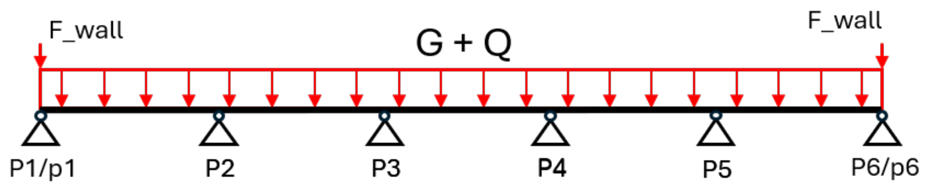

Where:

$$G = 3 \cdot (q_{\text{fl}} + q_{\text{fin}}) + q_{\text{wall}} = 7,2kN/m$$

$$Q = 2 \cdot q_{\text{var}} = 7,5kN/m$$

$$F_{\text{wall}} = 6,3kN$$

Load scheme calculation Ab & Ad

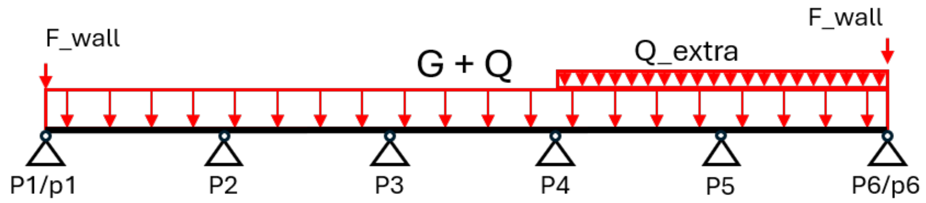

Where:

$$G = 3 \cdot (q_{\text{fl}} + q_{\text{fin}}) + q_{\text{wall}} = 7,2kN/m$$

$$Q = 2 \cdot q_{\text{var}} = 7,5kN/m$$

$$Q_{\text{extra}} = 2 \cdot \frac{1}{3} \cdot q_{\text{var}} = 2,5kN/m$$

$$F_{\text{wall}} = 6,3kN$$

Load scheme calculation Ba, Bc, Ca & Cc

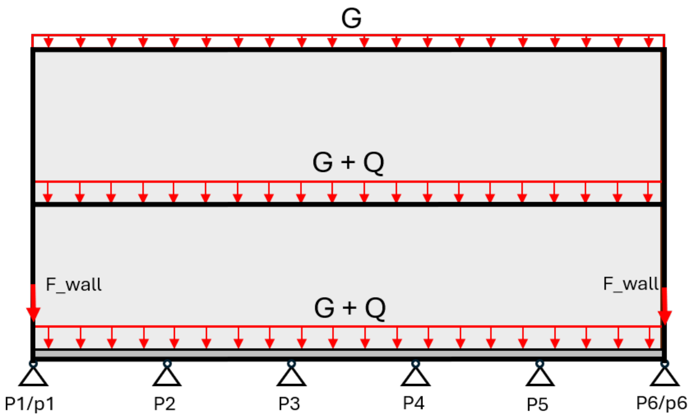

Where:

$G = q_{\text{fl}} + q_{\text{fin}} = 1,55kN/m$

$Q = q_{\text{var}} = 3,75kN/m$

$F_{\text{wall}} = 6,3kN$

Load scheme calculation Bb, Bd, Cb & Cd

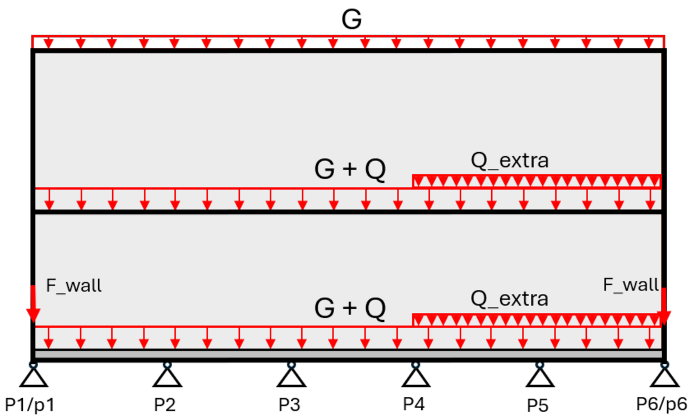

Where:

$G = q_{\text{fl}} + q_{\text{fin}} = 1,55kN/m$

$Q = q_{\text{var}} = 3,75kN/m$

$Q_{\text{extra}} = \frac{1}{3} \cdot q_{\text{var}} = 1,25kN/m$

$F_{\text{wall}} = 6,3kN$

5.3.3. Load combinations

To research the settlement of the structure, a load combination has to be chosen that estimates the loads that are present for a long period of time. Therefore the SLS factors are chosen in this calculation in combination with the Quasi-permanent load for the variable loads. The factor $\psi_{0;i}$ will become a value of 0.3 that is then multiplied with the variable loads. This represents the loads besides the self weight of the construction, for instance the furniture in the building. In this calculation, the loads on the roof of the building are not taken into account since it is assumed that they are not present for longer periods of time.

Table 5.9: Load combinations for the SLS(Nederlands Normalisatie-instituut, 2019a)

Design Situations	Permanent Load	Dominant Variable Load	Other Variable Loads
SLS	$1.0 \cdot G_{Kj,sup}$	$1.0 \cdot \psi_{0;i} Q_{j,1}$	$1.0 \cdot \psi_{0;i} Q_{j,i}$
SLS	$1.0 \cdot G_{Kj,sup}$	$1.0 \cdot 0,3 \cdot Q_{j,1}$	$1.0 \cdot 0,3 \cdot Q_{j,i}$

5.3.4. Mesh

A mesh is generated for 2D elements in SCIA Engineer. The wall system is connected to the continuous beam and a squared mesh is generated since there are no nodes on the wall where forces are concentrated. More nodes are created in the beam near the supports. Around these locations, the stresses are expected to be the highest.

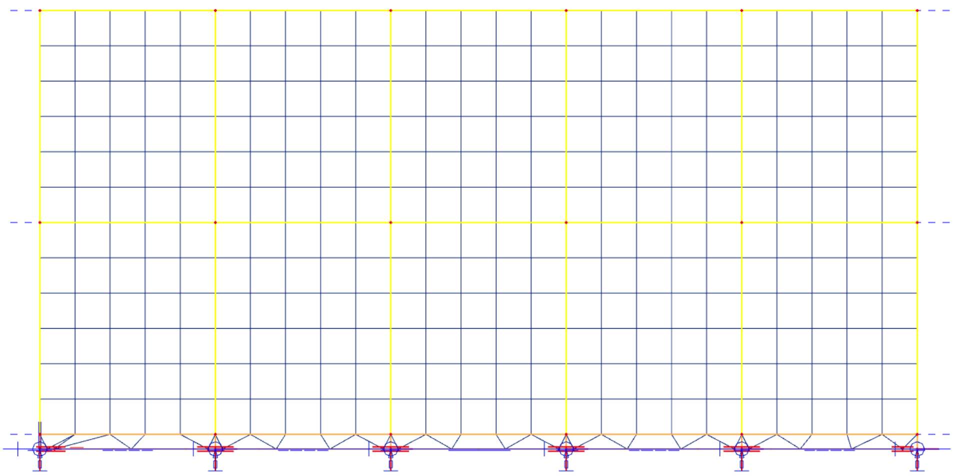

Figure 5.19: Generated mesh for calculations B and C

6
Results & Analysis

In this chapter, the results of the calculations will be presented. This will be done by giving the resulting deformations and support reactions of the piles at time steps T0 (immediately after the construction of the building is finished), T10 (10 days after construction), T100 (100 days after construction), and T1000 (1000 days after construction). The performance of the structure will be based on its deformations and the resulting internal stresses. Statements on these performances will be made on these performances and discussed. Each calculation presented in the flowchart shown in Figure 4.10 has been performed.

6.1. Results: Deformations

In this paragraph, each individual calculation will be presented with their support forces and support deformations at the given time steps. Each calculation will show the settlement of each pile over time and relative displacements between the piles that are next to one another. When tilt occurs, the relative displacement between the two most outer piles. The maximum total settlement (U), relative rotation (β) and tilt (ω) will be determined. In the end, a summarisation will be given of the maximum values for each calculation and how they perform on the boundary conditions given by the NEN.

6.1.1. Calculation Aa

For Calculation Aa, the displacements and reaction forces are calculated with the results given in Table 6.1.

Table 6.1: Displacements U in mm and support reactions F in kN over time (Calculation Aa)

	T0		T10		T100		T1000	
Supports	**U**	**F**	**U**	**F**	**U**	**F**	**U**	**F**
P1	80	20,3	89	20,6	116	21,0	159	21,4
P2	85	21,9	95	21,8	123	21,6	167	21,4
P3	88	23,1	98	23,0	126	22,7	171	22,6
P4	88	23,1	98	23,0	126	22,7	171	22,6
P5	85	21,9	95	21,8	123	21,6	167	21,4
P6	80	20,3	89	20,6	116	21,0	159	21,4

From the results, the relative displacement can be calculated at each time step. Figure 6.1 shows how the relative displacement change over time. Since P1 and P6 are at the same height at each time step, there is no tilt to be measured.

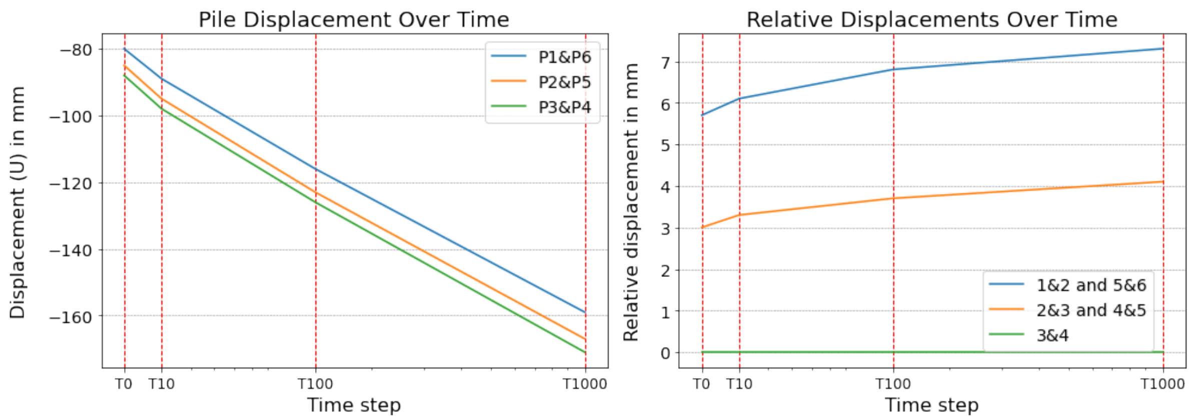

Figure 6.1: Resulting settlement calculation Aa

The maximum values of this calculation are:

Maximum U = 171 mm at T1000
Maximum β = 7.3 / 2400 at T1000

6.1.2. Calculation Ab

For Calculation Ab, the displacements and reaction forces are calculated with the results given in Table 6.2.

Table 6.2: Displacements U in mm and support reactions F in kN over time (Calculation Ab)

	T0		T10		T100		T1000	
Supports	**U**	**F**	**U**	**F**	**U**	**F**	**U**	**F**
1	79	20.2	88	20.4	115	20.9	159	21.1
2	86	22.0	95	22.0	123	21.6	167	21.4
3	89	23.5	99	23.4	128	23.1	172	23.0
4	90	23.9	100	23.5	129	23.7	173	23.9
5	88	23.0	98	23.0	126	22.7	171	22.2
6	83	21.7	92	22.0	120	22.3	164	22.7

From the results, the relative displacement can be calculated at each time step. Figure 6.2 shows how the relative displacement change over time. Due to the uneven loads applied, the building will tend to tilt (ω). The difference between the two most outer piles is given in Figure 6.3.

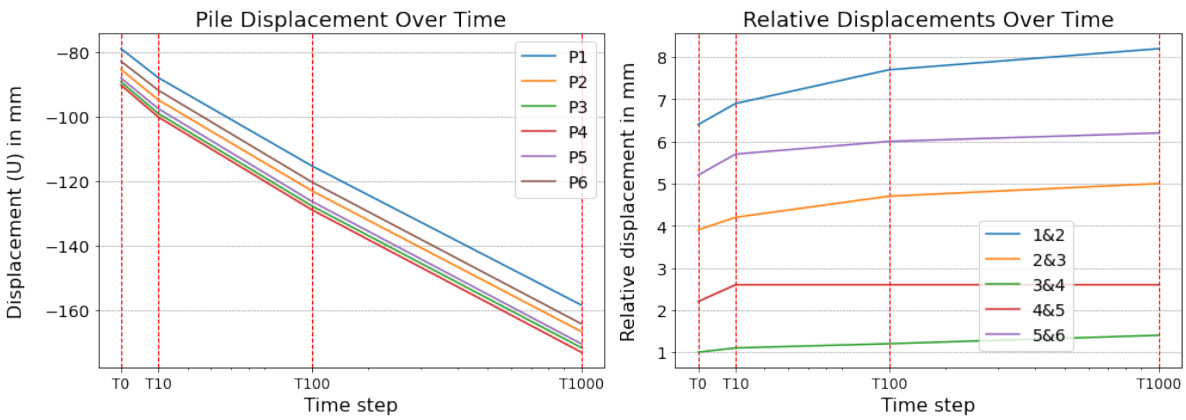

Figure 6.2: Resulting deformations (calculation Ab)

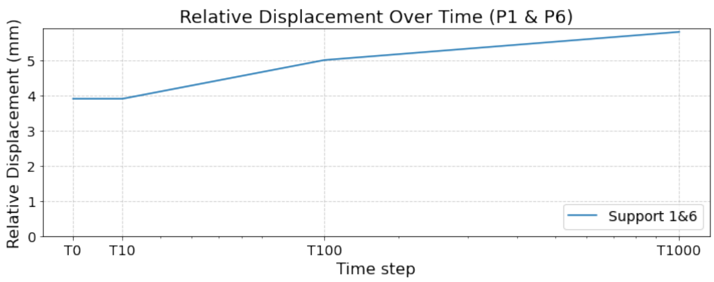

Figure 6.3: Result relative displacement P1&P6 (calculation Ab)

The maximum values of this calculation are:

Maximum U	= 173 mm	at T1000
Maximum β	= 8.2 / 2400	at T1000
Maximum ω	= 5.8 / 12000	at T1000

6.1.3. Calculation Ac

For Calculation Ac, the displacements and reaction forces are calculated with the results given in Table 6.3.

Table 6.3: Displacements U in mm and support reactions F in kN over time (Calculation Ac)

	T0		**T10**		**T100**		**T1000**	
Supports	**U**	**F**	**U**	**F**	**U**	**F**	**U**	**F**
1	85	16.4	96	16.4	121	16.8	162	16.9
2	90	23.9	101	24.0	129	23.2	172	23.1
3	90	23.7	100	23.7	130	24.0	173	24.0
4	90	23.7	100	23.7	130	24.0	173	24.0
5	90	23.9	101	24.0	129	23.2	172	23.1
6	85	16.4	96	16.4	121	16.8	162	16.9

From the results, the relative displacement can be calculated at each time step. Figure 6.4 shows how the relative displacement change over time. Since P1 and P6 are at the same height at each time step, there is no tilt to be measured.

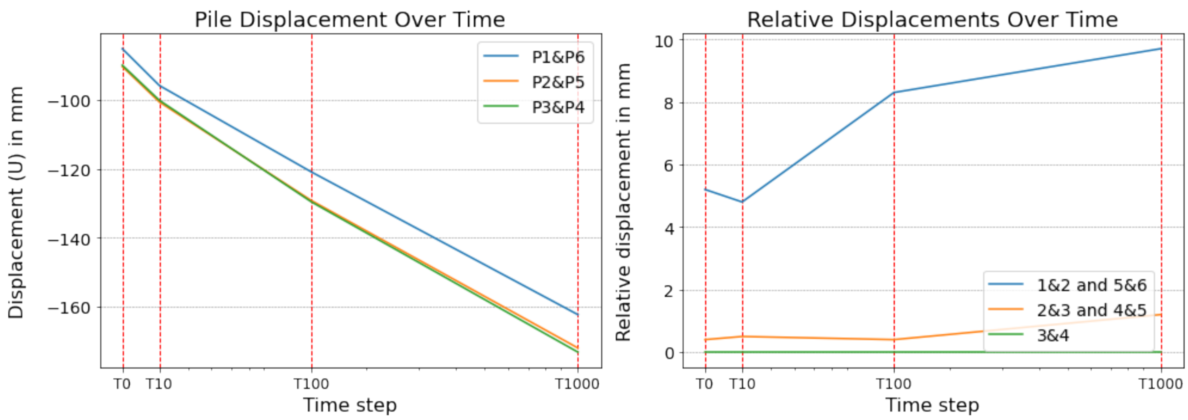

Figure 6.4: Resulting settlement calculation Ac

The maximum values of this calculation are:

Maximum U	= 173 mm	at T1000
Maximum β	= 9.7 / 2400	at T1000

6.1.4. Calculation Ad

For Calculation Ad, the displacements and reaction forces are calculated with the results given in Table 6.4.

Table 6.4: Displacements U in mm and support reactions F in kN over time (Calculation Ad)

	T0		T10		T100		T1000	
Supports	**U**	**F**	**U**	**F**	**U**	**F**	**U**	**F**
1	85	16.4	95	16.3	120	16.7	162	16.8
2	90	23.8	100	23.9	129	23.4	172	22.9
3	91	23.9	101	24.0	130	23.9	174	24.5
4	92	24.7	103	24.7	132	24.8	176	25.0
5	94	25.4	105	24.9	133	25.2	176	24.3
6	89	17.4	97	17.7	125	17.5	164	18.1

From the results, the relative displacement can be calculated at each time step. Figure 6.5 shows how the relative displacement change over time. Due to the uneven loads applied, the building will tend to tilt (ω). The difference between the two most outer piles is given in Figure 6.6.

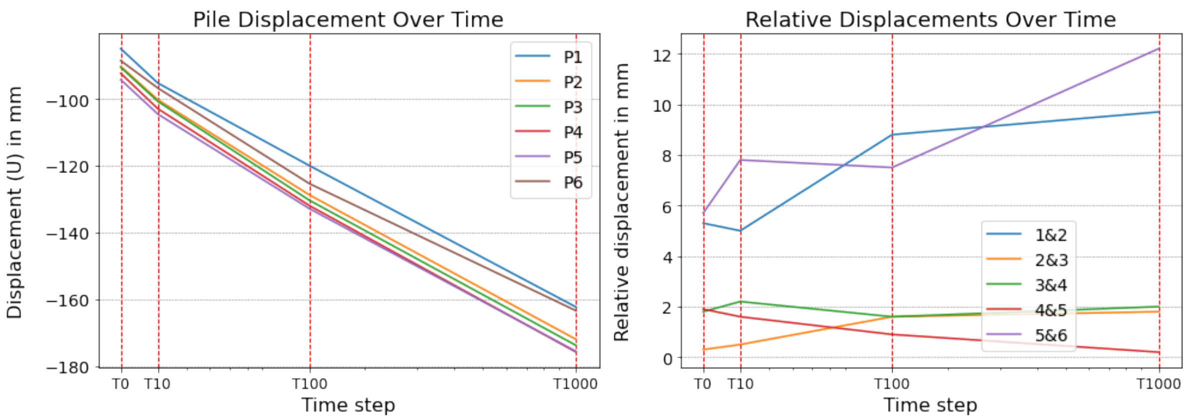

Figure 6.5: Resulting settlement calculation Ad

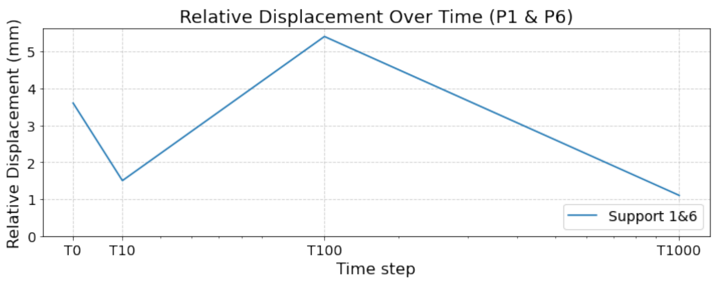

Figure 6.6: Result relative displacement P1&P6 (calculation Ad)

The maximum values of this calculation are:

Maximum U	= 176 mm	at T1000
Maximum β	= 12.2 / 2400	at T1000
Maximum ω	= 5.4 / 12000	at T100

6.1.5. Calculation Ba

For Calculation Ba, the displacements and reaction forces are calculated with the results given in Table 6.5.

Table 6.5: Displacements U in mm and support reactions F in kN over time (Calculation Ba)

	T0		T10		T100		T1000	
Supports	**U**	**F**	**U**	**F**	**U**	**F**	**U**	**F**
1	73	17.2	80	17.0	106	17.9	147	17.6
2	74	16.8	81	16.2	107	16.8	147	16.5
3	74	16.8	81	17.6	107	16.1	147	16.7
4	74	16.8	81	17.6	107	16.1	147	16.7
5	74	16.8	81	16.2	107	16.8	147	16.5
6	73	17.2	80	17.0	106	17.9	147	17.6

From the results, the relative displacement can be calculated at each time step. Figure 6.7 shows how the relative displacement change over time. Since P1 and P6 are at the same height at each time step, there is no tilt to be measured.

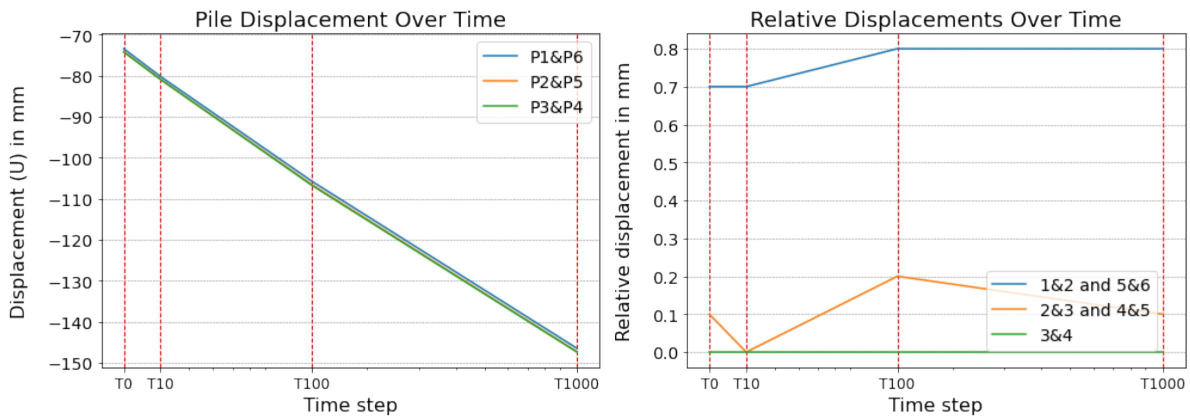

Figure 6.7: Resulting settlement calculation Ba

The maximum values of this calculation are:

Maximum U	= 147 mm	at T1000
Maximum β	= 0.8 / 2400	at T1000

6.1.6. Calculation Bb

For Calculation Bb, the displacements and reaction forces are calculated with the results given in Table 6.6.

Table 6.6: Displacements U in mm and support reactions F in kN over time (Calculation Bb)

	T0		T10		T100		T1000	
Supports	**U**	**F**	**U**	**F**	**U**	**F**	**U**	**F**
1	79	20.2	88	20.4	115	20.9	159	21.1
2	86	22.0	95	22.0	123	21.6	167	21.4
3	89	23.5	99	23.4	128	23.1	172	23.0
4	90	23.9	100	23.5	129	23.7	173	23.9
5	88	23.0	98	23.0	126	22.7	171	22.2
6	83	21.7	92	22.0	120	22.3	164	22.7

From the results, the relative displacement can be calculated at each time step. Figure 6.8 shows how the relative displacement change over time. Due to the uneven loads applied, the building will tend to tilt (ω). The difference between the two most outer piles is given in Figure 6.9.

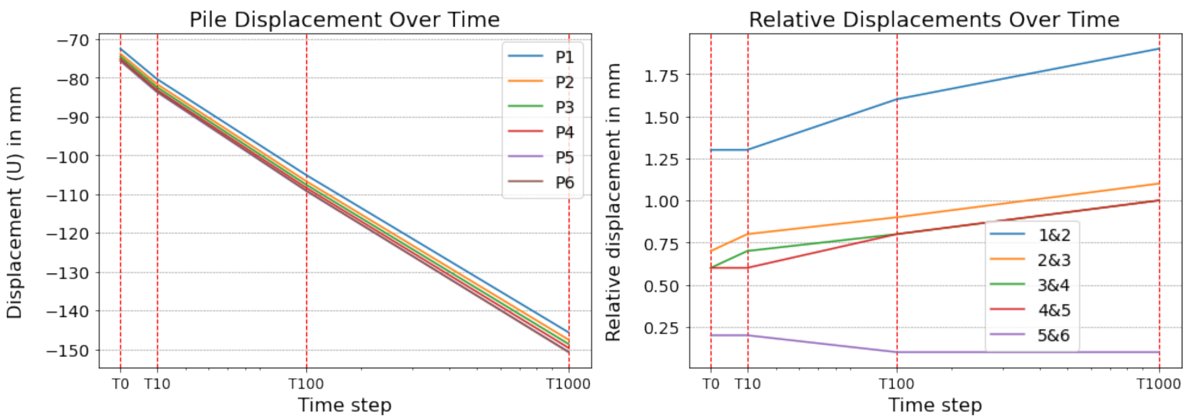

Figure 6.8: Resulting deformations (calculation Bb)

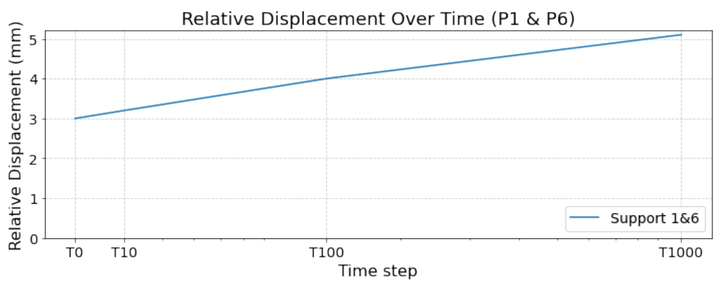

Figure 6.9: Result relative displacement P1&P6 (calculation Bb)

The maximum values of this calculation are:

Maximum U	= 151 mm	at T1000
Maximum β	= 0.3 / 2400	at T1000
Maximum ω	= 5.1 / 12000	at T1000

6.1.7. Calculation Bc

For Calculation Bc, the displacements and reaction forces are calculated with the results given in Table 6.7.

Table 6.7: Displacements U in mm and support reactions F in kN over time (Calculation Bc)

	T0		T10		T100		T1000	
Supports	**U**	**F**	**U**	**F**	**U**	**F**	**U**	**F**
1	79	20.2	88	20.4	115	20.9	159	21.1
2	86	22.0	95	22.0	123	21.6	167	21.4
3	89	23.5	99	23.4	128	23.1	172	23.0
4	90	23.9	100	23.5	129	23.7	173	23.9
5	88	23.0	98	23.0	126	22.7	171	22.2
6	83	21.7	92	22.0	120	22.3	164	22.7

From the results, the relative displacement can be calculated at each time step. Figure 6.10 shows how the relative displacement change over time. Since P1 and P6 are at the same height at each time step, there is no tilt to be measured.

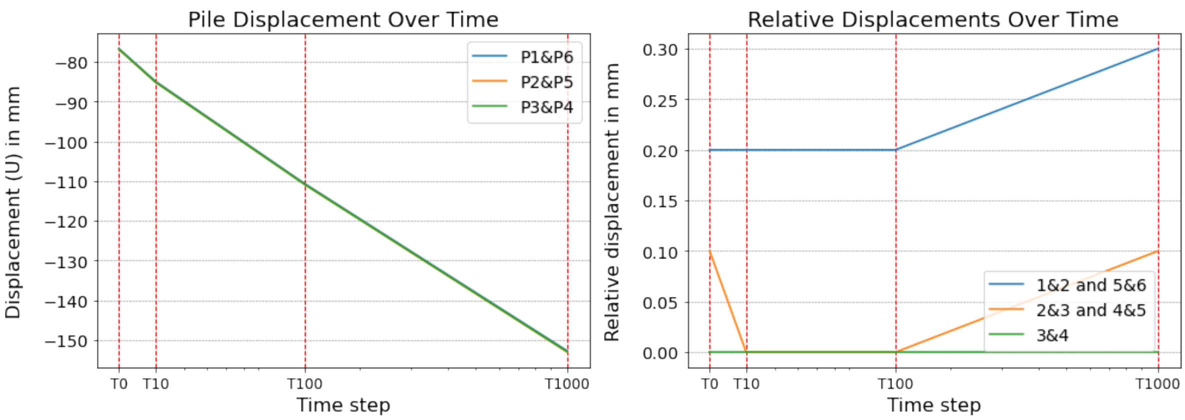

Figure 6.10: Resulting deformations (calculation Bc)

The maximum values of this calculation are:

Maximum U = 153 mm at T1000
Maximum β = 0.3 / 2400 at T1000

6.1.8. Calculation Bd

For Calculation Bd, the displacements and reaction forces are calculated with the results given in Table 6.8.

Table 6.8: Displacements U in mm and support reactions F in kN over time (Calculation Bd)

	T0		T10		T100		T1000	
Supports	**U**	**F**	**U**	**F**	**U**	**F**	**U**	**F**
1	79	20.2	88	20.4	115	20.9	159	21.1
2	86	22.0	95	22.0	123	21.6	167	21.4
3	89	23.5	99	23.4	128	23.1	172	23.0
4	90	23.9	100	23.5	129	23.7	173	23.9
5	88	23.0	98	23.0	126	22.7	171	22.2
6	83	21.7	92	22.0	120	22.3	164	22.7

From the results, the relative displacement can be calculated at each time step. Figure 6.11 shows how the relative displacement change over time. Due to the uneven loads applied, the building will tend to tilt (ω). The difference between the two most outer piles is given in Figure 6.12.

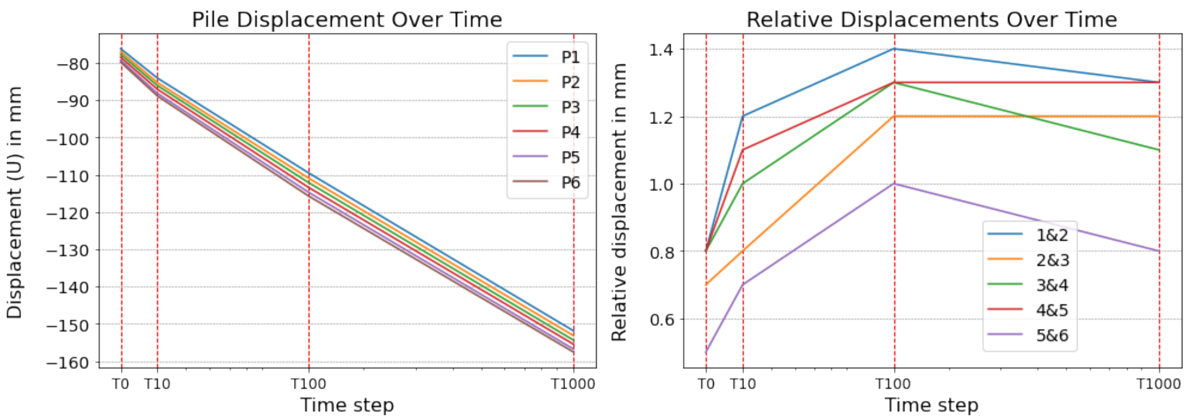

Figure 6.11: Resulting deformations (calculation Bd)

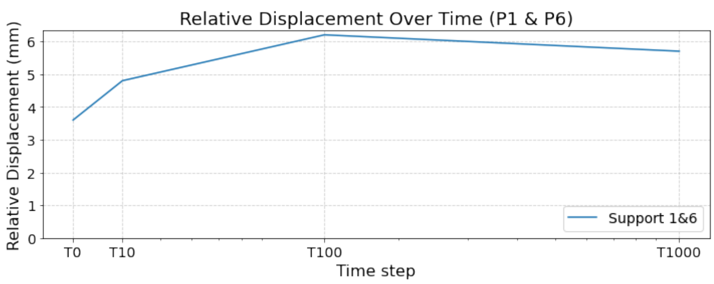

Figure 6.12: Result relative displacement P1&P6 (calculation Bd)

The maximum values of this calculation are:

Maximum U	= 158 mm	at T1000
Maximum β	= 1.3 / 2400	at T100
Maximum ω	= 6.2 / 12000	at T100

6.1.9. Calculation Ca

For Calculation Ba, the displacements and reaction forces are calculated with the results given in Table 6.9.

Table 6.9: Displacements U in mm and support reactions F in kN over time (Calculation Ca)

	T0		**T10**		**T100**		**T1000**	
Supports	**U**	**F**	**U**	**F**	**U**	**F**	**U**	**F**
1	83	21.7	92	22.0	120	22.1	164	22.7
2	83	21.2	93	21.0	120	21.1	164	20.5
3	83	21.2	93	21.0	120	20.9	164	20.9
4	83	21.2	93	21.0	120	20.9	164	20.9
5	83	21.2	93	21.0	120	21.1	164	20.5
6	83	21.7	92	22.0	120	22.1	164	22.7

From the results, the relative displacement can be calculated at each time step. Figure 6.13 shows how the relative displacement change over time. Since P1 and P6 are at the same height at each time step, there is no tilt to be measured.

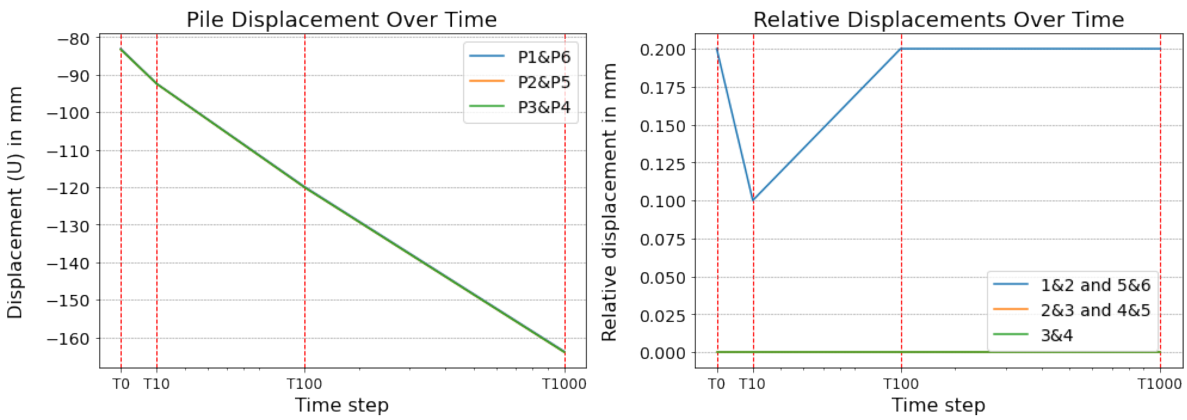

Figure 6.13: Resulting settlement calculation Ca

The maximum values of this calculation are:

Maximum U = 164 mm at T1000
Maximum β = 0.2 / 2400 at T1000

6.1.10. Calculation Cb

For Calculation Ba, the displacements and reaction forces are calculated with the results given in Table 6.10.

Table 6.10: Displacements U in mm and support reactions F in kN over time (Calculation Cb)

	T0		T10		T100		T1000	
Supports	**U**	**F**	**U**	**F**	**U**	**F**	**U**	**F**
1	83	21.5	92	21.8	120	21.9	164	22.7
2	84	21.3	93	21.2	121	21.2	165	20.9
3	84	21.6	94	21.4	122	21.5	166	20.9
4	85	21.9	95	21.8	123	21.7	167	21.2
5	86	22.2	95	22.2	124	21.8	167	21.4
6	87	23.1	96	23.3	124	23.6	168	24.5

From the results, the relative displacement can be calculated at each time step. Figure 6.14 shows how the relative displacement change over time. Due to the uneven loads applied, the building will tend to tilt (ω). The difference between the two most outer piles is given in Figure 6.15.

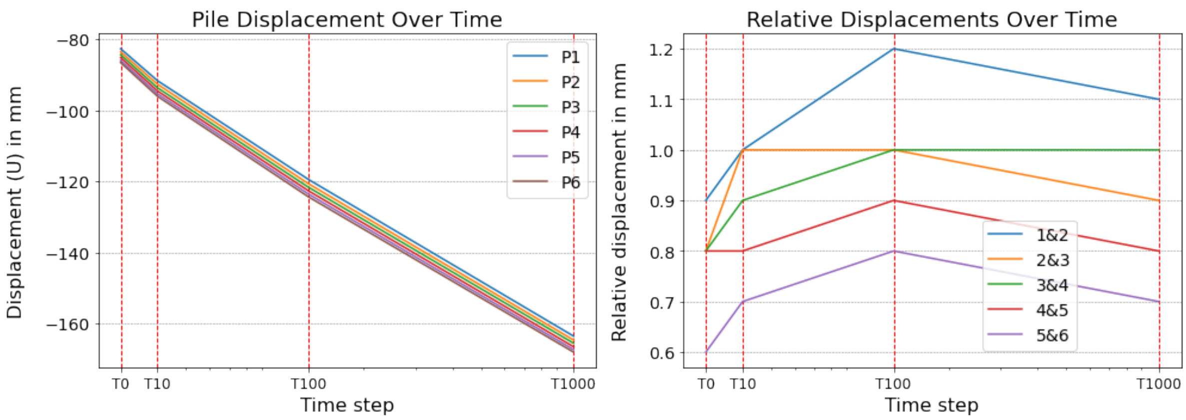

Figure 6.14: Resulting settlement calculation Cb

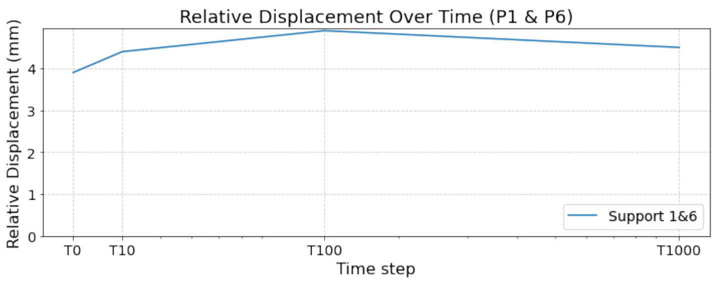

Figure 6.15: Result relative displacement P1&P6 (calculation Cb)

The maximum values of this calculation are:

Maximum U	= 168 mm	at T1000
Maximum β	= 0.2 / 2400	at T100
Maximum ω	= 4.9 / 12000	at T100

6.1.11. Calculation Cc

For Calculation Ba, the displacements and reaction forces are calculated with the results given in Table 6.11.

Table 6.11: Displacements U in mm and support reactions F in kN over time (Calculation Cc)

	T0		T10		T100		T1000	
Supports	**U**	**F**	**U**	**F**	**U**	**F**	**U**	**F**
1	89	17.5	98	17.7	127	18.2	171	18.7
2	89	23.3	99	23.2	127	22.9	171	22.7
3	89	23.3	99	23.2	127	22.9	171	22.7
4	89	23.3	99	23.2	127	22.9	171	22.7
5	89	23.3	99	23.2	127	22.9	171	22.7
6	89	17.5	98	17.7	127	18.2	171	18.7

From the results, the relative displacement can be calculated at each time step. Figure 6.16 shows how the relative displacement change over time. Since P1 and P6 are at the same height at each time step, there is no tilt to be measured.

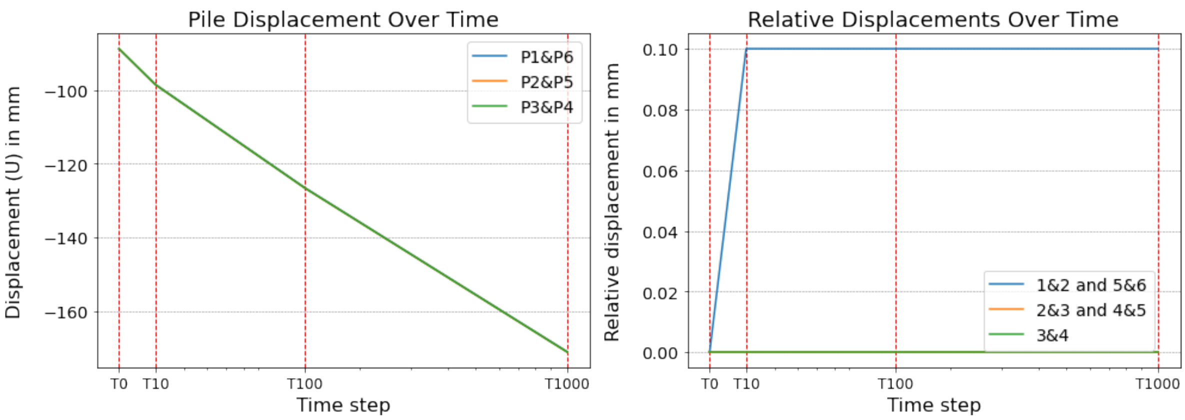

Figure 6.16: Resulting settlement calculation Cc

The maximum values of this calculation are:

Maximum U = 171 mm at T1000
Maximum β = 0.1 / 2400 at T1000

6.1.12. Calculation Cd

For Calculation Ba, the displacements and reaction forces are calculated with the results given in Table 6.12.

Table 6.12: Displacements U in mm and support reactions F in kN over time (Calculation Cd)

	T0		T10		T100		T1000	
Supports	**U**	**F**	**U**	**F**	**U**	**F**	**U**	**F**
1	88	17.3	98	17.8	126	17.7	170	18.2
2	89	23.4	99	23.1	127	23.1	171	23.1
3	90	23.7	100	23.5	128	23.6	172	22.6
4	91	24.1	101	23.3	129	24.2	173	23.9
5	92	24.5	102	24.9	130	23.9	174	24.8
6	93	18.7	103	18.9	131	19.2	175	19.0

From the results, the relative displacement can be calculated at each time step. Figure 6.17 shows how the relative displacement change over time. Due to the uneven loads applied, the building will tend to tilt (ω). The difference between the two most outer piles is given in Figure 6.15.

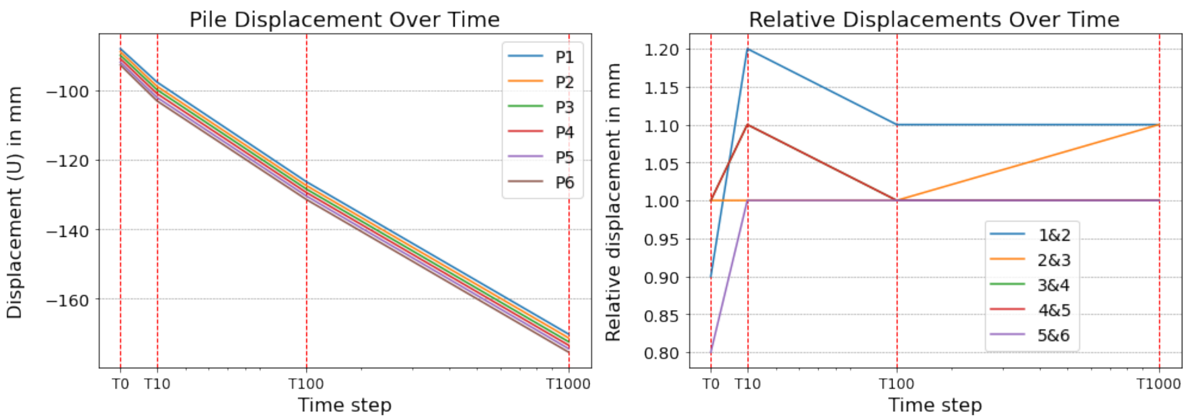

Figure 6.17: Resulting settlement calculation Cd

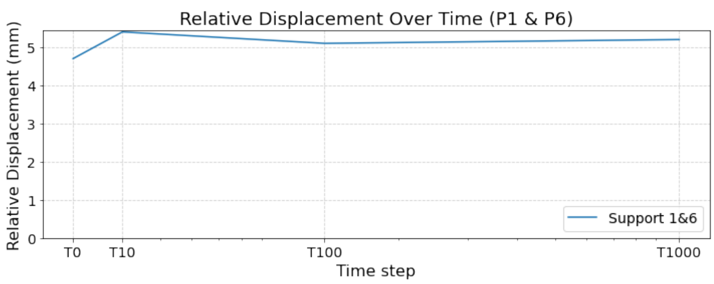

Figure 6.18: Result relative displacement P1&P6 (calculation Cd)

The maximum values of this calculation are:

Maximum U	= 175 mm	at T1000
Maximum β	= 0.1 / 2400	at T10
Maximum ω	= 5.4 / 12000	at T10

6.1.13. Summary: Deformations

The executed calculations are analysed on the structures performance. Table 6.13 gives a summarisation of the performance by outlining the maximum values for Total displacement, Relative Rotation, and Tilt. The latter two have been compared to their sufficiency on the given boundary conditions from the NEN.

Table 6.13: Calculation results of the maximum total displacement, relative rotation, tilt, and their sufficiency

Maximum:	**Total U [mm]**	**Rel. Rot. (β)**		**Tilt (ω)**		**Sufficient?**
Calc Aa	171	7.3	/2400	0	/12000	Yes
Calc Ab	173	8.2	/2400	5.8	/12000	No, $\beta > 1/300$
Calc Ac	173	9.7	/2400	0	/12000	No, $\beta > 1/300$
Calc Ad	176	12.2	/2400	5.4	/12000	No, $\beta > 1/300$
Calc Ba	147	0.8	/2400	0	/12000	Yes
Calc Bb	151	1.9	/2400	5.1	/12000	Yes
Calc Bc	153	0.3	/2400	0	/12000	Yes
Calc Bd	158	1.3	/2400	6.2	/12000	Yes
Calc Ca	164	0.2	/2400	0	/12000	Yes
Calc Cb	168	0.2	/2400	4.9	/12000	Yes
Calc Cc	171	0.1	/2400	0	/12000	Yes
Calc Cd	175	0	/2400	5.4	/12000	Yes

6.2. Discussion: Deformations

With the test results, a few observations can be made.

- *A stiffer superstructure decreases the maximum total settlement U;*
  Comparing the results from calculation Aa & Ab with those from Ca & Cb, it can be seen that despite having been applied to the same loads, the maximum settlement of the CLT wall system is less than of the continuous beam. This can be explained by the better distribution of the forces to the foundation piles. The wall system ensures that the piles at the side of the wall take more force and the middle piles less.
- *A stiffer superstructure lowers average settlement U over time;*
  If the average pile displacement is calculated for calculation Aa and Ca, it would result in an $U_{avg} = 165,4mm$ for calculation Aa and $U_{avg} = 163,9mm$ for calculation Ca at T1000. This suggests that a more equal distribution of the load, results in lower settlements overall.
- *The use of piles with lower capacity at the outer positions does not improve the performance of a less stiff superstructure;*
  Based on the methodology for meeting the requirements at T0, a 200×200 GL24h beam was determined to be adequate. However, the structure would not meet the requirements at later stages in time based on the boundary conditions for β.
- *Losing capacity on the outer piles of a stiff wall system, affects the total settlement and tilt more negatively then with a less stiff superstructure;*
  By decreasing the capacity of the outer piles, the maximum total settlement of a stiff structure increases more than that of a less stiff structure. It also makes the stiffer structures more susceptible for tilt. This can be explained by the fact that a stiffer structure is better able to distribute forces to the outer piles and uses them to their advantage. The
- *The tilt resulting from differential loading of the permanent load is minimal and exhibits a slight incremental increase over time;*

The differential displacements caused by tilting can increase over time, but never increase with more than half of the initial differential displacement between P1&P6. The deformations never come close to the boundary condition of 1/300 tilt in any of the calculations.

- *The tilt of the structure increases less over time for stiffer structures;*
  Comparing the results of calculation Ab and Cb, the difference between the relative displacement of supports 1&6 is 2 mm for calculation Ab and 1 mm for calculation Cb.

- *Using a lightweight wall system decreases the overall settlement.*
  With calculation Ba having a total vertical force of 102 kN on the foundation and calculation Ca 128 kN, a reduction in loads of 20% is achieved. Comparing the total settlement of the two, a reduction of 11% can be seen.

6.3. Results: Capacity

Each wall system has been calculated on the maximum bending stress within the structural elements. A clear distinction occurs in the stress propagation between the structure from calculation A and with the wall in calculation B and C.

6.3.1. Calculation A: Continuous beam

With the beam deforming in a U-shape in calculation Aa and Ab, the moment line is always positive. This results in the stresses at the top of the beam, always being in compression and at the bottom always in tension. Figure 6.19 shows the stresses that occur in calculation Aa.

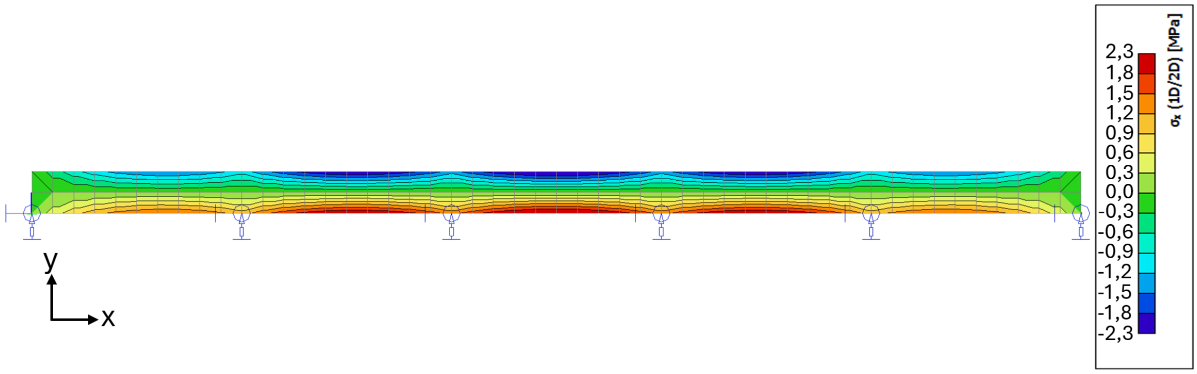

Figure 6.19: Calculation Aa: Resulting stress σ_x at T1000

The maximum stresses present in the beams from calculation A, are summarized in Table 6.14. From this table, it can be stated that even the beams with the smallest dimension and highest relative displacements, still do not surpass the bending strength of the material $f_{m,k} = 24MPa$.

Table 6.14: Resulting bending stress σ_x in Calculation A

	Max σ_x [MPa]	**Sufficient?**
Calc Aa	2.3	Yes
Calc Ab	2.2	Yes
Calc Ac	3.9	Yes
Calc Ad	5.0	Yes

6.3.2. Calculation B&C: Continuous beam + Wall

With a wall positioned on top of the continuous beam, the stress propagation will change. The wall acts as a large and slender beam, creating a high stiffness that has little deformations within its own elements. Above the supports, the continuous beam is undergoing compression at the bottom and tension at the top. Except for the outer supports, where it is the other way around. Figure 6.20 and 6.21 shows the stresses of the wall in calculation Ca at T1000.

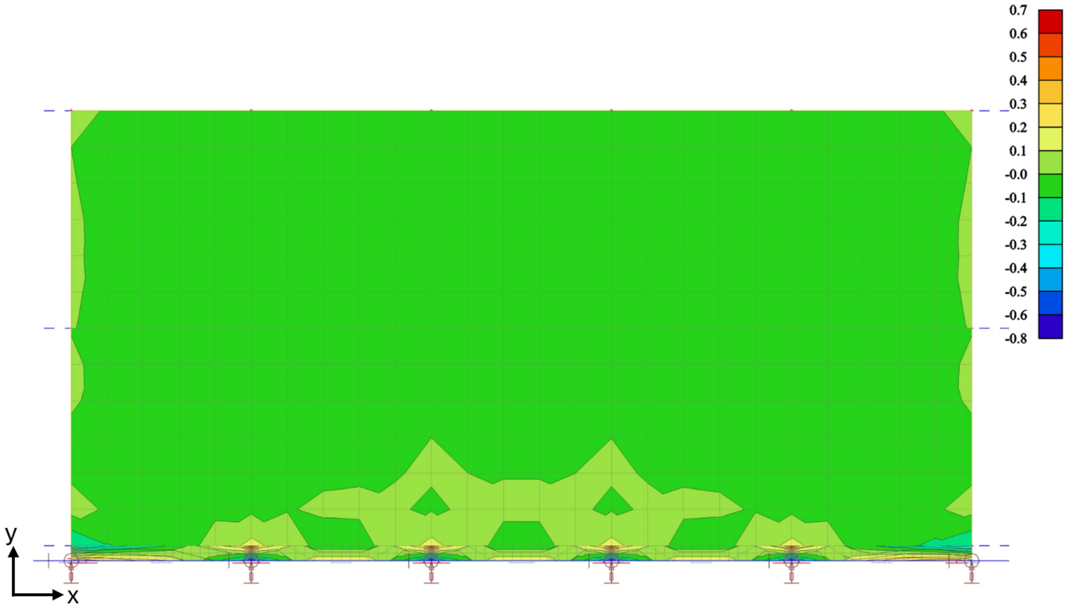

Figure 6.20: Resulting stress σ_x calculation Ca at T1000

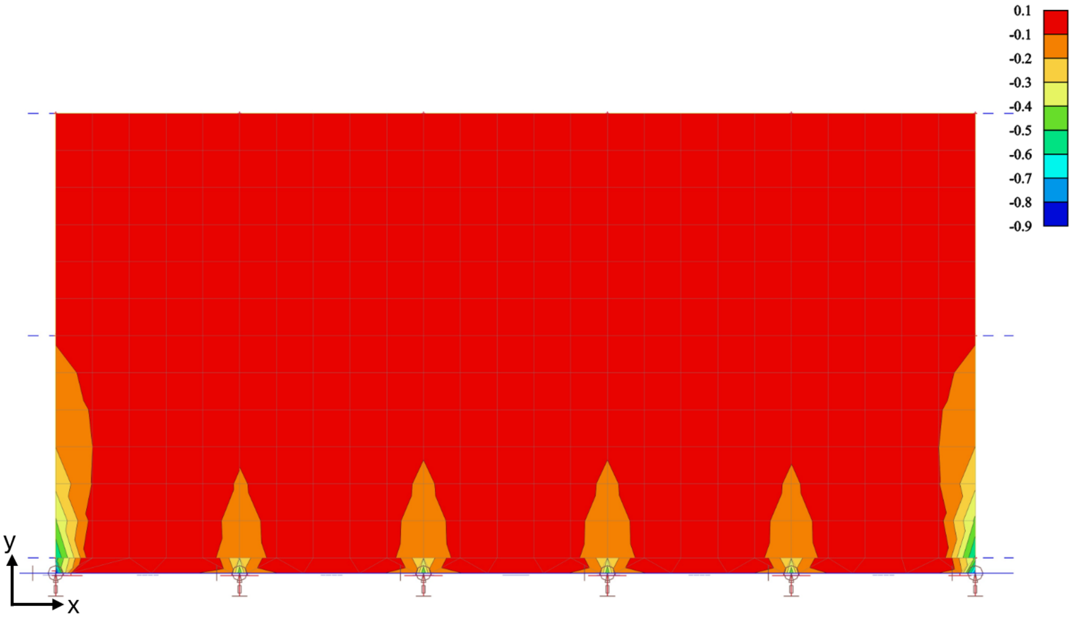

Figure 6.21: Resulting stress σ_y calculation Ca at T1000

Table 6.15 displays the maximum stresses in the x and y direction that occur in the wall system.

Table 6.15: Resulting stress σ_x and σ_y

Calculation	Max σ_x [MPa]	Max σ_y [MPa]	Max $f_{t,0,k}$ [MPa]	$f_{c,0,k}$ [MPa]	Sufficient?
Calc Ba	0.9	-4.2	9.4	15.4	Yes
Calc Bb	0.9	-4.8	9.4	15.4	Yes
Calc Bc	1.1	-2.5	9.4	15.4	Yes
Calc Bd	1.1	-3.1	9.4	15.4	Yes
Calc Ca	0.8	-0.9	14	21	Yes
Calc Cb	0.7	-1.0	14	21	Yes
Calc Cc	0.8	-0.7	14	21	Yes
Calc Cd	0.8	-0.7	14	21	Yes

6.4. Discussion: Capacity

Based on the results, it can be stated that no significant stress will occur that can cause failure. Even the calculation with the smallest profile does not come close to its maximum bending stress, even with the safety factors given in Section 3.3.1. That the results turn out this way, can be explained by the boundary conditions used for this research. Because each case is designed to meet the relative rotation requirements given by the NEN norm at T0, each calculation has a high stiffness to compensate for the lower stiffness of the pile foundation. Even the continuous beam of calculations Aa and Ab, that was supposed to represent a lower stiffness, has a relatively large profile. Therefore, it can be stated that the feasibility of this structure is not dependent on the capacity of the structural elements for this given case study.

Looking at the stress propagation in the wall, it can be seen that in the X direction most area of the wall is under compression stress. However, above the supports, a tension stress can be seen. The stress propagation in the x direction is a combination of behaviour of the whole structure on a large scale and small scale behaviour. Figures 6.22 and 6.23 give a schematisation of the expected stress propagation within the wall caused by global displacements and local displacements.

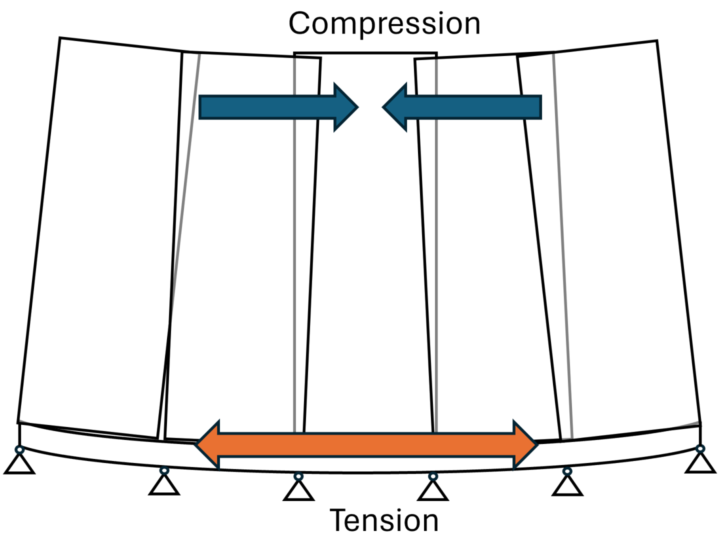

Figure 6.22: Schematisation of the global stress propagation of the wall system

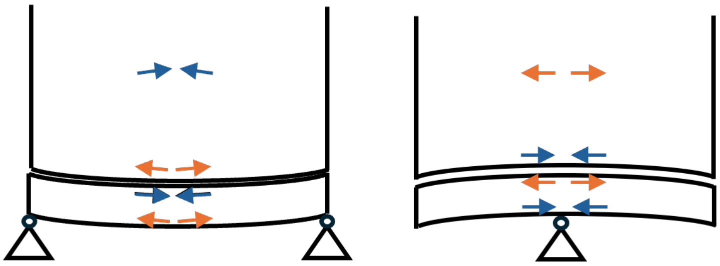

Figure 6.23: Schematisation of the local stress propagation of the wall system (Orange=Tension & Blue=Compression)

There are no tension stresses that are present at the top of the wall in any of the calculations, which means that there is no rocking of the panels. When constructing this system with individual panels, a proper connection should be made that takes these tension stresses into account. Especially if the design loads are increased.

7 Discussion

In this chapter, different model assumptions and their impact will be discussed. Furthermore, the influence of differentiations in the soil and foundation properties will be discussed.

7.1. Soil assumptions

In Appendix D, a few soil differentiations are investigated. The results show the importance of the soil properties on the settlement of a pile. In this study several assumptions were made regarding the soil conditions:

- **Assumed soil properties**: The soil properties used in this research are based on Table 5.3 in Appendix A. This table is used to give an approximation of the soil parameters that can be expected. However, there are multiple factors that influence the properties of the soil. For instance, deeper clay layers have been subjected to prolonged compression over time, likely resulting in increased consolidation and greater resistance to further compression.

- **Homogeneous soil properties**: The soil is assumed to be homogeneous across the entire foundation area. In reality, variations in soil composition, stiffness, and bearing capacity can occur due to natural inconsistencies. Small-scale inhomogeneities may lead to differential settlement. Additionally, natural variations in soil composition, moisture content, and previous loading conditions may lead to localized deviations from the assumed values, potentially affecting settlement predictions.

- **Groundwater level stability**: The analysis assumes that the groundwater level remains stable over time. However, groundwater fluctuations due to seasonal changes or drainage variations can significantly affect settlement behaviour. Changes in groundwater levels could influence the total settlement or even the differential settlement if the level is not equal over the whole 12 meters.

7.2. Structure assumptions

The structural analysis in this study relies on several assumptions regarding material behaviour, load distribution, and structural connections. These simplifications, while necessary for feasibility, introduce certain limitations:

- **Connection behaviour and creep:** The timber elements require mechanical connections, which may experience deformation over time due to creep or cyclic loading. These deformations are not explicitly modelled, as they are considered negligible compared to the overall structural deformations and the relatively low stress levels in the structure. However, for larger or multi-story buildings, connection slip and creep effects could become more significant. Research by Pim Mol (Mol, 2023) demonstrates that fastener slip can increase total deformation in wooden structures, an aspect that should be considered in future studies.

- **2D Structural modelling limitations:** The structure was modelled in a two-dimensional (2D) environment, which inherently omits out-of-plane effects and the three-dimensional behaviour of load redistribution. In reality, torsional effects, lateral stiffness contributions, and localized connection flexibility could influence performance. A full 3D structural interaction analysis would provide a more comprehensive understanding of these effects.
- **Material performance over time:** The timber material is assumed to exhibit homogeneous elastic behaviour throughout its service life. However, long-term factors such as moisture variations, ageing effects, and material degradation may influence its structural performance.

7.3. Modelling approach

The numerical modelling approach adopted in this study provides valuable insights but comes with limitations. These constraints must be considered when interpreting the results:

- **Iterative numerical rounding errors:** The modelling process involves iterative calculations that can lead to numerical noise due to rounding errors. While these errors remain within acceptable tolerances, they may slightly influence predicted settlement values.
- **Group effect approximation:** The interaction between closely spaced piles was not possible to model in an axisymmetric model, but was estimated using empirical correlations. The general settlement patterns obtained in this study align with findings from Angeliki E. Arapakou and Vasileios P. Papadopoulos (Arapakou & Papadopoulos, 2012). While the approach provides a reasonable approximation, more refined finite element modelling could improve accuracy.

7.4. Case study: Influence foundation differentiations

The case study in this project is based on the relation between the stiffness of the superstructure and the settlements. However, changes in the soil composition or foundation elements have mostly been left out. To still investigate these changes, a separate case study has been done in Appendix D.2. The differentiations investigated are: the use of longer piles, piles with multiple helices and changes in the soil profile. The information obtained from this case study can be summarized as follows:

- Using a longer foundation pile with a lower helix lessens the settlement of the pile. The difference in settlement increases over time.
- A weaker soil layer than estimated, will increase the settlement.
- A depth change of the Pleistocene soil layer is less impactful than a depth change of the helical plate.
- Using two helical plates improves the resistance of the pile to settlement. This resistance is not expected to increase at later stages in time. Secondary settlement is therefore similar to a pile with a single helix.
- When using two helical plates on a pile, a wider spacing between the helical plates is more beneficial for resisting settlements.

With the obtained knowledge, better advise can be given on the optimisation of this structure.

8 Conclusion

In an attempt to find a sustainable solution for the housing crisis at short notice, a lightweight, timber building design is proposed that is placed on short foundation piles. This research investigates the impact of helical foundation piles on the settlement of the structure and how the stiffness of the superstructure can influence these settlements. The research aims to provide an answer to the question:

”What is the structural feasibility of a lightweight, modular wooden building design on short, screwed foundation piles that is expected to have large amount of settlement?”

Starting with the foundation methodology of using short, screwed, helical foundation piles, it is feasible to support a lightweight structure without structural problems if the present soil is homogeneous over the length of the structure. These piles transfer vertical loads to deeper soil that have a higher effective stress. This provides a higher bearing capacity and reduces settlement over time to some extent. A minimum spacing of two times the diameter of the helical plate is required when positioned in soft soil, to ensure that the interaction between the foundation piles is minimise. The helical plate provides most of the bearing capacity and the position is therefore important. Placing the plate in peat soil will lead to a lower capacity and higher settlements, risking the stability of the structure, and should be avoided. Lastly, when helical piles are installed in soft soil, large amount of settlement will occur in both the short and long term. To prove that a structure is sufficient, the settlements should be considered at multiple points in time in terms of total settlement (U), differential rotations (β), tilt (ω), and element capacity (σ).

Creating a proper design for the wall system, contributes to a structure that is more resistant to total settlements and differential settlements. A stiffer wall system has the ability to redistribute more force to the foundation piles at the most outer position. This reduces the differential settlement between piles, but also reduces the maximum total settlement of the wall. The resistance to deformations of the outer foundation piles is therefore more impactful with a stiffer superstructure.

The redistribution of forces within the wall does lead to an increase in compressive vertical stress above the outer supports that also increase over time. For this case study, where the boundary conditions are based of the differential displacements, these stresses do not cause failure. Tension stresses will occur within the wall, but none will lead to rocking of the panels for the cases in this research.

Overall, the settlements caused by permanent and uneven live loads do not threaten the structural integrity of the building. Utilising the wall system of the building to redistribute forces over the foundation piles, improves the resilience of the structure to differential displacements and makes it save for use. The main concern for this structure in a location with a homogeneous soil profile is overall settlement. This is particularly important for utility connections and timber components, which have specific limitations regarding decay prevention.

9 Recommendations

This chapter will give recommendations for the design based on the information obtained in the results and will give suggestions for future research to increase the validity of this design methodology.

9.1. Concept design

Time dependency

This research demonstrates promising results for the construction of small-scale lightweight structures using this methodology. However, the calculations show that constructions that fulfil the requirements at the start of its life time, do not guarantee a sufficient structure later on. That is why in future projects with the same building concept, it is recommended to investigate the structure at multiple stages throughout its lifetime. The following three stages are recommended:

- At the end of the construction;
- After 100 days. This gives insight on if the structure is sufficient after the primary consolidation has ended;
- At the intended end of the structures lifetime. This ensures that the structure is sufficient after large amount of secondary settlement.

Importance of the outer piles with stiff wall systems

In structures where significant settlement is not expected, the outer foundation piles are often designed with smaller dimensions. These piles typically bear less load, allowing for cost reductions by minimising their size. However, in this research, stiffer systems demonstrate a greater reliance on the capacity of the outer piles. Increasing the load-bearing capacity of these outer piles could help mitigate the tilt of the structure.

It is important to note that enhancing the capacity of the outer piles also leads to greater force redistribution within the system, potentially causing the overall capacity to be reached sooner. Measurements such as using multiple helices or positioning the helix deeper in the soil, can be used to improve the capacity of the outer piles. These measurements will also increase the piles resistance to settlement, meaning that over time the stiffness of the support increases in comparison to the other piles. The stresses within the structural elements will over time increase as well.

Sustainability

The main concept design of this project, aims to find a sustainable, short term solution to address the housing crisis. This should be achieved by using mostly environmental friendly and reusable materials. The structure consists of steel helical piles for the foundation and wooden elements for the superstructure to match this philosophy.

Steel helical piles are selected for their reusability and ease of retrieval. Their short length and screw-in installation allow for quick deployment and removal, making them a low-impact alternative to traditional deep foundations. However, the steel is susceptible for corrosion, especially when exposed to fluctuating groundwater levels. To ensure longevity, proper treatments such as hot-dip galvanization or protective coatings should be applied to prevent corrosion.

Lastly, the wooden components come from sustainable sources. However, their longevity is dependent on the moisture exposure. With a proper design this will not cause big problems, but it might be worth considering hardwood or even steel as foundation beams on top of the piles. This would make the building design better at dealing with unexpectedly high settlements that result in the structure getting in contact with the soil surface. Treating the wood with chemicals would also make it more resistant to moisture exposure, but it will make the components less reusable and environmental friendly. Ideally, this should be avoided.

9.2. Future research

While this study has provided valuable insights into the structural feasibility of this building design, several aspects require further investigation to refine and optimize the design. Future research should focus on a 3D model for the settlements, the impact of dynamic loading on the structure and a more detailed structural model on the connections of the timber structure.

3D PLAXIS model
In this research, multiple assumptions were done to represent the 3D effects of the short helical pile foundation. To better understand the real effects of this foundation methodology, a 3D model should be developed. This would provide insights into:

- The effect of a non homogeneous soil profile;
- The effect of using a group of helical piles on the displacements of each pile;
- The effect of other nearby structures on the settlement of the building.

The use of a single 3D model will also take away the rounding errors caused by the iterative process between PLAXIS 2D and SCIA Engineer.

Connection design of the timber elements
The use of timber elements in construction introduces additional mechanisms that this research has not explored in detail. Future studies should focus on the long-term effects of differential settlement on timber structures, particularly in relation to joint behaviour and creep. Investigating how connections perform over time under varying settlement conditions would provide valuable insights into the durability and serviceability of timber construction.

Field test
To validate the predicted settlements and assess the behaviour of the structure under real-world conditions, it is essential to conduct full-scale field tests. Such tests would provide empirical data to confirm the performance of the design. It will also be helpful in researching the influence of the modelling assumptions used in this study.

More locations
In this research, a single soil profile is used that represents a location with large layers of soft soil. While variations within this profile have been considered, the study does not account for other geographical locations with different soil conditions. Expanding the research to include diverse soil profiles and locations would offer a broader understanding of how the foundation system performs under varying ground conditions.

Dynamic behaviour
Lastly, future research should look into the dynamic loads caused by wind or seismic activity. This is especially relevant for lightweight timber structures, which may exhibit different responses to dynamic forces compared to heavier materials.

Bibliography

Reference manual 2d. (2024, May). Bentley.

Arapakou, A. E., & Papadopoulos, V. P. (2012). Factors affecting differential settlements of framed structures. *30*, 1323–1333. https://doi.org/10.1007/s10706-012-9546-x

Backhausen, U., & van der Stoel, A. (2014, July). *Reader geotechniek*. KIVI, Den Haag.

Björdal, C. G. (2012). Microbial degradation of waterlogged archaeological wood. *Journal of Cultural Heritage 13*, *13*, 118–122. https://doi.org/10.1016/j.culher.2012.02.003

Blaß, H. J., & Görlacher, R. (2017). *Timber engineering principles for design*. KIT Scientific Publishing.

Bodemkaart nederland [Accessed: 2024-06-28]. (2014). https://versestad.nl/2015/01/jaar-van-de-bodem-2015/bodemkaartnl/

Brandner, R., Tomasi, R., thomas moosbrugger, Serrano, E., & Dietsch, P. (2018, September). *A state-of-the-art report: Properties, testing and design of cross laminated timber*. Shaker. https://doi.org/10.2370/9783844061437

The clt handbook. (2019, May). Swedish Wood. https://www.swedishwood.com/publications/list_of_swedish_woods_publications/the-clt-handbook/

Coduto, D. P., Kitch, W. A., & Kitch, W. A. (2016). *Foundation design, principles and practices* (Vol. 3). PEARSON. https://istasazeh-co.com/pdf/Foundation-design-principles-and-practices-Donald-P-Coduto.pdf

D'Amicoa, B., Kermani, A., Porteous, J., Dhonju, R., & Zhang, B. (2016). Racking performance of platform timber framed walls assessed by rigid body relaxation technique. *Construction and Building Materials*, *129*, 148–158. https://doi.org/10.1016/j.conbuildmat.2016.10.106

Elsherbiny, Z., & Naggar, M. E. (2013). The performance of helical pile groups under compressive loads: A numerical investigation. *Proceedings of the 18th International Conference on Soil Mechanics and Geotechnical Engineering*, 2723–2726. https://www.researchgate.net/publication/278405899_The_Performance_of_Helical_Pile_Groups_Under_Compressive_Loads_A_Numerical_Investigation

Engineersview. (2024). *Pile foundations : Necessity, types on different basis* [Accessed: 2024-09-20]. https://engineersviews.com/pile-foundations-necessity-types-on-different-basis/

Farhad Nabizadeh, A. J. C. (2017). Field study of capacity helical piles in sand and silty clay. https://doi.org/10.1007/s40515-016-0036-0

Forest Products Laboratory. (2021, March). *Wood handbook: Wood as an engineering material*.

Hogerheijde, S. (2023, November). *Lowering eci/mpg value by implementing sustainable foundations for houses* [Master's thesis, Delft University of Technology].

Huizinga, T. K. (1969). *Gondmechanica, en haar toepassingen bij grond- en kunstwerken*. Agon Elsevier.

Jahanshahinowkandeh, M., & Choobbasti, A. J. (2021). Numerical study of single helical piles and helical pile groups under compressive loading in cohesive and cohesionless soils. *80*, 4001–4023. https://doi.org/10.1007/s10064-021-02158-w

Karami, M., Basack, S., Das, G., Bhadra, D., & Karakouzian, M. (2023). Experimental and numerical evaluations of load settlement response of helical piles in soft clay. *61*. https://doi.org/10.1016/j.ibiod.2007.07.006

Klaassen, R. K. W. M. (2007). Bacterial decay in wooden foundation. *International Biodeterioration & Biodegradation*, *61*, 45–60. https://doi.org/10.1016/j.ibiod.2007.07.006

Lai, V. Q., Keawsawasvong, S., & Do, H. (2022). Performance analysis of pile under negative skin friction by load-transfer method. *Lecture Notes in Civil Engineering*. https://doi.org/10.1007/978-981-19-3303-5_56

Mol, P. (2023, February). *Structural analysis of clt walls in façades of a multistory building* [Master's thesis, TU Delft]. http://resolver.tudelft.nl/uuid:2ff8ea83-76ba-4913-8eec-2d558e775d11

The natural pavilion [Accessed: 25-Feb-2025]. (2022). https://www.thenaturalpavilion.eu/

Nederlands Normalisatie-instituut. (2011). Nen-en 1995: Design of timber structures. https://connect.nen.nl/Standard/Detail/161458?compId=10037&collectionId=0

Nederlands Normalisatie-instituut. (2017). Nen 9997: Geotechnisch ontwerp van constructies. https://connect.nen.nl/Standard/Detail/3535337?compId=10037&collectionId=0

Nederlands Normalisatie-instituut. (2019a). NEN 1990: Grondslagen voor het constructief ontwerp. https://connect.nen.nl/Standard/Detail/3622790?compId=10037&collectionId=0

Nederlands Normalisatie-instituut. (2019b). NEN 1991: Belastingen op constructies. https://connect.nen.nl/Standard/Detail/3622772?compId=10037&collectionId=0

Perko, H. A. (2009). *Helical piles, practice guide* (Vol. 1). John Wiley Sons.

Prakash, S., & Sharma, H. D. (1990). *Pile foundations in practice*. John Wiley & Sons, Inc.

Trutalli, D. (2017). Durability of timber structures [Lecture presentation, Università degli Studi di Padova].

Rijksoverheid. (2024). *900.000 nieuwe woningen om aan groeiende vraag te voldoen* [Accessed: 2024-07-15]. https://www.rijksoverheid.nl/onderwerpen/volkshuisvesting/nieuwe-woningen

Sandanayake, M., Zhang, G., & Setunge, S. (2016). Environmental emissions at foundation construction stage of buildings. *95*, 189–198. https://doi.org/10.1016/j.buildenv.2015.09.002

Shuman, N. M., Khan, S., & Amini, F. (2022). Settlement based load capacity curve for single helix helical pile. *63*, 101265. https://doi.org/10.1016/j.sandf.2022.101265

Singh, A., Kim, Y., & Singh, T. (2016). Bacterial degradation of wood. In *Secondary xylem biology* (pp. 169–190). Elsevier. https://doi.org/10.1016/B978-0-12-802185-9.00009-7

Syahbana, A. J., & Sarah, D. (2013). Comparison of overconsolidated clay settlements calculated by analytical 1d terzaghi consolidation and biot numerical analysis. *RISET Geologi dan Pertambangan*, *22*, 81–91. https://doi.org/10.14203/risetgeotam2012.v22.60

TNO. (2016). Diktekaart holocene slappe lagen nederland. https://www.cob.nl/document/diktekaart-holocene-slappe-lagen-nederland/

TNO. (2024). *Data and information on the dutch subsurface* [Accessed: 2024-10-02]. https://www.dinoloket.nl/

Türedi, Y., & Örnek, M. (2020). Analysis of model helical piles subjected to axial compression. *72*, 759–769. https://doi.org/10.14256/JCE.2660.2019

Verruijt, A. (1999). *Gondmechanica*. Delft University. https://geo.verruijt.net/software/GrondMechBoek.pdf

A

Appendix A: Soil properties

In this Appendix, the soil properties used for the calculation are given and the determination of the chosen soil profile is explained. First Table A.1 gives the soil properties obtained from the NEN9997.

Grondsoort			Karakteristieke waarde [a] van grondeigenschap											
Hoofdnaam	Bijmengsel	Consistentie [b]	γ [c] kN/m^3	γ_{sat} kN/m^3	q_c [d g] MPa	C'_p [g]	C'_s	$C_c/(1+e_0)$ [g] [-]	C_α [f] [-]	$C_{sw}/(1+e_0)$ [g] [-]	E_{100} [g h] MPa	φ' [g] Graden	c' kPa	c_u kPa
Grind	Zwak siltig	Los	17	19	15	500	∞	0,004 6	0	0,001 5	45	32,5	0	
		Matig	18	20	25	1 000	∞	0,002 3	0	0,000 8	75	35,0	0	N.v.t.
		Vast	19 20	21 22	30	1 200 1 400	∞	0,001 9 0,001 6	0	0,000 6 0,000 5	90 105	37,5 40,0	0	
	Sterk siltig	Los	18	20	10	400	∞	0,005 8	0	0,001 9	30	30,0	0	
		Matig	19	21	15	600	∞	0,003 8	0	0,001 3	45	32,5	0	N.v.t.
		Vast	20 21	22 22,5	25	1 000 1 500	∞	0,002 3 0,001 5	0	0,000 8 0,000 5	75 110	35,0 40,0	0	
Zand	Schoon	Los	17	19	5	200	∞	0,011 5	0	0,003 8	15	30,0	0	
		Matig	18	20	15	600	∞	0,003 8	0	0,001 3	45	32,5	0	N.v.t.
		Vast	19 20	21 22	25	1 000 1 500	∞	0,002 3 0,001 5	0	0,000 8 0,000 5	75 110	35,0 40,0	0	
	Zwak siltig, kleiig		18 19	20 21	12	450 650	∞	0,005 1 0,003 5	0	0,001 7 0,001 2	35 50	27,0 32,5	0	N.v.t.
	Sterk siltig, kleiig		18 19	20 21	8	200 400	∞	0,011 5 0,005 8	0	0,003 8 0,001 9	15 30	25,0 30,0	0	N.v.t.
Leem [e]	Zwak zandig	Slap	19	19	1	25	650	0,092 0	0,003 7	0,030 7	2	27,5 30,0	0	50
		Matig	20	20	2	45	1 300	0,051 1	0,002 0	0,017 0	3	27,5 32,5	1	100
		Vast	21 22	21 22	3	70 100	1 900 2 500	0,032 9 0,023 0	0,001 3 0,000 9	0,011 0 0,007 7	5 7	27,5 35,0	2,5 3,8	200 300
	Sterk zandig		19 20	19 20	2	45 70	1 300 2 000	0,051 1 0,032 9	0,002 0 0,001 3	0,017 0 0,011 0	3 5	27,5 35,0	0 1	50 100
Klei	Schoon	Slap	14	14	0,5	7	80	0,328 6	0,013 1	0,109 5	1	17,5	0	25
		Matig	17	17	1,0	15	160	0,153 3	0,006 1	0,051 1	2	17,5	5	50
		Vast	19 20	19 20	2,0	25 30	320 500	0,092 0 0,076 7	0,003 7 0,003 1	0,030 7 0,025 6	4 10	17,5 25,0	13 15	100 200
	Zwak zandig	Slap	15	15	0,7	10	110	0,230 0	0,009 2	0,076 7	1,5	22,5	0	40
		Matig	18	18	1,5	20	240	0,115 0	0,004 6	0,038 3	3	22,5	5	80
		Vast	20 21	20 21	2,5	30 50	400 600	0,076 7 0,046 0	0,003 1 0,001 8	0,025 6 0,015 3	5 10	22,5 27,5	13 15	120 170
	Sterk zandig	-	18 20	18 20	1,0	25 140	320 1 680	0,092 0 0,016 4	0,003 7 0,000 7	0,030 7 0,005 5	2 5	27,5 32,5	0 1	0 10
	Organisch	Slap	13	13	0,2	7,5	30	0,306 7	0,015 3	0,102 2	0,5	15,0	0 1	10
		Matig	15 16	15 16	0,5	10 15	40 60	0,230 0 0,153 3	0,011 5 0,007 7	0,076 7 0,051 1	1,0 2,0	15,0	0 1	25 30
Veen	Niet voorbelast	Slap	10 12	10 12	0,1	5 7,5	20 30	0,460 0 0,306 7	0,023 0 0,015 3	0,153 3 0,102 2	0,2 0,5	15,0	1 2,5	10 20
	Matig voorbelast	Matig	12 13	12 13	0,2	7,5 10	30 40	0,306 7 0,230 0	0,015 3 0,011 5	0,102 2 0,076 7	0,5 1,0	15,0	2,5 5	20 30
Variatiecoëfficiënt v			0,05		–	0,25					0,10		0,20	

[a] De tabel geeft van de desbetreffende grondsoort de lage, respectievelijk de hoge karakteristieke waarde van gemiddelden. Binnen een gebied, vastgesteld door de rij van het bijmengsel en de kolom van de parameter (een cel), geldt:

— als een verhoging van de waarde van een van de grondeigenschappen tot een ongunstiger situatie leidt dan de toepassing van de in de tabel gepresenteerde lagere karakteristieke waarde, moet de rechterwaarde op dezelfde regel zijn gebruikt. Is er rechts geen waarde vermeld, dan moet de waarde er recht onder zijn toegepast;
OPMERKING Dit is bijvoorbeeld het geval bij negatieve kleef op een paal waar een hogere waarde van φ', c' en c_u ook een hogere waarde van de negatieve kleef oplevert.

— voor $C_c/(1+e_0)$, C_α en $C_{sw}/(1+e_0)$ zijn in de tabel de hoge karakteristieke gemiddelde waarden vermeld.

Figure A.1: Soil properties(Nederlands Normalisatie-instituut, 2017)

Determining ground profile of a location can be done by doing a cone penetration test (CPT). This test measures the resistance on the cone and the friction over a certain depth. By analysing these measurements the soil type at a given depth can be determined. Figure A.3 and Table A.1 show the estimated values for different soil types with their values in relation to the cone penetration test.

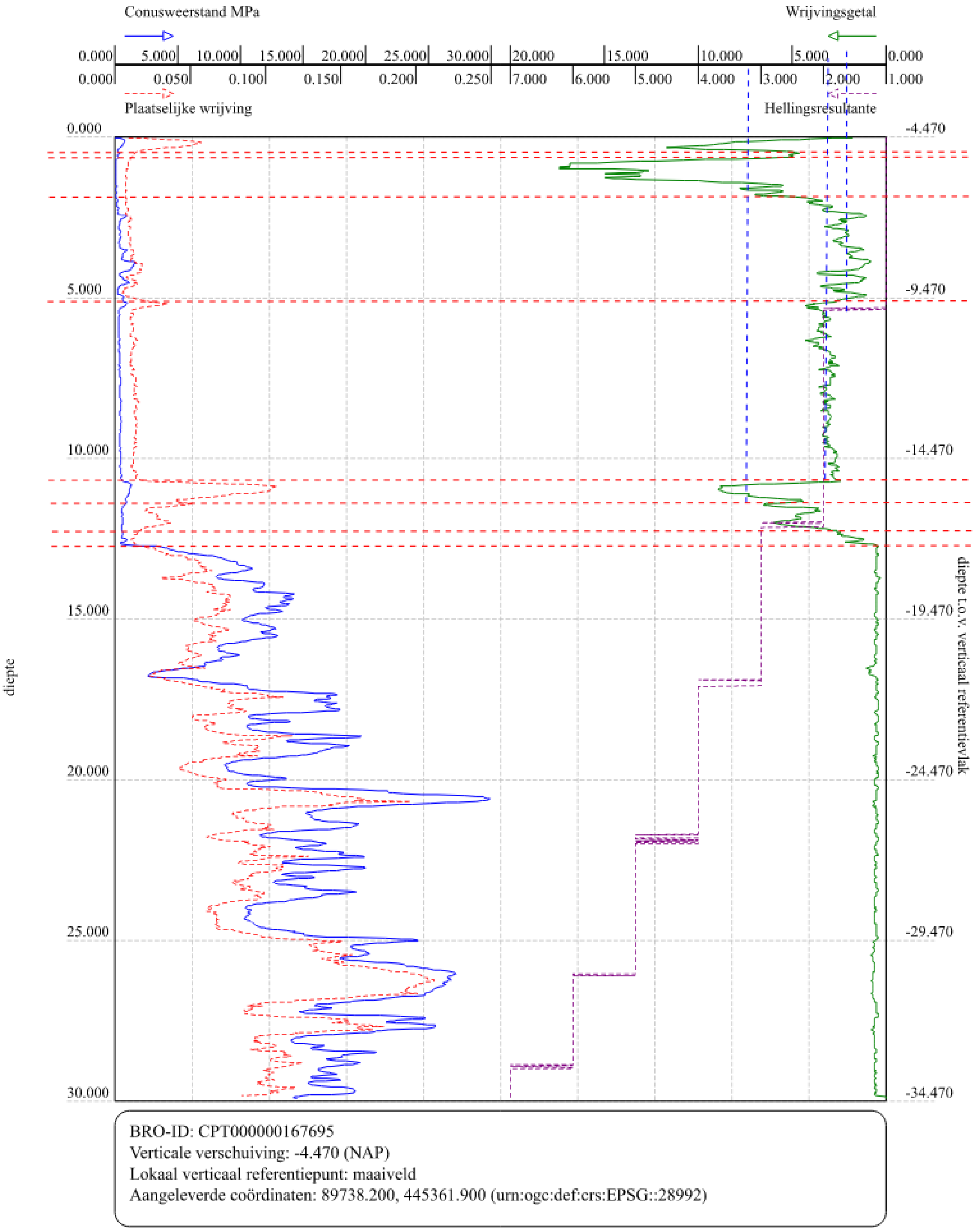

Figure A.2: CPT Oude Leedenweg (TNO, 2024)

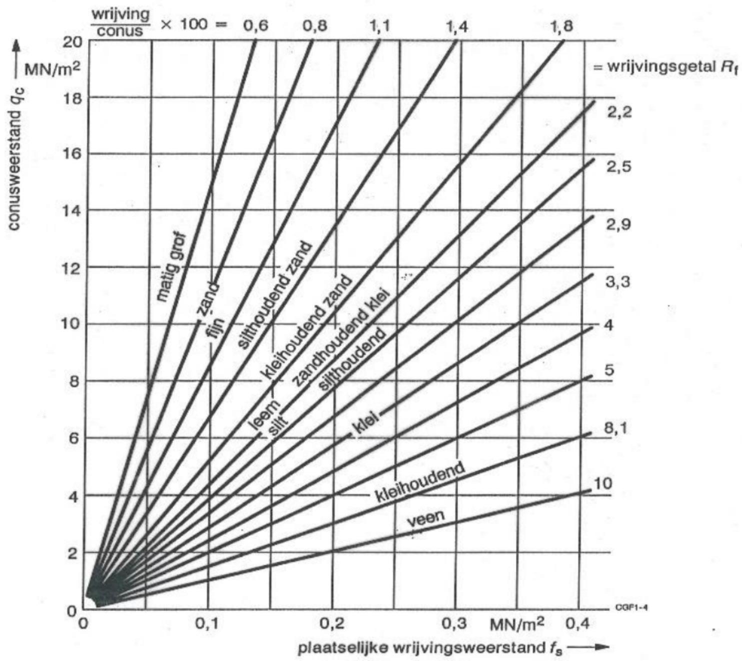

Figure A.3: Relation friction ratio with soil (Backhausen & van der Stoel, 2014)

Table A.1: Friction ratio and cone resistance for different soil types.

Soil Type	Friction Ratio [%]	Cone Resistance [MPa]
Clay	3.0 – 6.0	2.0 – 5.0
Peat	> 6.0	5.0 – 10.0
Loam	1.2 – 3.0	2.0 – 4.0
Sand	0.5 – 2.0	> 5.0
Gravel	0.2 – 0.5	15 – 30

This results in the following soil profile:

Top Layer (m)	Bottom Layer (m)	Soil Type
0.0	-0.5	Peat weak
-0.5	-0.6	Clay weak mod
-0.6	-1.8	Peat mod
-1.8	-5.0	Clay sandy mod
-5.0	-10.6	Clay clean mod
-10.6	-11.3	Peat mod
-11.3	-12.2	Clay clean weak
-12.2	-12.7	Clay sandy mod
-12.7	-16.0	Sand clean mod

The groundwater level will be assumed to be at 4.5 meters underneath NAP. This value is estimated by available information in Dinoloket. From the database the Groundwater level graph of a nearby location is obtained and after 2004 the groundwater has exceeded -4.5m NAP once, see Figure. With ground level being at -4m NAP, the phreatic level in the model will be at -0.5.

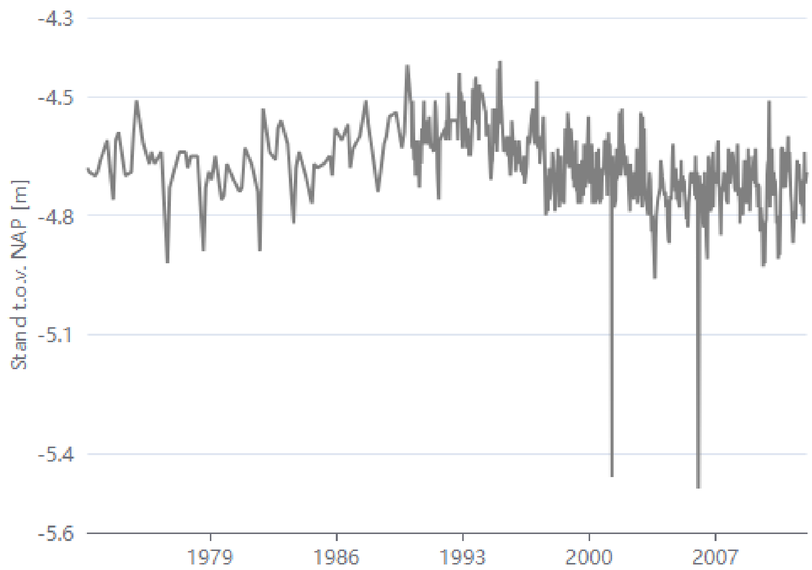

Figure A.4: Groundwater level Oude Leedenweg (TNO, 2024)

B

Appendix B: Validation of the settlement

For the calculations done by using PLAXIS software, a soft soil creep model is used to determine the settlements of a helical pile. This model takes into account the immediate, primary, and secondary settlements. To validate the model, a hand calculation is done from which the results will be compared to the PLAXIS model.

The stress increase in the soil is most apparent underneath the helical plate. Looking at the stress increase deeper in the soil, it can be seen that it spreads out as discussed in Section **??**. Of the soil, the first 2 meters underneath the helical plate will be investigated. This soil consist of clay soil that is moderately sandy. The input for moderately sandy clay soil is as follows:

Properties of Clay sandy moderate soil:

γ_{unsat}	18	kN/m^3
γ_{sat}	18	kN/m^3
E_{ref}	3	MPa
ν	0.3	$-$
c'_{ref}	5	kPa
ϕ	22.5	$degrees$
C_c	0.173	$-$
C_s	0.017	$-$
C_a	0.004	$-$
C'_p	20	$-$
C'_s	240	$-$

The pile properties are:

Unit weight	$78,5kN/m^3$;
E_{ref}	$2,0 * 10^5 N/mm^2$;
d	$0,1m$;
D	$0,6m$.

A force of 20 kN is chosen for this validation. The equivalent stress underneath the surface pile is 70,7 kPa.

The soil layer of moderately sandy soil is split into layers with the size of 200 mm. This is done to take into account the non linear spreading of the stress, described in Section 2.2.2.

B.1. Effective stress

To calculate the settlement underneath the pile the effective stress within the soil has to be determined. This can be done by using the soil properties found in Appendix A and equations 2.1, 2.2 and 2.3. The soil profile given in Table 4.1 results in the stresses shown in Table B.1at depth where there is a change in soil condition.

$$\sigma'_{zz} = \sigma_{zz} - pwp \tag{2.1}$$

$$\sigma_{zz} = \gamma \cdot z \tag{2.2}$$

$$pwp = \gamma_w \cdot z_w \tag{2.3}$$

Table B.1: Stresses at different depths for the location

Depth [m]	σ_{zz} [kPa]	pwp [kPa]	σ'_{zz} [kPa]
0.0	0.0	0.0	0.0
0.5	5.5	0.0	5.5
0.6	6.9	0.0	6.9
1.0	11.7	0.0	11.7
1.8	21.3	8.0	13.3
5.0	78.9	40.0	38.9
10.6	174.1	96.0	78.1
11.3	183.9	103.0	80.9
12.2	200.1	112.0	88.1
12.7	210.1	117.0	93.1
16.0	276.1	150.0	126.1

The groundwater level is estimated at a depth of one meter underneath the surface. Each meter going downwards the water stress will increase with 10 kPa. A schematisation of the soil stress and water stress is given in Figure B.1

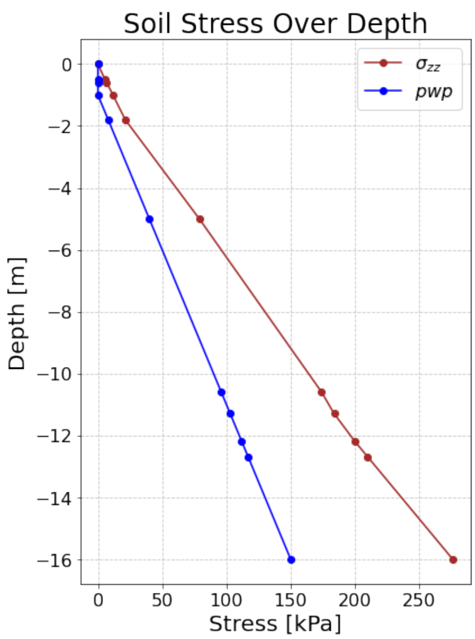

Figure B.1: Stress propagation of σ_{zz} and pwp over depth with the estimated soil profile

B.2. Stress spreading underneath a helical pile

The stress underneath a circular surface spreads out over the depth. A conservative value of the stress at a certain depth can be calculated with formula 2.4.

$$\Delta\sigma'_{v,z,d} = p_{\text{gem},d} \times \left(1 - \frac{1}{\sqrt{\left(1+\frac{a^2}{z^2}\right)^3}}\right) \tag{2.4}$$

Where:

$\Delta\sigma'_{v,z,d}$:	The calculated value of the effective stress increase at a depth z, in kPa;
$p_{\text{gem},d}$:	The calculated value of the uniformly distributed load, in kPa;
a:	Radius of the circular load, in m;
z:	Depth underneath the circular load, in m;

For each segment of 200 mm soil, the average effective stress increase is calculated. For instance, the first segment has stress of 70,7 kPa at the top and, by using equation, 2.4 the bottom stress at a depth of 0,2 m is calculated to be 58,7 kPa. The average stress in the segment is therefore 64,7 kPa. This is done for 10 segments covering 2 meters of soil underneath the helical plate.

Table B.2: Segment stress increase overview

Segment	p_{top} [kPa]	p_{bot} [kPa]	a [m]	z [m]	p_{avg} [kPa]
1	70.7	58.7	0.3	0.2	64.7
2	58.7	34.5	0.3	0.4	46.6
3	34.5	20.1	0.3	0.6	27.3
4	20.1	12.7	0.3	0.8	16.4
5	12.7	8.6	0.3	1.0	10.6
6	8.6	6.1	0.3	1.2	7.4
7	6.1	4.6	0.3	1.4	5.4
8	4.6	3.6	0.3	1.6	4.1
9	3.6	2.8	0.3	1.8	3.2
10	2.8	2.3	0.3	2.0	2.6

B.3. Hand calculation pile settlement

For each segment a hand calculation is done to estimate the expected settlements and validate the model. The formulas 2.5, 2.7 and 2.9 are used to make this estimation.

$$\Delta D = -\frac{(1+\nu)(1-2\nu)}{E(1-\nu)} * p * D \tag{2.5}$$

$$s_1 = \sum_{j=n}^{j=0} \frac{1}{C'_{p;j}} * d_j * log(\frac{\sigma'_{v;z;0;d} + \Delta\sigma'_{v;z;d}}{\sigma'_{v;z;0;d}}) \tag{2.7}$$

$$s_2 = \sum_{j=n}^{j=0} \frac{1}{C'_{s;j}} * d_j * log(\frac{t}{t_0}) * ln(\frac{\sigma'_{v;z;0;d} + \Delta\sigma'_{v;z;d}}{\sigma'_{v;z;0;d}}) \tag{2.9}$$

Immediate settlement
Each segment is has a thickness D of 200 mm and an elasticity modulus E of 3 MPa (obtained from Table A.1. The deeper the immediate settlement is calculated, the less the deformations become. The values found in B.2 are used for p in the equation.

Table B.3: Immediate settlement segment Overview

Segment	p [kPa]	D [mm]	ν	E_m [MPa]	ΔD [mm]
1	64.7	200	0.3	3	-3.2
2	46.6	200	0.3	3	-2.3
3	27.3	200	0.3	3	-1.4
4	16.4	200	0.3	3	-0.8
5	10.6	200	0.3	3	-0.5
6	7.4	200	0.3	3	-0.4
7	5.4	200	0.3	3	-0.3
8	4.1	200	0.3	3	-0.2
9	3.2	200	0.3	3	-0.2
10	2.6	200	0.3	3	-0.1

This results in a deformation of $\Delta D = -9,3mm$ in the first 2 meters under the helical plate.

Primary settlement

For the primary and secondary settlement, the existing effective stress affects the impact of the increase in stress. The existing effective soil stress is dependent on the depth and can be calculated for a depth between -3m and -5m by using the linear increase of the effective stress between depth -1,8m and -5m.

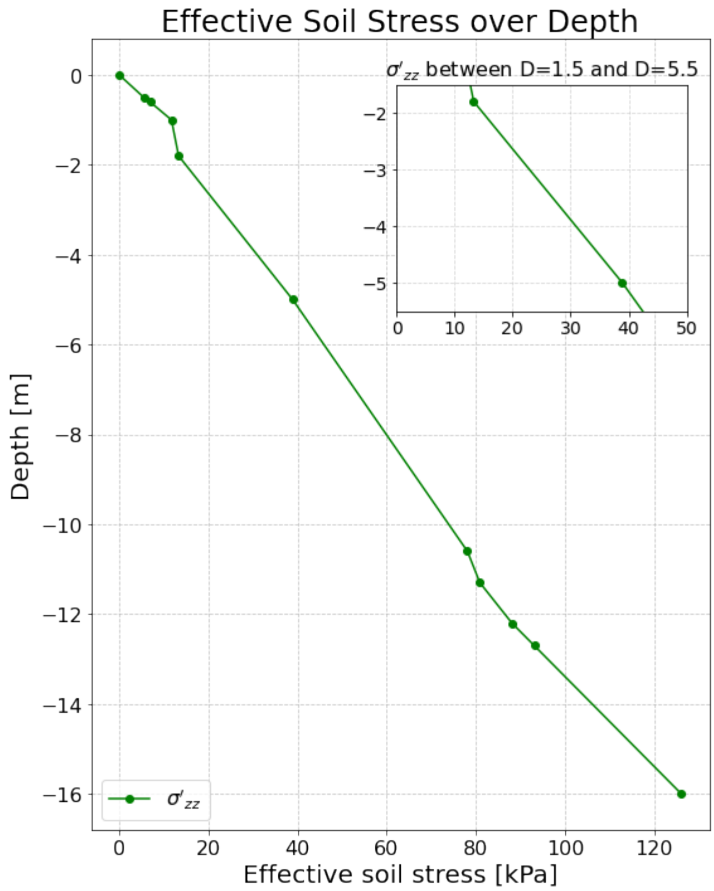

Figure B.2: Effective soil stress σ'_{zz} propagation over depth

This part of the effective stress can be described by the following formula:

$\sigma'_{zz} = \frac{D-1{,}8}{5{,}0-1{,}8} * (38{,}9 - 13{,}3) + 13{,}3$, for $1{,}8 < D < 5$

With the knowledge of the existing effective stress in the soil, the primary settlement s_1 can be calculated. Each s_1 is calculated by equation 2.7. This results in the calculation found in Table B.4.

Table B.4: Primary settlement segment Overview

Segment	$C'_{p:j}$	dj [mm]	D_{avg} [m]	σ [kPa]	s_1 [mm]
1	20	200	3.1	23.7	13.2
2	20	200	3.3	25.3	10.4
3	20	200	3.5	26.9	7.0
4	20	200	3.7	28.5	4.5
5	20	200	3.9	30.1	3.0
6	20	200	4.1	31.7	2.1
7	20	200	4.3	33.3	1.5
8	20	200	4.5	34.9	1.1
9	20	200	4.7	36.5	0.8
10	20	200	4.9	38.1	0.7

Adding the s_1 of each segment results in a total primary settlement of *44,4 mm*.

Secondary settlement

The same existing effective stress from the last calculation, is applicable for the secondary settlement of the pile s_2. The calculation results of each segment can be seen in Table B.5.

Table B.5: Secondary settlement segment Overview

Segment	$C'_{s:j}$	dj [mm]	Log(T/t0)	σ [kPa]	s_2 [mm]
1	240	200	2.1	23.7	2.3
2	240	200	2.1	25.3	1.8
3	240	200	2.1	26.9	1.2
4	240	200	2.1	28.5	0.8
5	240	200	2.1	30.1	0.5
6	240	200	2.1	31.7	0.4
7	240	200	2.1	33.3	0.3
8	240	200	2.1	34.9	0.2
9	240	200	2.1	36.5	0.1
10	240	200	2.1	38.1	0.1

Adding all the values of s_2 results in a settlement of 7,8 mm for this 2 meter thick segment of soil.

In conclusion the settlement of this 2 meter thick segment after 130 days, can be summarized as follows:

Settlement after 130 days

Immediate settlement $D = 9.3\,\text{mm}$
Primary settlement $s_1 = 44.4\,\text{mm}$
Secondary settlement $s_2 = 7.8\,\text{mm}$

Total settlement $s_2 = 61,5\,\text{mm}$

From the calculation it can be observed that around 75% of the total settlement in the first 100 days is caused by the primary settlement.

B.4. PLAXIS simulation

The same soil conditions stated in Table 5.3 are applied in the soft soil creep calculation in PLAXIS 2D. For this validation, the 2 meters underneath the helical plate will be investigated. The displacement of the pile will be distracted with the displacement of the soil at a depth of 5 meter. This will result in a value for the compression of the soil.

To simulate the calculation, the pile is placed and a load of 20 kN is applied at day 1. Afterwards the load stays for 99 days. The model will calculate the deformations at day 100 which results in a deformation schematisation shown in Figure B.3. The output shows a large displacement of the soil around the helical pile, but the differential displacement within the soil lessens at deeper levels.

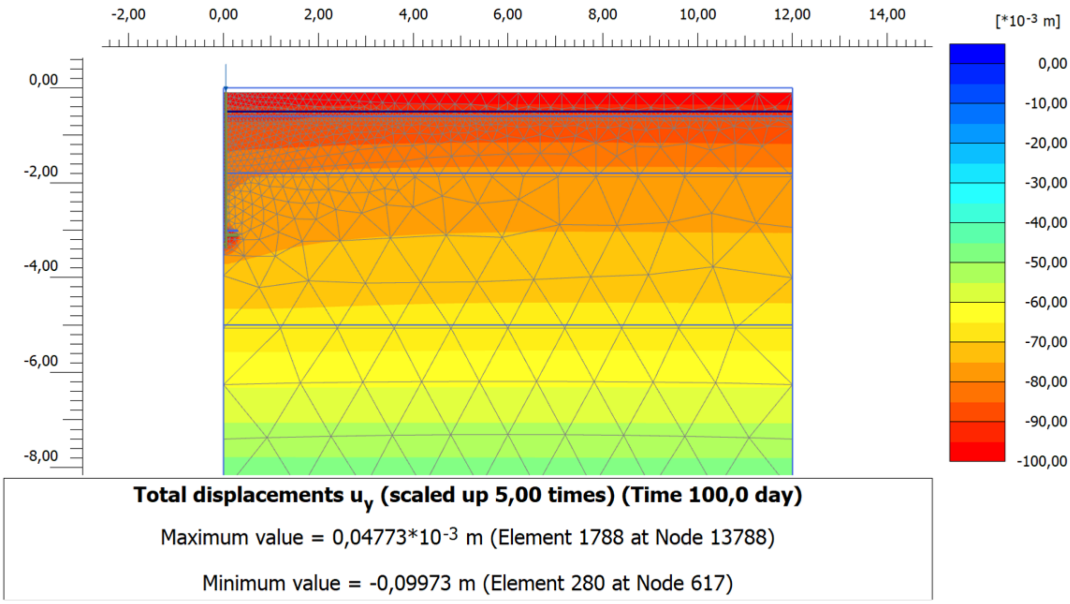

Figure B.3: Deformation results of a helical pile applied with 20 kN for 100 days

The helical plate settles 99,7 mm while the soil positioned at Y = -5 m settles with a value of 62,7 mm. The total compression of the soil body with thickness of 2 meters is therefore $99,7 - 61,7 = 38mm$.

B.5. Comparing results

When comparing the results of the hand calculation $(61,5mm)$ with the results of the PLAXIS model $(38mm)$, a difference of $22,5mm$ can be observed. The PLAXIS model expects the pile to settle 38% less than when it is calculated by hand. However, the order of magnitude is in line with the hand calculations. Several reasons can be given for the difference in settlement, but the intention of the hand calculation is the biggest.

Immediate settlement

The immediate settlement obtained from the hand calculation is based on drained soil conditions. With the position of the helical plate being underneath the groundwater level, the soil is not drained. The pore water pressure present in the soil adds resistance to the immediate deformations, since the soil is more difficult to move to the gabs in the soil.

Shaft friction

For the hand calculation, the shaft resistance is not taken into account. The shaft resistance leads to a reduction in stress at the helical plate.

Load not equally distributed

For the hand calculation, it is assumed that the point load applied on top of the helical pile is equally distributed. The software shows that this is not the case. Figure B.4 shows a stress distribution at the bottom of the foundation pile where the helical plate appears to apply less stress than assumed in the calculation and the stress increases just below the tip of the pile.

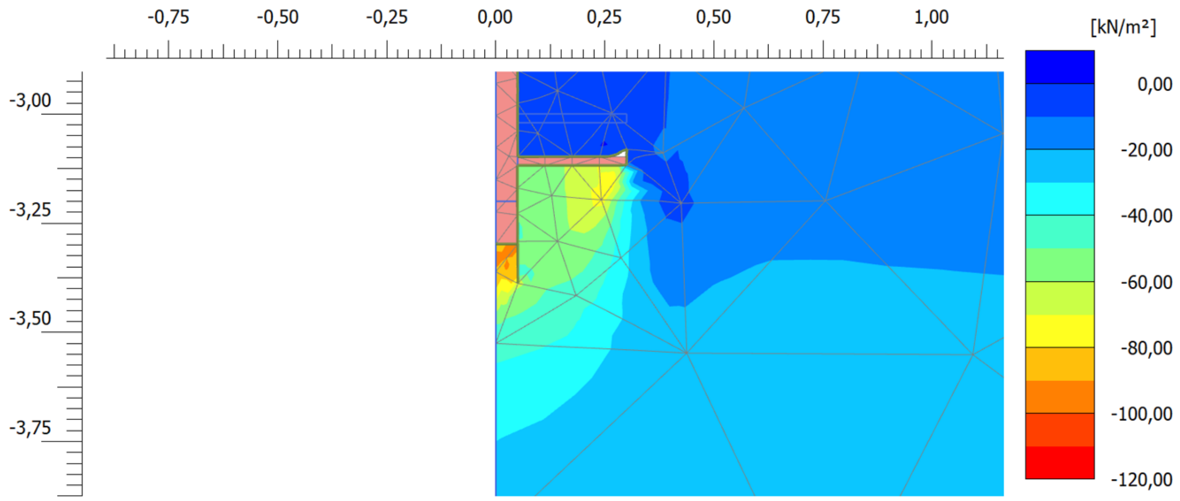

Figure B.4: Soil stress within the soil underneath the helical plate

Stress spreading assumption

A last reason for the results not matching, is the assumptions done in the hand calculation. In Figure 2.6 it is shown that the stress calculated is the maximum stress within the soil. The actual stress underneath the surface area of the plate is less than calculated. This is also supported with the results shown in Figure B.4, where a higher soil stress is shown underneath the tip of the helical pile. PLAXIS does take this into account and the deformation will therefore be less.

Shear effects

The formulas for the hand calculations are intended for an applied load over a big surface area. In this situation, the soil displacement can be calculated as a 1D compression. In the PLAXIS model, the shear stresses and horizontal strains do play a role in the calculation. Research from Arifan Jaya Syahbana and Dwi Sarah (Syahbana & Sarah, 2013) confirms this by comparing the two. The conclusion from this paper explains that for low loads ($< 40kN/m^2$) and loads with a smaller surface area, the expected settlement is lower in a 3D numerical model than with the 1D method of Terzaghi. Figure B.4 shows that most of the loads present in this part of the settlement calculation are lower than $< 40kN/m^2$ and since the helical plate has a relatively small area, compared to for instance an embankment, the settlement calculated in PLAXIS can be assumed to be representative.

B.6. Conclusion on validation

The settlement of a helical pile can be calculated by hand and with a program such as PLAXIS 2D. The calculation has a large difference, but it can be explained by multiple factors. The order of magnitude is correct and the behaviour of the soil matches the theory. Therefore, it can be concluded that PLAXIS is a good tool for estimating the settlement of a helical pile for this particular research.

C

Appendix C: Group effect

The current model in PLAXIS 2D is an axisymmetrical model. This type of model is not able replicate the multiple piles positioned underneath the structure at the same time. However, the group effect is important for the overall behaviour of the structure. The applied stress will spread out over the depth and eventually increase the soil stress underneath other piles, leading to larger settlement.

C.1. Methodology

The group effect will be implemented by looking at the deformation of soil at different distances from the pile. The deformation at $X = 12m$ is taken as the 0 point for these deformations since the influence of helical pile is neglectable at this distance. Figure C.1 Gives a schematisation of the calculation setup.

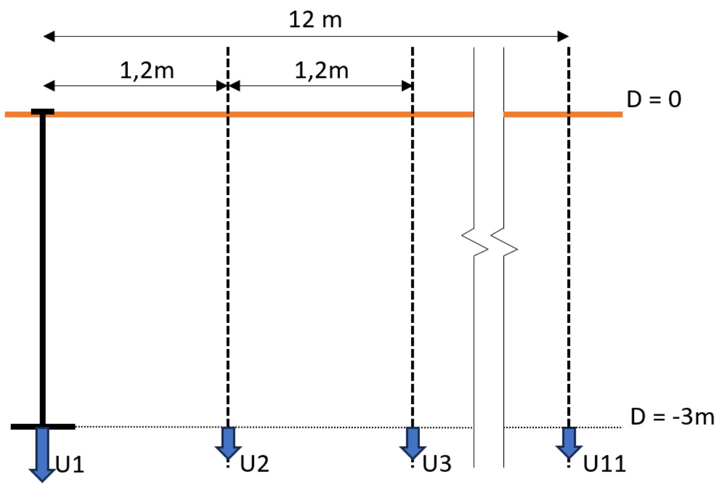

Figure C.1: Schematisation of the calculation setup for the pile influence at different distances

The calculation will investigate the situation of $F = 20kN$, $F = 30kN$ and $F = 40kN$ at day 30 (T0), day 130 (T100) and day 1030 (T1000) similar to the phases in from the research. Table C.1 summarizes this calculation setup.

Table C.1: Displacement soil at different distances setup

F	Day	U2 [mm]	U3 [mm]	U4 [mm]	U5 [mm]	U11 [mm]
20 kN	30	-	-	-	-	-
30 kN	30	-	-	-	-	-
40 kN	30	-	-	-	-	-
20 kN	130	-	-	-	-	-
30 kN	130	-	-	-	-	-
40 kN	130	-	-	-	-	-
20 kN	1030	-	-	-	-	-
30 kN	1030	-	-	-	-	-
40 kN	1030	-	-	-	-	-

By using the cross section tool in PLAXIS 2D, the vertical deformations at the desired height can be simulated. Figure shows the output of this tool for a load of 40 kN at T100.

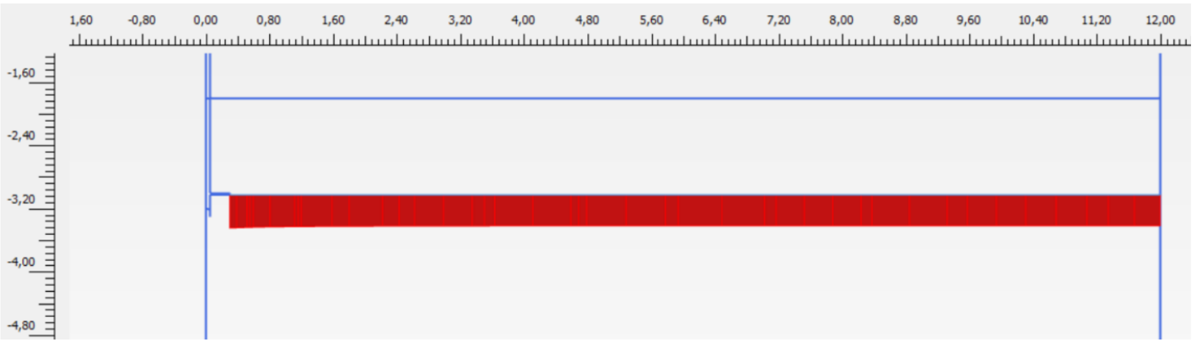

Figure C.2: Cross section of the soil showing the deformation at depth 3m for a pile loaded with 40 kN at T100

Each cross section can generate a table that shows the displacement of the local node. The deformations can be obtained giving the following result:

Table C.2: Displacement soil at different distances

F	Day	U2 [mm]	U3 [mm]	U4 [mm]	U5 [mm]	U11 [mm]
20 kN	30	56.2	55.5	55.2	55.1	55.2
30 kN	30	56.9	55.9	55.5	55.3	55.3
40 kN	30	57.7	56.2	55.7	55.4	55.4
20 kN	40	61.2	60.4	60.1	59.9	59.9
30 kN	40	62.0	60.8	60.4	60.1	60.0
40 kN	40	62.9	61.3	60.6	60.3	60.1
20 kN	130	81.2	80.1	79.6	79.4	79.2
30 kN	130	82.4	80.8	80.1	79.7	79.4
40 kN	130	83.5	81.4	80.5	80.0	79.5
20 kN	1030	115.8	114.3	113.7	113.4	113.0
30 kN	1030	117.3	115.2	114.3	113.8	113.2
40 kN	1030	118.7	115.9	114.7	114.1	113.3

The differential displacement of each support in comparison with support 11, is increasing over time. A table is constructed as an overview of these differential displacements:

Table C.3: Differential displacement of the supports in comparison to support 11

Δ U2_11 [mm]	Δ DU3_11 [mm]	Δ DU4_11 [mm]	Δ DU5_11 [mm]
1.0	0.3	0.0	-0.1
1.6	0.6	0.2	0.0
2.3	0.8	0.3	0.0
2.0	0.9	0.4	0.2
3.0	1.4	0.7	0.3
4.0	1.9	1.0	0.5
2.8	1.3	0.7	0.4
4.1	2.0	1.1	0.6
5.4	2.6	1.4	0.8

A matrix can be constructed that shows the displacement of each support as a consequence of other piles. At a distance of 4,8 meter from a pile, the influence of the load is less than 1 mm at all time stages and different loads. As a demonstration the matrix of the supports being loaded with a force of 30 KN at time stages T100 is constructed. The other calculated matrices are located in Appendix C.3.

Table C.4: Support Interactions $F = 30$ kN at T_{100} (U is in mm)

	Sup 1	**Sup 2**	**Sup 3**	**Sup 4**	**Sup 5**	**Sup 6**	**Sup 7**	**Sup 8**	**Sup 9**	**Sup 10**	**Sup 11**	**Sum**
U1	-	3.0	1.4	0.7	0.0	0.0	0.0	0.0	0.0	0.0	0.0	**5.1**
U2	3.0	-	3.0	1.4	0.7	0.0	0.0	0.0	0.0	0.0	0.0	**8.1**
U3	1.4	3.0	-	3.0	1.4	0.7	0.0	0.0	0.0	0.0	0.0	**9.5**
U4	0.7	1.4	3.0	-	3.0	1.4	0.7	0.0	0.0	0.0	0.0	**10.2**
U5	0.0	0.7	1.4	3.0	-	3.0	1.4	0.7	0.0	0.0	0.0	**10.2**
U6	0.0	0.0	0.7	1.4	3.0	-	3.0	1.4	0.7	0.0	0.0	**10.2**
U7	0.0	0.0	0.0	0.7	1.4	3.0	-	3.0	1.4	0.7	0.0	**10.2**
U8	0.0	0.0	0.0	0.0	0.7	1.4	3.0	-	3.0	1.4	0.7	**10.2**
U9	0.0	0.0	0.0	0.0	0.0	0.7	1.4	3.0	-	3.0	1.4	**9.5**
U10	0.0	0.0	0.0	0.0	0.0	0.0	0.7	1.4	3.0	-	3.0	**8.1**
U11	0.0	0.0	0.0	0.0	0.0	0.0	0.0	0.7	1.4	3.0	-	**5.1**

C.2. Conclusion

From the results of all the calculations, a few conclusions can be made. Firstly, the differential settlement of a support caused by other helical piles, increases over time. Secondly, the most inner positioned piles will have twice as much settlement caused by others, compared to the most outer positioned piles. Thirdly, the differential settlement is less than 5% in comparison with the total deformations caused by a maximum force of 40 kN.

For this research however, a difference in settlement of this order of magnitude is important. The relative rotations (β) between the piles should not exceed 1/300 and with a pile spacing of 1,2 meters, the difference in settlement should not exceed 4 mm. That is why a group settlement applicable to the load, should be implemented in the calculations. Section 5.1.2 goes into detail on how the additional deformations are implemented in SCIA.

C.3. Calculations group effect

In this section, the calculations are given for the group effect of the piles under different loads at different stages in time.

Table C.5: Support Interactions $F = 20$ kN at T_0

	Sup 1	**Sup 2**	**Sup 3**	**Sup 4**	**Sup 5**	**Sup 6**	**Sup 7**	**Sup 8**	**Sup 9**	**Sup 10**	**Sup 11**	**Sum**
U1	-	1.0	0.3	0.0	0.0	0.0	0.0	0.0	0.0	0.0	0.0	**1.3**
U2	1.0	-	1.0	0.3	0.0	0.0	0.0	0.0	0.0	0.0	0.0	**2.3**
U3	0.3	1.0	-	1.0	0.3	0.0	0.0	0.0	0.0	0.0	0.0	**2.6**
U4	0.0	0.3	1.0	-	1.0	0.3	0.0	0.0	0.0	0.0	0.0	**2.6**
U5	0.0	0.0	0.3	1.0	-	1.0	0.3	0.0	0.0	0.0	0.0	**2.6**
U6	0.0	0.0	0.0	0.3	1.0	-	1.0	0.3	0.0	0.0	0.0	**2.6**
U7	0.0	0.0	0.0	0.0	0.3	1.0	-	1.0	0.3	0.0	0.0	**2.6**
U8	0.0	0.0	0.0	0.0	0.0	0.3	1.0	-	1.0	0.3	0.0	**2.6**
U9	0.0	0.0	0.0	0.0	0.0	0.0	0.3	1.0	-	1.0	0.3	**2.6**
U10	0.0	0.0	0.0	0.0	0.0	0.0	0.0	0.3	1.0	-	1.0	**2.3**
U11	0.0	0.0	0.0	0.0	0.0	0.0	0.0	0.0	0.3	1.0	-	**1.3**

Table C.6: Support Interactions $F = 20$ kN at T_{10}

	Sup 1	**Sup 2**	**Sup 3**	**Sup 4**	**Sup 5**	**Sup 6**	**Sup 7**	**Sup 8**	**Sup 9**	**Sup 10**	**Sup 11**	**Sum**
U1	-	1.3	0.5	0.2	0.0	0.0	0.0	0.0	0.0	0.0	0.0	**2.0**
U2	1.3	-	1.3	0.5	0.2	0.0	0.0	0.0	0.0	0.0	0.0	**3.3**
U3	0.5	1.3	-	1.3	0.5	0.2	0.0	0.0	0.0	0.0	0.0	**3.8**
U4	0.2	0.5	1.3	-	1.3	0.5	0.2	0.0	0.0	0.0	0.0	**4.0**
U5	0.0	0.2	0.5	1.3	-	1.3	0.5	0.2	0.0	0.0	0.0	**4.0**
U6	0.0	0.0	0.2	0.5	1.3	-	1.3	0.5	0.2	0.0	0.0	**4.0**
U7	0.0	0.0	0.0	0.2	0.5	1.3	-	1.3	0.5	0.2	0.0	**4.0**
U8	0.0	0.0	0.0	0.0	0.2	0.5	1.3	-	1.3	0.5	0.2	**4.0**
U9	0.0	0.0	0.0	0.0	0.0	0.2	0.5	1.3	-	1.3	0.5	**3.8**
U10	0.0	0.0	0.0	0.0	0.0	0.0	0.2	0.5	1.3	-	1.3	**3.3**
U11	0.0	0.0	0.0	0.0	0.0	0.0	0.0	0.2	0.5	1.3	-	**2.0**

Table C.7: Support Interactions $F = 20$ kN at T_{100}

	Sup 1	Sup 2	Sup 3	Sup 4	Sup 5	Sup 6	Sup 7	Sup 8	Sup 9	Sup 10	Sup 11	Sum
U1	-	2.0	0.9	0.4	0.0	0.0	0.0	0.0	0.0	0.0	0.0	**3.3**
U2	2.0	-	2.0	0.9	0.4	0.0	0.0	0.0	0.0	0.0	0.0	**5.3**
U3	0.9	2.0	-	2.0	0.9	0.4	0.0	0.0	0.0	0.0	0.0	**6.2**
U4	0.4	0.9	2.0	-	2.0	0.9	0.4	0.0	0.0	0.0	0.0	**6.6**
U5	0.0	0.4	0.9	2.0	-	2.0	0.9	0.4	0.0	0.0	0.0	**6.6**
U6	0.0	0.0	0.4	0.9	2.0	-	2.0	0.9	0.4	0.0	0.0	**6.6**
U7	0.0	0.0	0.0	0.4	0.9	2.0	-	2.0	0.9	0.4	0.0	**6.6**
U8	0.0	0.0	0.0	0.0	0.4	0.9	2.0	-	2.0	0.9	0.4	**6.6**
U9	0.0	0.0	0.0	0.0	0.0	0.4	0.9	2.0	-	2.0	0.9	**6.2**
U10	0.0	0.0	0.0	0.0	0.0	0.0	0.4	0.9	2.0	-	2.0	**5.3**
U11	0.0	0.0	0.0	0.0	0.0	0.0	0.0	0.4	0.9	2.0	-	**3.3**

Table C.8: Support Interactions $F = 20$ kN at T_{1000}

	Sup 1	Sup 2	Sup 3	Sup 4	Sup 5	Sup 6	Sup 7	Sup 8	Sup 9	Sup 10	Sup 11	Sum
U1	-	2.8	1.3	0.7	0.0	0.0	0.0	0.0	0.0	0.0	0.0	**4.8**
U2	2.8	-	2.8	1.3	0.7	0.0	0.0	0.0	0.0	0.0	0.0	**7.6**
U3	1.3	2.8	-	2.8	1.3	0.7	0.0	0.0	0.0	0.0	0.0	**8.9**
U4	0.7	1.3	2.8	-	2.8	1.3	0.7	0.0	0.0	0.0	0.0	**9.6**
U5	0.0	0.7	1.3	2.8	-	2.8	1.3	0.7	0.0	0.0	0.0	**9.6**
U6	0.0	0.0	0.7	1.3	2.8	-	2.8	1.3	0.7	0.0	0.0	**9.6**
U7	0.0	0.0	0.0	0.7	1.3	2.8	-	2.8	1.3	0.7	0.0	**9.6**
U8	0.0	0.0	0.0	0.0	0.7	1.3	2.8	-	2.8	1.3	0.7	**9.6**
U9	0.0	0.0	0.0	0.0	0.0	0.7	1.3	2.8	-	2.8	1.3	**8.9**
U10	0.0	0.0	0.0	0.0	0.0	0.0	0.7	1.3	2.8	-	2.8	**7.6**
U11	0.0	0.0	0.0	0.0	0.0	0.0	0.0	0.7	1.3	2.8	-	**4.8**

Table C.9: Support Interactions $F = 25$ kN at T_0

	Sup 1	Sup 2	Sup 3	Sup 4	Sup 5	Sup 6	Sup 7	Sup 8	Sup 9	Sup 10	Sup 11	Sum
Sup 1	-	1.20	0.40	0.00	0.00	0.00	0.00	0.00	0.00	0.00	0.00	**1.6**
Sup 2	1.20	-	1.20	0.40	0.00	0.00	0.00	0.00	0.00	0.00	0.00	**2.8**
Sup 3	0.40	1.20	-	1.20	0.40	0.00	0.00	0.00	0.00	0.00	0.00	**3.2**
Sup 4	0.00	0.40	1.20	-	1.20	0.40	0.00	0.00	0.00	0.00	0.00	**3.2**
Sup 5	0.00	0.00	0.40	1.20	-	1.20	0.40	0.00	0.00	0.00	0.00	**3.2**
Sup 6	0.00	0.00	0.00	0.40	1.20	-	1.20	0.40	0.00	0.00	0.00	**3.2**
Sup 7	0.00	0.00	0.00	0.00	0.40	1.20	-	1.20	0.40	0.00	0.00	**3.2**
Sup 8	0.00	0.00	0.00	0.00	0.00	0.40	1.20	-	1.20	0.40	0.00	**3.2**
Sup 9	0.00	0.00	0.00	0.00	0.00	0.00	0.40	1.20	-	1.20	0.40	**3.2**
Sup 10	0.00	0.00	0.00	0.00	0.00	0.00	0.00	0.40	1.20	-	1.20	**2.8**
Sup 11	0.00	0.00	0.00	0.00	0.00	0.00	0.00	0.00	0.40	1.20	-	**1.6**

Table C.10: Support Interactions $F = 25$ kN at T_{10}

	Sup 1	Sup 2	Sup 3	Sup 4	Sup 5	Sup 6	Sup 7	Sup 8	Sup 9	Sup 10	Sup 11	Sum
Sup 1	-	1.60	0.60	0.20	0.00	0.00	0.00	0.00	0.00	0.00	0.00	**2.4**
Sup 2	1.60	-	1.60	0.60	0.20	0.00	0.00	0.00	0.00	0.00	0.00	**4.0**
Sup 3	0.60	1.60	-	1.60	0.60	0.20	0.00	0.00	0.00	0.00	0.00	**4.6**
Sup 4	0.20	0.60	1.60	-	1.60	0.60	0.20	0.00	0.00	0.00	0.00	**4.8**
Sup 5	0.00	0.20	0.60	1.60	-	1.60	0.60	0.20	0.00	0.00	0.00	**4.8**
Sup 6	0.00	0.00	0.20	0.60	1.60	-	1.60	0.60	0.20	0.00	0.00	**4.8**
Sup 7	0.00	0.00	0.00	0.20	0.60	1.60	-	1.60	0.60	0.20	0.00	**4.8**
Sup 8	0.00	0.00	0.00	0.00	0.20	0.60	1.60	-	1.60	0.60	0.20	**4.8**
Sup 9	0.00	0.00	0.00	0.00	0.00	0.20	0.60	1.60	-	1.60	0.60	**4.6**
Sup 10	0.00	0.00	0.00	0.00	0.00	0.00	0.20	0.60	1.60	-	1.60	**4.0**
Sup 11	0.00	0.00	0.00	0.00	0.00	0.00	0.00	0.20	0.60	1.60	-	**2.4**

Table C.11: Support Interactions $F = 25$ kN at T_{100}

	Sup 1	Sup 2	Sup 3	Sup 4	Sup 5	Sup 6	Sup 7	Sup 8	Sup 9	Sup 10	Sup 11	Sum
Sup 1	-	2.50	1.10	0.60	0.00	0.00	0.00	0.00	0.00	0.00	0.00	**4.2**
Sup 2	2.50	-	2.50	1.10	0.60	0.00	0.00	0.00	0.00	0.00	0.00	**6.7**
Sup 3	1.10	2.50	-	2.50	1.10	0.60	0.00	0.00	0.00	0.00	0.00	**7.8**
Sup 4	0.60	1.10	2.50	-	2.50	1.10	0.60	0.00	0.00	0.00	0.00	**8.4**
Sup 5	0.00	0.60	1.10	2.50	-	2.50	1.10	0.60	0.00	0.00	0.00	**8.4**
Sup 6	0.00	0.00	0.60	1.10	2.50	-	2.50	1.10	0.60	0.00	0.00	**8.4**
Sup 7	0.00	0.00	0.00	0.60	1.10	2.50	-	2.50	1.10	0.60	0.00	**8.4**
Sup 8	0.00	0.00	0.00	0.00	0.60	1.10	2.50	-	2.50	1.10	0.60	**8.4**
Sup 9	0.00	0.00	0.00	0.00	0.00	0.60	1.10	2.50	-	2.50	1.10	**7.8**
Sup 10	0.00	0.00	0.00	0.00	0.00	0.00	0.60	1.10	2.50	-	2.50	**6.7**
Sup 11	0.00	0.00	0.00	0.00	0.00	0.00	0.00	0.60	1.10	2.50	-	**4.2**

Table C.12: Support Interactions $F = 25$ kN at T_{1000}

	Sup 1	Sup 2	Sup 3	Sup 4	Sup 5	Sup 6	Sup 7	Sup 8	Sup 9	Sup 10	Sup 11	Sum
Sup 1	-	3.40	1.70	0.90	0.00	0.00	0.00	0.00	0.00	0.00	0.00	**6.0**
Sup 2	3.40	-	3.40	1.70	0.90	0.00	0.00	0.00	0.00	0.00	0.00	**9.4**
Sup 3	1.70	3.40	-	3.40	1.70	0.90	0.00	0.00	0.00	0.00	0.00	**11.1**
Sup 4	0.90	1.70	3.40	-	3.40	1.70	0.90	0.00	0.00	0.00	0.00	**12.0**
Sup 5	0.00	0.90	1.70	3.40	-	3.40	1.70	0.90	0.00	0.00	0.00	**12.0**
Sup 6	0.00	0.00	0.90	1.70	3.40	-	3.40	1.70	0.90	0.00	0.00	**12.0**
Sup 7	0.00	0.00	0.00	0.90	1.70	3.40	-	3.40	1.70	0.90	0.00	**12.0**
Sup 8	0.00	0.00	0.00	0.00	0.90	1.70	3.40	-	3.40	1.70	0.90	**12.0**
Sup 9	0.00	0.00	0.00	0.00	0.00	0.90	1.70	3.40	-	3.40	1.70	**11.1**
Sup 10	0.00	0.00	0.00	0.00	0.00	0.00	0.90	1.70	3.40	-	3.40	**9.4**
Sup 11	0.00	0.00	0.00	0.00	0.00	0.00	0.00	0.90	1.70	3.40	-	**6.0**

Table C.13: Support Interactions $F = 30$ kN at T_0

	Sup 1	Sup 2	Sup 3	Sup 4	Sup 5	Sup 6	Sup 7	Sup 8	Sup 9	Sup 10	Sup 11	Sum
U1	-	1.6	0.6	0.2	0.0	0.0	0.0	0.0	0.0	0.0	0.0	**2.4**
U2	1.6	-	1.6	0.6	0.2	0.0	0.0	0.0	0.0	0.0	0.0	**4.0**
U3	0.6	1.6	-	1.6	0.6	0.2	0.0	0.0	0.0	0.0	0.0	**4.6**
U4	0.2	0.6	1.6	-	1.6	0.6	0.2	0.0	0.0	0.0	0.0	**4.8**
U5	0.0	0.2	0.6	1.6	-	1.6	0.6	0.2	0.0	0.0	0.0	**4.8**
U6	0.0	0.0	0.2	0.6	1.6	-	1.6	0.6	0.2	0.0	0.0	**4.8**
U7	0.0	0.0	0.0	0.2	0.6	1.6	-	1.6	0.6	0.2	0.0	**4.8**
U8	0.0	0.0	0.0	0.0	0.2	0.6	1.6	-	1.6	0.6	0.2	**4.8**
U9	0.0	0.0	0.0	0.0	0.0	0.2	0.6	1.6	-	1.6	0.6	**4.6**
U10	0.0	0.0	0.0	0.0	0.0	0.0	0.2	0.6	1.6	-	1.6	**4.0**
U11	0.0	0.0	0.0	0.0	0.0	0.0	0.0	0.2	0.6	1.6	-	**2.4**

Table C.14: Support Interactions $F = 30$ kN at T_{10}

	Sup 1	Sup 2	Sup 3	Sup 4	Sup 5	Sup 6	Sup 7	Sup 8	Sup 9	Sup 10	Sup 11	Sum
U1	-	2.0	0.8	0.4	0.1	0.0	0.0	0.0	0.0	0.0	0.0	**3.3**
U2	2.0	-	2.0	0.8	0.4	0.1	0.0	0.0	0.0	0.0	0.0	**5.3**
U3	0.8	2.0	-	2.0	0.8	0.4	0.1	0.0	0.0	0.0	0.0	**6.1**
U4	0.4	0.8	2.0	-	2.0	0.8	0.4	0.1	0.0	0.0	0.0	**6.5**
U5	0.1	0.4	0.8	2.0	-	2.0	0.8	0.4	0.1	0.0	0.0	**6.6**
U6	0.0	0.1	0.4	0.8	2.0	-	2.0	0.8	0.4	0.1	0.0	**6.6**
U7	0.0	0.0	0.1	0.4	0.8	2.0	-	2.0	0.8	0.4	0.1	**6.6**
U8	0.0	0.0	0.0	0.1	0.4	0.8	2.0	-	2.0	0.8	0.4	**6.5**
U9	0.0	0.0	0.0	0.0	0.1	0.4	0.8	2.0	-	2.0	0.8	**6.1**
U10	0.0	0.0	0.0	0.0	0.0	0.1	0.4	0.8	2.0	-	2.0	**5.3**
U11	0.0	0.0	0.0	0.0	0.0	0.0	0.1	0.4	0.8	2.0	-	**3.3**

Table C.15: Support Interactions $F = 30$ kN at T_{100} (U is in mm)

	Sup 1	Sup 2	Sup 3	Sup 4	Sup 5	Sup 6	Sup 7	Sup 8	Sup 9	Sup 10	Sup 11	Sum
U1	-	3.0	1.4	0.7	0.0	0.0	0.0	0.0	0.0	0.0	0.0	**5.1**
U2	3.0	-	3.0	1.4	0.7	0.0	0.0	0.0	0.0	0.0	0.0	**8.1**
U3	1.4	3.0	-	3.0	1.4	0.7	0.0	0.0	0.0	0.0	0.0	**9.5**
U4	0.7	1.4	3.0	-	3.0	1.4	0.7	0.0	0.0	0.0	0.0	**10.2**
U5	0.0	0.7	1.4	3.0	-	3.0	1.4	0.7	0.0	0.0	0.0	**10.2**
U6	0.0	0.0	0.7	1.4	3.0	-	3.0	1.4	0.7	0.0	0.0	**10.2**
U7	0.0	0.0	0.0	0.7	1.4	3.0	-	3.0	1.4	0.7	0.0	**10.2**
U8	0.0	0.0	0.0	0.0	0.7	1.4	3.0	-	3.0	1.4	0.7	**10.2**
U9	0.0	0.0	0.0	0.0	0.0	0.7	1.4	3.0	-	3.0	1.4	**9.5**
U10	0.0	0.0	0.0	0.0	0.0	0.0	0.7	1.4	3.0	-	3.0	**8.1**
U11	0.0	0.0	0.0	0.0	0.0	0.0	0.0	0.7	1.4	3.0	-	**5.1**

Table C.16: Support Interactions $F = 30$ kN at T_{1000}

	Sup 1	Sup 2	Sup 3	Sup 4	Sup 5	Sup 6	Sup 7	Sup 8	Sup 9	Sup 10	Sup 11	Sum
U1	-	4.1	2.0	1.1	0.0	0.0	0.0	0.0	0.0	0.0	0.0	**7.2**
U2	4.1	-	4.1	2.0	1.1	0.0	0.0	0.0	0.0	0.0	0.0	**11.3**
U3	2.0	4.1	-	4.1	2.0	1.1	0.0	0.0	0.0	0.0	0.0	**13.3**
U4	1.1	2.0	4.1	-	4.1	2.0	1.1	0.0	0.0	0.0	0.0	**14.4**
U5	0.0	1.1	2.0	4.1	-	4.1	2.0	1.1	0.0	0.0	0.0	**14.4**
U6	0.0	0.0	1.1	2.0	4.1	-	4.1	2.0	1.1	0.0	0.0	**14.4**
U7	0.0	0.0	0.0	1.1	2.0	4.1	-	4.1	2.0	1.1	0.0	**14.4**
U8	0.0	0.0	0.0	0.0	1.1	2.0	4.1	-	4.1	2.0	1.1	**14.4**
U9	0.0	0.0	0.0	0.0	0.0	1.1	2.0	4.1	-	4.1	2.0	**13.3**
U10	0.0	0.0	0.0	0.0	0.0	0.0	1.1	2.0	4.1	-	4.1	**11.3**
U11	0.0	0.0	0.0	0.0	0.0	0.0	0.0	1.1	2.0	4.1	-	**7.2**

Table C.17: Support Interactions $F = 40$ kN at T_0

	Sup 1	Sup 2	Sup 3	Sup 4	Sup 5	Sup 6	Sup 7	Sup 8	Sup 9	Sup 10	Sup 11	Sum
U1	-	2.3	0.8	0.3	0.0	0.0	0.0	0.0	0.0	0.0	0.0	**3.4**
U2	2.3	-	2.3	0.8	0.3	0.0	0.0	0.0	0.0	0.0	0.0	**5.7**
U3	0.8	2.3	-	2.3	0.8	0.3	0.0	0.0	0.0	0.0	0.0	**6.5**
U4	0.3	0.8	2.3	-	2.3	0.8	0.3	0.0	0.0	0.0	0.0	**6.8**
U5	0.0	0.3	0.8	2.3	-	2.3	0.8	0.3	0.0	0.0	0.0	**6.8**
U6	0.0	0.0	0.3	0.8	2.3	-	2.3	0.8	0.3	0.0	0.0	**6.8**
U7	0.0	0.0	0.0	0.3	0.8	2.3	-	2.3	0.8	0.3	0.0	**6.8**
U8	0.0	0.0	0.0	0.0	0.3	0.8	2.3	-	2.3	0.8	0.3	**6.8**
U9	0.0	0.0	0.0	0.0	0.0	0.3	0.8	2.3	-	2.3	0.8	**6.5**
U10	0.0	0.0	0.0	0.0	0.0	0.0	0.3	0.8	2.3	-	2.3	**5.7**
U11	0.0	0.0	0.0	0.0	0.0	0.0	0.0	0.3	0.8	2.3	-	**3.4**

Table C.18: Support Interactions $F = 40$ kN at T_{10}

	Sup 1	Sup 2	Sup 3	Sup 4	Sup 5	Sup 6	Sup 7	Sup 8	Sup 9	Sup 10	Sup 11	Sum
U1	-	2.8	1.2	0.5	0.0	0.0	0.0	0.0	0.0	0.0	0.0	**4.5**
U2	2.8	-	2.8	1.2	0.5	0.0	0.0	0.0	0.0	0.0	0.0	**7.3**
U3	1.2	2.8	-	2.8	1.2	0.5	0.0	0.0	0.0	0.0	0.0	**8.5**
U4	0.5	1.2	2.8	-	2.8	1.2	0.5	0.0	0.0	0.0	0.0	**9.0**
U5	0.0	0.5	1.2	2.8	-	2.8	1.2	0.5	0.0	0.0	0.0	**9.0**
U6	0.0	0.0	0.5	1.2	2.8	-	2.8	1.2	0.5	0.0	0.0	**9.0**
U7	0.0	0.0	0.0	0.5	1.2	2.8	-	2.8	1.2	0.5	0.0	**9.0**
U8	0.0	0.0	0.0	0.0	0.5	1.2	2.8	-	2.8	1.2	0.5	**9.0**
U9	0.0	0.0	0.0	0.0	0.0	0.5	1.2	2.8	-	2.8	1.2	**8.5**
U10	0.0	0.0	0.0	0.0	0.0	0.0	0.5	1.2	2.8	-	2.8	**7.3**
U11	0.0	0.0	0.0	0.0	0.0	0.0	0.0	0.5	1.2	2.8	-	**4.5**

Table C.19: Support Interactions $F = 40$ kN at T_{100}

	Sup 1	Sup 2	Sup 3	Sup 4	Sup 5	Sup 6	Sup 7	Sup 8	Sup 9	Sup 10	Sup 11	Sum
U1	-	4.0	1.9	1.0	0.0	0.0	0.0	0.0	0.0	0.0	0.0	**6.9**
U2	4.0	-	4.0	1.9	1.0	0.0	0.0	0.0	0.0	0.0	0.0	**10.9**
U3	1.9	4.0	-	4.0	1.9	1.0	0.0	0.0	0.0	0.0	0.0	**12.8**
U4	1.0	1.9	4.0	-	4.0	1.9	1.0	0.0	0.0	0.0	0.0	**13.8**
U5	0.0	1.0	1.9	4.0	-	4.0	1.9	1.0	0.0	0.0	0.0	**13.8**
U6	0.0	0.0	1.0	1.9	4.0	-	4.0	1.9	1.0	0.0	0.0	**13.8**
U7	0.0	0.0	0.0	1.0	1.9	4.0	-	4.0	1.9	1.0	0.0	**13.8**
U8	0.0	0.0	0.0	0.0	1.0	1.9	4.0	-	4.0	1.9	1.0	**13.8**
U9	0.0	0.0	0.0	0.0	0.0	1.0	1.9	4.0	-	4.0	1.9	**12.8**
U10	0.0	0.0	0.0	0.0	0.0	0.0	1.0	1.9	4.0	-	4.0	**10.9**
U11	0.0	0.0	0.0	0.0	0.0	0.0	0.0	1.0	1.9	4.0	-	**6.9**

Table C.20: Support Interactions $F = 40$ kN at T_{1000}

	Sup 1	Sup 2	Sup 3	Sup 4	Sup 5	Sup 6	Sup 7	Sup 8	Sup 9	Sup 10	Sup 11	Sum
U1	-	5.4	2.6	1.4	0.0	0.0	0.0	0.0	0.0	0.0	0.0	**9.4**
U2	5.4	-	5.4	2.6	1.4	0.0	0.0	0.0	0.0	0.0	0.0	**14.8**
U3	2.6	5.4	-	5.4	2.6	1.4	0.0	0.0	0.0	0.0	0.0	**17.4**
U4	1.4	2.6	5.4	-	5.4	2.6	1.4	0.0	0.0	0.0	0.0	**18.8**
U5	0.0	1.4	2.6	5.4	-	5.4	2.6	1.4	0.0	0.0	0.0	**18.8**
U6	0.0	0.0	1.4	2.6	5.4	-	5.4	2.6	1.4	0.0	0.0	**18.8**
U7	0.0	0.0	0.0	1.4	2.6	5.4	-	5.4	2.6	1.4	0.0	**18.8**
U8	0.0	0.0	0.0	0.0	1.4	2.6	5.4	-	5.4	2.6	1.4	**18.8**
U9	0.0	0.0	0.0	0.0	0.0	1.4	2.6	5.4	-	5.4	2.6	**17.4**
U10	0.0	0.0	0.0	0.0	0.0	0.0	1.4	2.6	5.4	-	5.4	**14.8**
U11	0.0	0.0	0.0	0.0	0.0	0.0	0.0	1.4	2.6	5.4	-	**9.4**

D

Appendix D: Pile specific calculations

In this research, additional calculations have been done besides the main one. This appendix will go into aspects that did not fit in the main document, but can be helpful for future research. It will start with calculating the capacity of the helical pile in soil. Afterwards, different variations for the pile settlement calculations will be shown including the settlement for piles with a deeper positioned helical plate, soil differentiations, and the impact of an additional helix. Then, the settlement of the helical pile will be compared to the compression of the soil without any foundation elements. The appendix will end with the comparison of different mesh generations to substantiate the chosen mesh.

D.1. Pile capacity

In Section 2.3.2, the capacity of a helical pile is discussed. From this paragraph the capacity of a helical pile in fine grained soil can be calculated with the following formula:

$$q_{ult} = 9s_u \qquad (2.25)$$

The helical plate is positioned in a moderately sandy clay soil. This soil has an s_u of 80 kPa and would therefore have a capacity of around 720 kPa. To validate this, the equation 2.14 is also used for the calculation.

$$q_{ult} = cN_cs_cd_c + q' * (N_qs_qd_q - 1) + 0.5\gamma DN_\gamma s_\gamma d_\gamma \qquad (2.14)$$

In the equation, the following properties can already be determined for a short term capacity:

ϕ	22.5 degrees
c	80 kPa (the value of c_u is used obtained from Appendix A Figure A.1)
q'	23.7 kPa (obtained from Appendix B Table B.1)
γ	42.9 kPa (obtained from Appendix B Table B.1)
B	0.6 m
L	3 m

These values are used to calculate the factors that influence the q_{ult}.

$$\begin{array}{lcll}
N_q & = & 8.2 & (Eq : 2.15) \\
s_q & = & 1.1 & (Eq : 2.19) \\
d_q & = & 1.3 & (Eq : 2.22) \\
N_c & = & 17.5 & (Eq : 2.16) \\
s_c & = & 1.1 & (Eq : 2.18) \\
d_c & = & 1.4 & (Eq : 2.21) \\
N_y & = & 4.4 & (Eq : 2.17) \\
s_y & = & 0.9 & (Eq : 2.20) \\
d_y & = & 1.0 & (Eq : 2.23)
\end{array}$$

With equation 2.14 the q_{ult} has a value of:

$$q_{ult} = 2139 + 254,2 + 52,5 = 2447kPa$$

This value is more than 3 times larger than the earlier found value due to the friction angle being taken into account in the calculation.

If a force of 50 kN is applied on top of the helical pile and all force is taken by the helical plate, this would result in a stress increase of $50/(\pi * r^2) = 176,8kPa$ for a plate with a diameter of 600 mm. This stress increase in addition to the existing vertical stress of 42,9 kPa, is much lower than the obtained capacity. However, the diameter should not be changed for this research.

The value used for c in a short term calculation, is the cohesion c_u with a value of 80 kPa. However, for long term calculations the value T for drained shear strength should be used.

$$T = c' + \sigma_n' \tan\phi \tag{2.28}$$

Where:

T	is the drained shear strength;
c'	is the effective cohesion;
σ_n'	effective confining stress;

$$T = 5 + 23.7 \times \tan 22.5 = 15\,\text{kPa}$$

This reduces the value of $\underline{q_{ult}\text{ to }708kPa}$, which is closer to the expected value of $9s_u$. Since there is an uncertainty to the soil profile, certain assumed values can be lower than expected. The handbook "Helical Piles in Practice" advises to use a pile which at least has a q_{ult} that is twice as high as the expected load increase (Perko, 2009).

Soil uncertainty

The reason for this advise is the uncertainty of the soil properties. In Appendix A the soil properties are read from a CPT test, but this is an estimation. If the estimation is wrong and the soil layer *Moderate Sandy Clay* in actuality is *Moderate Clean Clay*, the capacity would be lower. The properties would change to the following:

ϕ	17.5 degrees
c	50 kPa (the value of c_u is used obtained from Appendix A Figure A.1)
q'	23.6 kPa
γ	41.7
B	0.6 m
L	3 m
T	12 kPa $(= 5 + 23,6 * \tan 17,5)$

These values are used to calculate the factors that influence the q_{ult}.

$$\begin{aligned}
N_q &= 5.0 && (Eq: 2.15)\\
s_q &= 1.1 && (Eq: 2.19)\\
d_q &= 1.3 && (Eq: 2.22)\\
N_c &= 12.7 && (Eq: 2.16)\\
s_c &= 1.1 && (Eq: 2.18)\\
d_c &= 1.4 && (Eq: 2.21)\\
N_y &= 1.8 && (Eq: 2.17)\\
s_y &= 0.9 && (Eq: 2.20)\\
d_y &= 1.0 && (Eq: 2.23)
\end{aligned}$$

With equation 2.14 the q_{ult} for long term capacity has a value of:

$$q_{ult} = 624 + 141 + 21 = 392kPa$$

This is a decrease of 45 % compared with the earlier found $708kPa$. A good estimation of the soil properties is therefore need to make an accurate prediction of the capacity. Since this research does not have the resources for such an accurate prediction, the capacity should be underestimated.

D.2. Pile differentiations

As discussed in Chapter 2, the differentiations that affect the settlement of a structure are discussed. In this section, some differentiations will be investigated to get a better view of their impact. In PLAXIS 2D the same pile used in the research is modelled with a load of 25 kN on top at T0. The helix is originally positioned at a depth of 3 meters underneath the surface. The model will be adjusted with the following points:

- A longer pile with the helix positioned lower in the soil;
- The *Moderate Sandy Clay* layer changed into a *Moderate Clean Clay* layer;
- The sand layer being less deep than it is now (at a depth of 12,7m);
- The use of a helical pile with 2 helices.

In the calculations, the lowest helical plate is positioned at a depth of 3m unless stated otherwise. Thus in the double helix calculation, the lowest helix is at a depth of 3m and the second is x meters above that.

Table D.1: Displacements of helical pile modifications over time

		U_T0 [mm]	**U_T10** [mm]	**U_T100** [mm]	**U_T1000** [mm]
(1)	Depth helix 3m	90	99	124	164
(2)	Depth helix 4m	72	80	102	140
(3)	Depth helix 5m	65	72	94	130
(4)	Depth helix 6m	58	63	82	115
(5)	Sandy clay to clean clay	110	122	154	205
(6)	Sand layer depth at 11,7m	83	92	113	149
(7)	Sand layer depth at 10m	65	72	89	116
(8)	Sand layer depth at 5m	40	45	53	63
(9)	Double helix (spacing 0.5m)	77	84	108	148
(10)	Double helix (spacing 1m)	70	77	100	140

The impact of the modifications are shown in Table D.2.

Table D.2: Difference in Displacement Between Configurations

Comparison	Diff U_T0 [mm]	Diff U_T10 [mm]	Diff U_T100 [mm]	Diff U_T1000 [mm]
1 & 2	18	20	22	24
1 & 3	25	27	30	34
1 & 4	32	37	42	49
1 & 5	-20	-23	-30	-41
1 & 6	7	7	11	15
1 & 7	25	27	35	49
1 & 8	50	54	72	102
1 & 9	13	15	17	16
1 & 10	20	22	24	24

From these results, a few statements can be made:

- Using a longer foundation pile with a lower helix lessens the settlement of the pile. The difference in settlement increases over time.
- A weaker soil layer than estimated, will increase the settlement.
- A depth change of the Pleistocene soil layer is less impactful than a depth change of the helical plate.
- Using two helical plates improves the resistance of the pile to settlement. This resistance is not expected to increase at later stages in time. Secondary settlement is therefore similar to a pile with a single helix.
- When using two helical plates on a pile, a wider spacing between the helical plates is more beneficial for resisting settlements.

D.3. Pile settlement in comparison to soil settlement

In this research, the total settlement of a pile is based on the displacement of the pile. With the formulas obtained from the Eurocode (Nederlands Normalisatie-instituut, 2017) the soil is not expected to deform without an increase of the effective stress. However, the soft soil creep model in PLAXIS does expect soil settlement. This model bases the creep of the soil on only the effective stress and not the change in effective stress. This leads to more realistic results, but also results in soil settlement that is not caused by the helical pile.

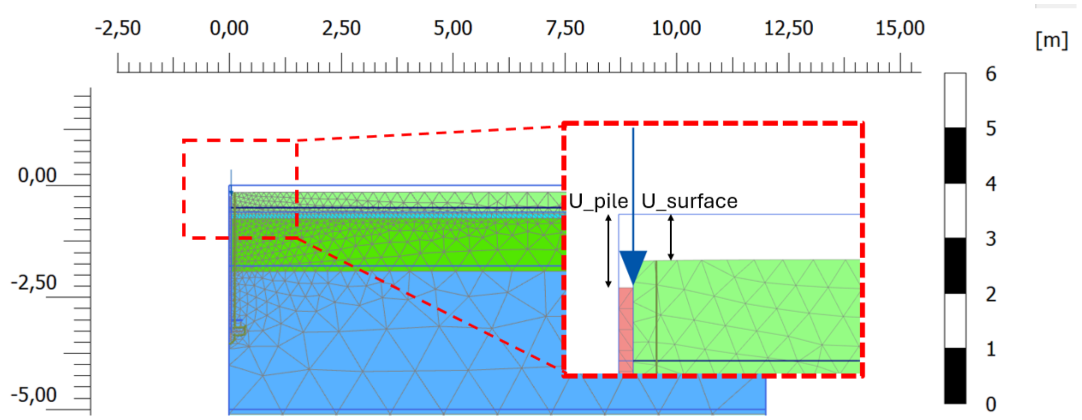

Figure D.1: Pile displacement (U_{pile}) in comparison to the surface displacement ($U_{surface}$)

The distance between the top of the helical pile and the surface is therefore not as simple as just the displacement of the helical pile. The expected settlement of the soil without the pile should be subtracted from these values.

To give insight on the pile displacement in comparison to the displacement of the ground surface, four calculations have been done. A helical pile is modelled in the same soil profile that is used for this research. Three different loads ($F = 25kN$, $F = 35kN$ and $F = 45kN$) are used to calculated the settlements of the pile at T0, T10, T100 and T1000. Furthermore, the settlement calculation is done for a model without the helical pile. The results can be seen in Table D.3

Force	Time	U Pile [mm]	U Surface [mm]	Difference [mm]
F = 25 kN	T0	90	73	17
	T10	99	79	20
	T100	124	105	19
	T1000	164	149	15
F = 35 kN	T0	116	73	43
	T10	127	79	48
	T100	156	105	51
	T1000	203	149	54
F = 45 kN	T0	151	73	78
	T10	165	79	86
	T100	199	105	94
	T1000	251	149	102

Table D.3: Comparison of the pile settlement applied with different loads to the surface settlement without any additional load calculated with the soft soil creep model of PLAXIS 2D

Looking at the results of the calculation, it can be seen that for the lowest applied force the difference between the pile and the soil stays within a range of 5 mm. When higher forces are applied, the difference increases over time. For the pile applied with 25 kN, the 3 meters of soil above the helical plate are expected to compress at a relatively similar rate as the settlement of the helical pile. This can be beneficial for the structures connection with for instance pipes. However, for higher forces, the increasing difference might lead to problems for designs that do not take this into account.

D.4. Mesh determination

Determining what mesh should be used for the settlement calculations is dependent on the accuracy and time it takes for a calculation of the mesh. PLAXIS 2D lets the user choose between a very coarse, coarse, medium, fine, and very fine mesh. For this research, a comparison will be drawn between the medium, fine, and very fine mesh.
The model used is the same for each mesh:

- Soil properties determined from the CPT in Appendix A;
- A helical pile with the plate at a depth of 3m;
- A force on top of the pile of 25 kN;
- Displacement calculations at T0, T10, T100, T1000.

This results in the following deformations:

Table D.4: Displacement of the pile with different meshes

mesh	**U_T0** [mm]	**U_T10** [mm]	**U_T100** [mm]	**U_T1000** [mm]
(1) Medium	90.0	99.0	124.0	164.0
(2) Fine	91.8	102.6	128.2	168.6
(3) Very Fine	91.0	99.5	124.5	165.9

Comparing the results leads to the following table:

Table D.5: Displacement comparison between the meshes

Comparison	**Diff U_T0**	**Diff U_T10**	**Diff U_T100**	**Diff U_T1000**
1 & 2	2%	3.3%	3.1%	2.7%
1 & 3	1.1%	0.2%	0.2%	1.1%

The maximum difference between the meshes can be up to 3,3%. The difference in deformation between the medium mesh and the very fine mesh, is less than between the medium and fine mesh. The medium mesh seems therefore the best option for this research, since it saves time compared to calculations with a finer mesh, and is closer to the most accurate calculation compared to the fine mesh.

E

Appendix E: Final calculations

In this Appendix, the calculation sheets for the settlement are given. Each calculation consists of multiple steps:

- **SCIA results** are the displacements and forces obtained from the calculation software SCIA engineer. Each foundation pile has been calculated at T0, T10, T100, and T1000.
- **Input Plaxis** is the translation of point loads to a line load on the circumference of the top of the pile.
- **Output Plaxis** are the displacements calculated by PLAXIS 2D. These values, in combination with the displacement caused by soil stress increase from other piles, will form the non-linear spring function used in SCIA Engineer.
- **Resulting differential displacement** are the differences in settlement between the piles.

With the obtained values from these calculations, the results in Chapter 6 are constructed.
First, calculation Aa is fully worked out to show an example of a full calculation. After that all calculation results will be given.

E.1. Calculation Aa worked out

This section will work through the four calculation steps.

E.1.1. Step 1: Deformation graph

A helical pile with helical plate at a depth of 3 meters is modelled in PLAXIS 2D. Different forces are applied to it increasing from day 0 till day 30. Day 30 is set as T0 in this research. This results in the following displacement graph:

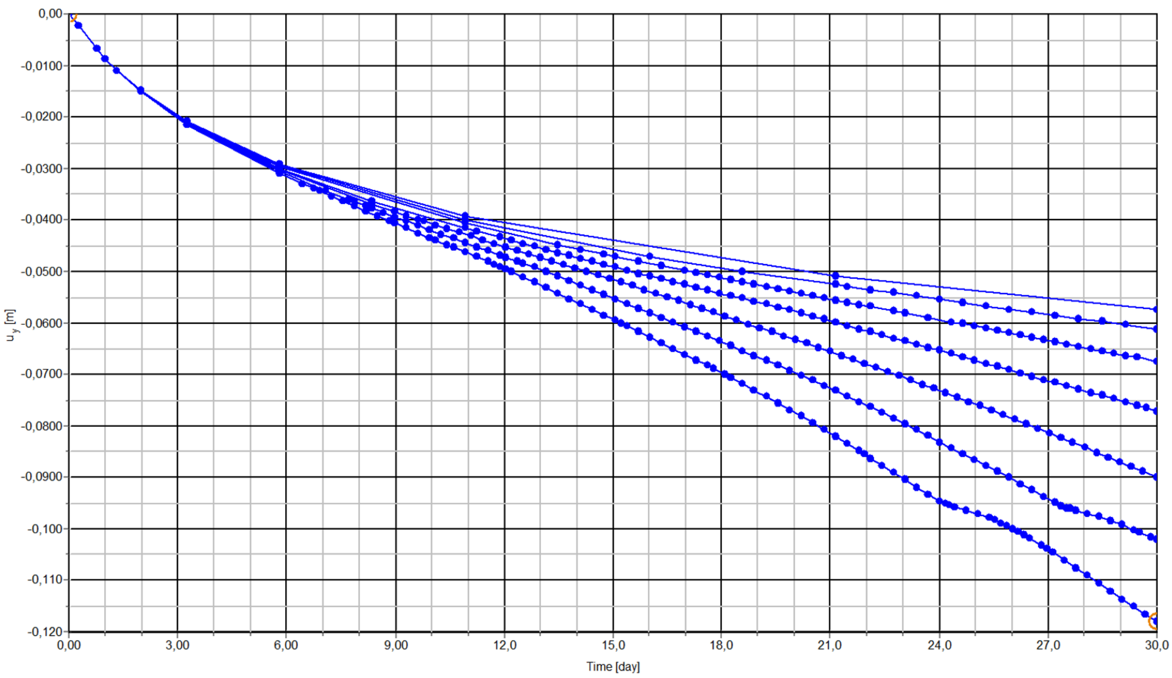

Figure E.1: Displacement over time for calculation Aa step 1

E.1.2. Step 2: Implementation to SCIA engineer

In SCIA, the supports underneath the structure need to be modelled in a way that they represent the settlement behaviour of the helical piles. This is done by using non-linear spring supports. These supports can be modelled to give a non-linear response to the applied load. Using the deformation graph of Figure E.1 a non-linear function can be constructed:

	u [m]	F [MN]
1	-0,1180	-0,0350
2	-0,1020	-0,0300
3	-0,0900	-0,0250
4	-0,0771	-0,0200
5	-0,0675	-0,0150
6	-0,0612	-0,0100
7	-0,0575	-0,0050
8	0,0000	0,0000

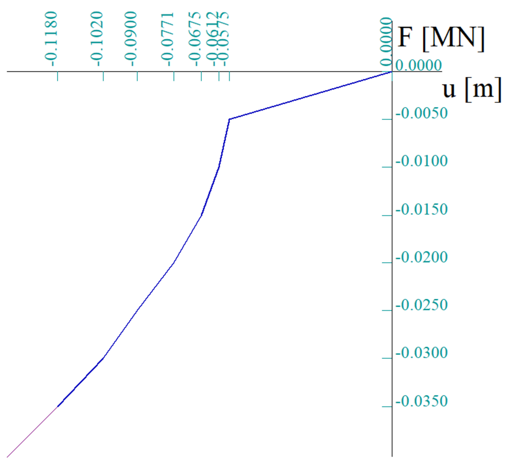

Figure E.2: Non-linear function for supports at T0

Since each foundation pile is similar in this calculation, this function should represent each support at T0. However, neighbouring piles will also influence the settlement, leading to additional settlement. The expected support reactions will be between the 20 kN and 25 kN. For this calculation, the expected additional settlement will be based on the group effect of piles loaded with 25 kN. This assumption leads to more differential settlement and impacts the results therefore more negatively. The additional settlement is 1,6 mm for the outer piles and 3,2 mm for the inner piles at T0, see Appendix C. Adding these values to the earlier function results in the following support functions:

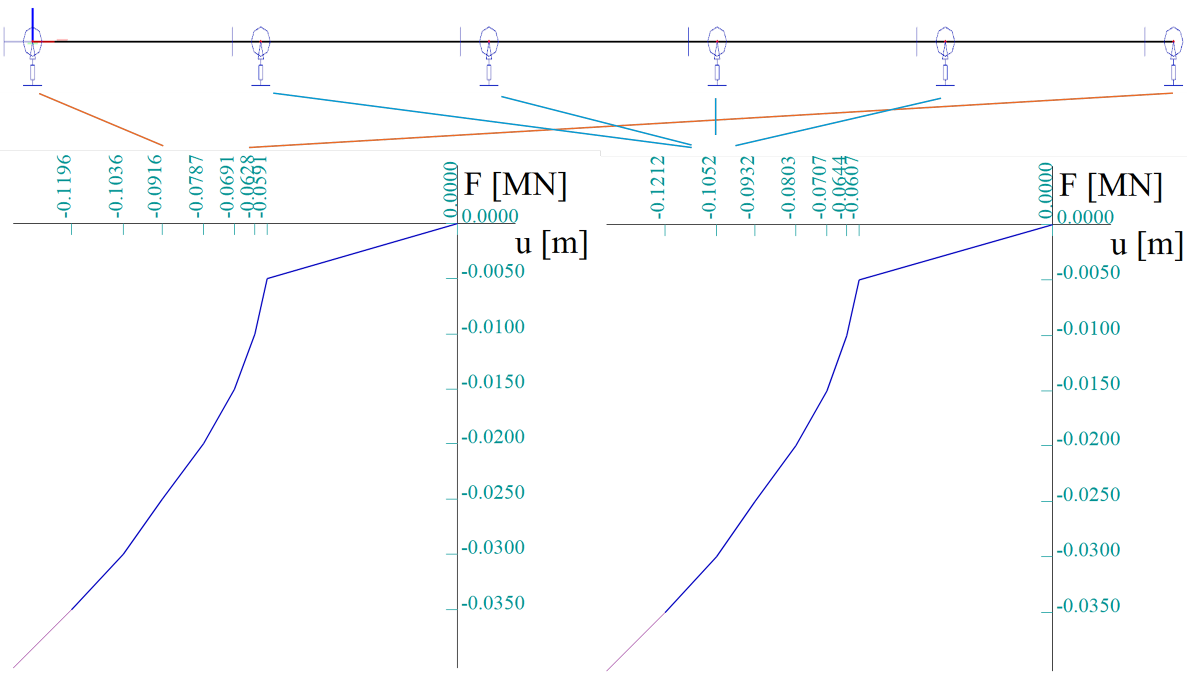

Figure E.3: Support functions for the outer supports (left) and Inner supports (right)

Calculating the model with a non-linear calculation results in the displacements and support reactions given in Figures E.4 and E.5.

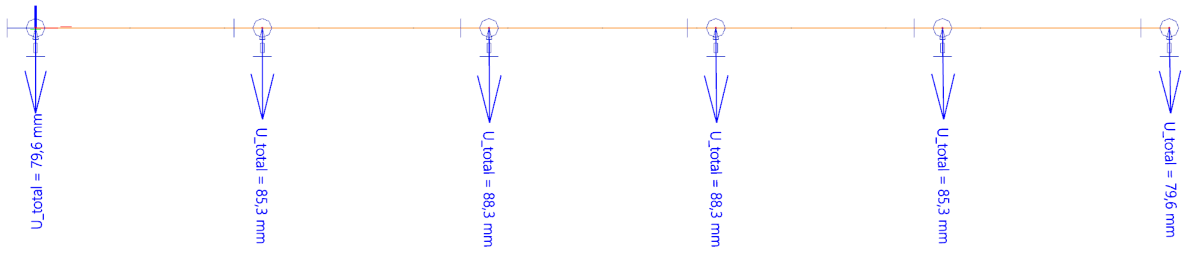

Figure E.4: Support displacement U calculation Aa at T0

Figure E.5: Support reaction F calculation Aa at T0

The occurring stresses can also be obtained.

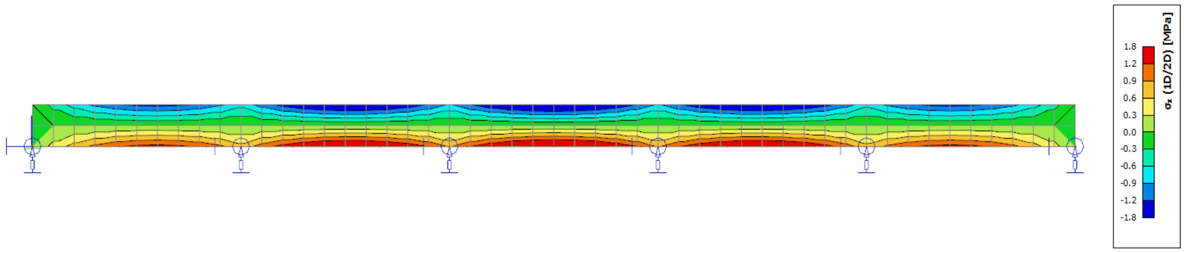

Figure E.6: Stress σ_x calculation Aa at T0

E.1.3. Step 3: Long term calculations

Now that the support reactions are determined at T0, they can be used for calculating the long term settlement. This will be done with the following method:

The support settlement of each pile will be run for a second time between 0 and 30 days, so till T0, but with the obtained support reaction in step 2. This will simulate the estimated settlement for that time period. Afterwards, the next 10 days for the pile will be simulated. This will be done by running the simulation with three different loads on top of the pile: $0.9F_{T0}$, F_{T0}, and $1.1F_{T0}$.

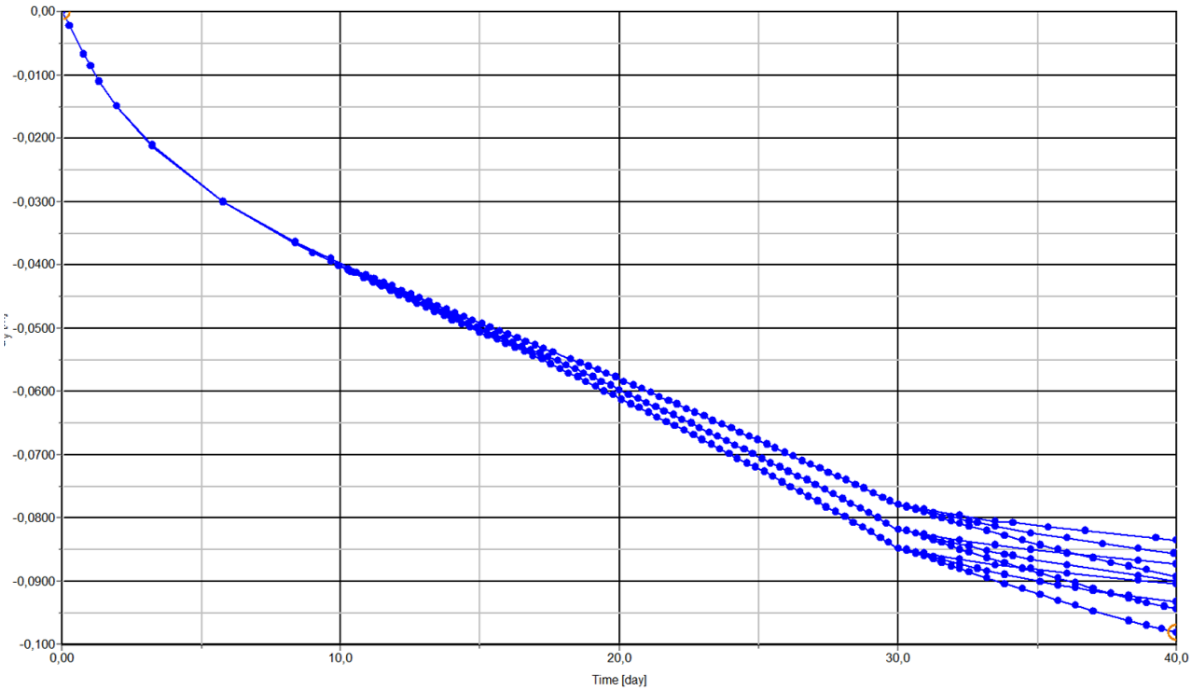

Figure E.7: Deformation graph supports calculation Aa T10

This results in three force vs displacement values for each pile that can be implemented in SCIA as a new non-linear function. The functions have to make sure to add the additional settlements caused by neighbouring piles at T10 for a load of 25 kN. Figure E.8 shows the resulting support functions.

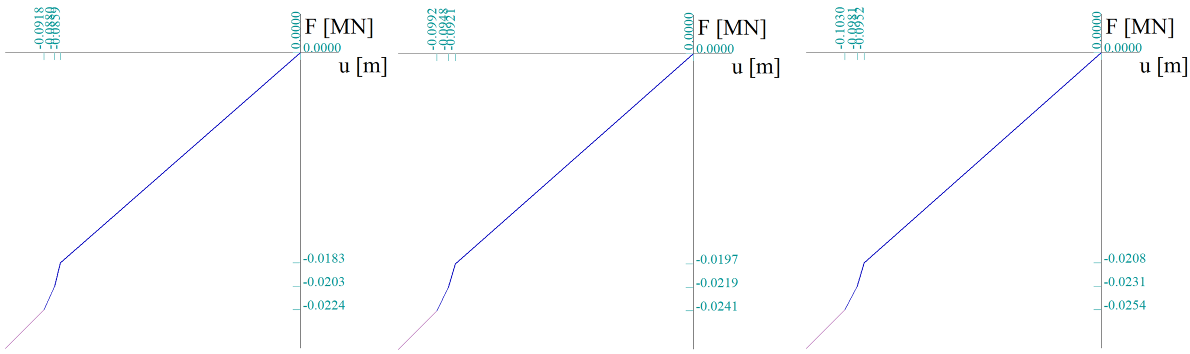

Figure E.8: Load displacement functions at T10 P1&P6 (left), P2&P5 (middle), P3&P4 (right)

This results in new support deformations and reaction forces:

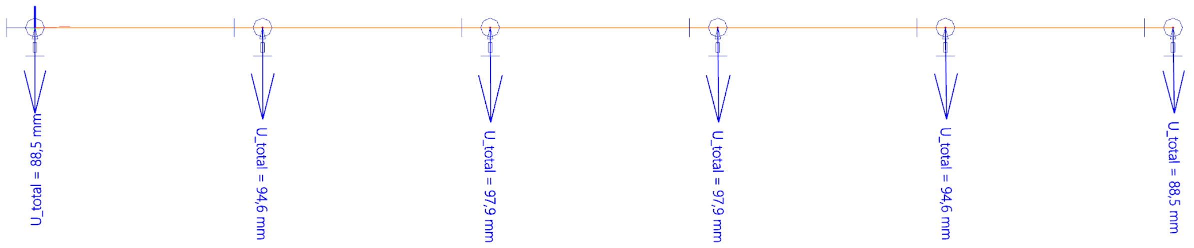

Figure E.9: Support displacement U calculation Aa at T10

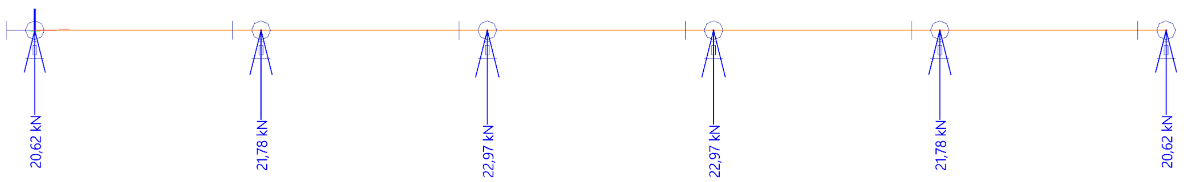

Figure E.10: Support reaction F calculation Aa at T10

Now the same step can be repeated for time steps T100 and T1000.

E.1.4. Step 4: Structural analysis

In the end, results of the construction over time can be described with the following tables and figures:

Table E.1: Displacements U in mm and support reactions F in kN over time (Calculation Aa)

	T0		T10		T100		T1000	
Supports	**U**	**F**	**U**	**F**	**U**	**F**	**U**	**F**
P1	80	20,3	89	20,6	116	21,0	159	21,4
P2	85	21,9	95	21,8	123	21,6	167	21,4
P3	88	23,1	98	23,0	126	22,7	171	22,6
P4	88	23,1	98	23,0	126	22,7	171	22,6
P5	85	21,9	95	21,8	123	21,6	167	21,4
P6	80	20,3	89	20,6	116	21,0	159	21,4

This results in new support deformations and reaction forces:

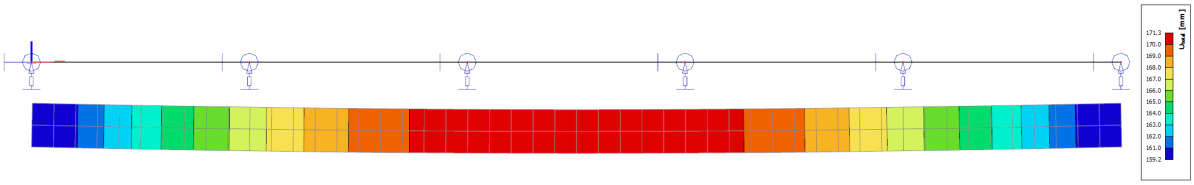

Figure E.11: Support displacement U calculation Aa at T1000

Figure E.12: Support reaction F calculation Aa at T1000

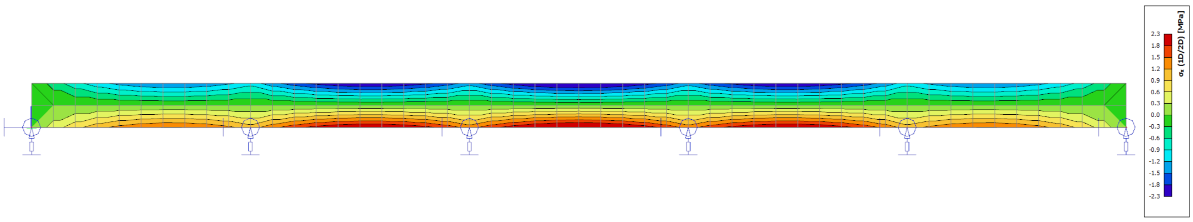

Figure E.13: Stress σ_x calculation Aa at T1000

E.2. Calculation documentation

In this final section, the calculation process is documented with the different input and output values for the calculation software.

Calc Aa

SCIA results

	T0				T10				T100				T1000	
Supports	Disp [mm]	F [kN]	Upper lim	Lower lim	Disp [mm]	F [kN]	Upper lim	Lower lim	Disp [mm]	F [kN]	Upper lim	Lower lim	Disp [mm]	F [kN]
1	79,6	20,34	22,37	18,31	88,5	20,62	22,68	18,56	115,7	21,02	23,12	18,92	159,2	21,4
2	85,3	21,92	24,11	19,73	94,6	21,78	23,96	19,60	122,5	21,61	23,77	19,45	166,5	21,37
3	88,3	23,11	25,42	20,80	97,9	22,97	25,27	20,67	126,2	22,74	25,01	20,47	170,6	22,59
4	88,3	23,11	25,42	20,80	97,9	22,97	25,27	20,67	126,2	22,74	25,01	20,47	170,6	22,59
5	85,3	21,92	24,11	19,73	94,6	21,78	23,96	19,60	122,5	21,61	23,77	19,45	166,5	21,37
6	79,6	20,34	22,37	18,31	88,5	20,62	22,68	18,56	115,7	21,02	23,12	18,92	159,2	21,40

Input Plaxis

Force in circle for input Plaxis

T0			T10			T100		
64,7	71,2	58,3	65,6	72,2	59,1	66,9	73,6	60,2
69,8	76,8	62,8	69,3	76,3	62,4	68,8	75,7	61,9
73,6	80,9	66,2	73,1	80,4	65,8	72,4	79,6	65,1
73,6	80,9	66,2	73,1	80,4	65,8	72,4	79,6	65,1
69,8	76,8	62,8	69,3	76,3	62,4	68,8	75,7	61,9
64,7	71,2	58,3	65,6	72,2	59,1	66,9	73,6	60,2

Output Plaxis

					Non lin spring					
T10	u_max	u_mid	u_min	Group	U_max	U_mid	U_min	Fmax	Fmid	Fmin
Sup 1	89,4	85,6	83,5	2,4	91,8	88	85,9	22,37	20,34	18,31
Sup 2	94,4	90	87,3	4,8	99,2	94,8	92,1	24,11	21,92	19,73
Sup 3	98,2	93,3	90,4	4,8	103	98,1	95,2	25,42	23,11	20,80

					Non lin spring					
T100	u_max	u_mid	u_min	Group	U_max	U_mid	U_min	Fmax	Fmid	Fmin
Sup 1	114,9	110,7	107,7	4,2	119,1	114,9	111,9	22,68	20,62	18,56
Sup 2	119,1	114,3	111,3	8,4	127,5	122,7	119,7	23,96	21,78	19,60
Sup 3	123,7	118,1	114,7	8,4	132,1	126,5	123,1	25,27	22,97	20,67

					Non lin spring					
T1000	u_max	u_mid	u_min	Group	U_max	U_mid	U_min	Fmax	Fmid	Fmin
Sup 1	156,4	152,4	149,3	6	162,4	158,4	155,3	23,12	21,02	18,92
Sup 2	158,6	154,9	151,7	12	170,6	166,9	163,7	23,77	21,61	19,45
Sup 3	161,4	158,8	155,6	12	173,4	170,8	167,6	25,01	22,74	20,47

Resulting differential displacement

Rel. disp.	T0	T10	T100	T1000
Supports	D_u	D_u	D_u	D_u
1&2	5,7	6,1	6,8	7,3
2&3	3	3,3	3,7	4,1
3&4	0	0	0	0
4&5	3	3,3	3,7	4,1
grid	5,7	6,1	6,8	7,3

Calc Ab

SCIA results

	T0				T10				T100				T1000	
Supports	Disp [mm]	F [kN]	Upper lim	Lower lim	Disp [mm]	F [kN]	Upper lim	Lower lim	Disp [mm]	F [kN]	Upper lim	Lower lim	Disp [mm]	F [kN]
1	79,1	20,17	22,19	18,15	88,1	20,42	22,46	18,38	115,4	20,93	23,02	18,84	158,5	21,13
2	85,5	22,03	24,23	19,83	95,0	22,03	24,23	19,83	123,1	21,6	23,76	19,44	166,7	21,42
3	89,4	23,54	25,89	21,19	99,2	23,42	25,76	21,08	127,8	23,1	25,41	20,79	171,7	23,02
4	90,4	23,91	26,30	21,52	100,3	23,52	25,87	21,17	129	23,73	26,10	21,36	173,1	23,94
5	88,2	23,04	25,34	20,74	97,7	22,98	25,28	20,68	126,4	22,67	24,94	20,40	170,5	22,19
6	83,0	21,65	23,82	19,49	92,0	21,98	24,18	19,78	120,4	22,32	24,55	20,09	164,3	22,65

Input Plaxis Force in circle for input Plaxis

T0			T10			T100		
64,2	70,6	57,8	65,0	71,5	58,5	66,6	73,3	60,0
70,1	77,1	63,1	70,1	77,1	63,1	68,8	75,6	61,9
74,9	82,4	67,4	74,5	82,0	67,1	73,5	80,9	66,2
76,1	83,7	68,5	74,9	82,4	67,4	75,5	83,1	68,0
73,3	80,7	66,0	73,1	80,5	65,8	72,2	79,4	64,9
68,9	75,8	62,0	70,0	77,0	63,0	71,0	78,2	63,9

Outpout Plaxis

					Non lin spring					
T10	u_max	u_mid	u_min	Group	U_max	U_mid	U_min	Fmax	Fmid	Fmin
Sup 1	89	85,2	83,1	2,4	91,4	87,6	85,5	22,19	20,17	18,15
Sup 2	94,7	90,2	87,5	4,8	99,5	95	92,3	24,23	22,03	19,83
Sup 3	99,4	94,6	91,5	4,8	104,2	99,4	96,3	25,89	23,54	21,19
Sup 4	100,4	96	92,6	4,8	105,2	100,8	97,4	26,30	23,91	21,52
Sup 5	98,1	93	90,1	4,8	102,9	97,8	94,9	25,34	23,04	20,74
Sup 6	93,6	88,9	86,7	2,4	96	91,3	89,1	23,82	21,65	19,49

					Non lin spring					
T100	u_max	u_mid	u_min	Group	U_max	U_mid	U_min	Fmax	Fmid	Fmin
Sup 1	114,1	110,2	107,2	4,2	118,3	114,4	111,4	22,46	20,42	18,38
Sup 2	120,5	115,4	111,8	8,4	128,9	123,8	120,2	24,23	22,03	19,83
Sup 3	124,1	120	116	8,4	132,5	128,4	124,4	25,76	23,42	21,08
Sup 4	124,6	120,2	116,5	8,4	133	128,6	124,9	25,87	23,52	21,17
Sup 5	123,5	118,5	114,5	8,4	131,9	126,9	122,9	25,28	22,98	20,68
Sup 6	119,1	115,6	112	4,2	123,3	119,8	116,2	24,18	21,98	19,78

					Non lin spring					
T1000	u_max	u_mid	u_min	Group	U_max	U_mid	U_min	Fmax	Fmid	Fmin
Sup 1	156,2	152,1	149,3	6	162,2	158,1	155,3	23,02	20,93	18,84
Sup 2	158,6	154,9	152,0	12	170,6	166,9	164,0	23,76	21,60	19,44
Sup 3	162,7	159,8	157,8	12	174,7	171,8	169,8	25,41	23,10	20,79
Sup 4	164,6	160,7	158,6	12	176,6	172,7	170,6	26,10	23,73	21,36
Sup 5	161,7	159,1	156,1	12	173,7	171,1	168,1	24,94	22,67	20,40
Sup 6	160,2	158,0	155,4	6	166,2	164,0	161,4	24,55	22,32	20,09

Resulting differential settlement

Rel. disp.	T0	T10	T100	T1000
Supports	D_u	D_u	D_u	D_u
1&2	6,4	6,9	7,7	8,2
2&3	3,9	4,2	4,7	5
3&4	1	1,1	1,2	1,4
4&5	2,2	2,6	2,6	2,6
5&6	5,2	5,7	6	6,2

Rel. disp	T0	T10	T100	T1000
Supports	D_u	D_u	D_u	D_u
1 & 6	3,9	3,9	5	5,8

Calc Ac

SCIA results

	T0				T10				T100				T1000	
Supports	Disp [mm]	F [kN]	Upper lim	Lower lim	Disp [mm]	F [kN]	Upper lim	Lower lim	Disp [mm]	F [kN]	Upper lim	Lower lim	Disp [mm]	F [kN]
1	85,1	16,41	18,05	14,77	95,8	16,36	18,00	14,72	120,9	16,76	18,44	15,08	162,4	16,85
2	90,3	23,86	26,25	21,47	100,6	23,95	26,35	21,56	129,2	23,22	25,54	20,90	172,1	23,12
3	89,9	23,71	26,08	21,34	100,1	23,67	26,04	21,30	129,6	24,01	26,41	21,61	173,3	24,02
4	89,9	23,71	26,08	21,34	100,1	23,67	26,04	21,30	129,6	24,01	26,41	21,61	173,3	24,02
5	90,3	23,86	26,25	21,47	100,6	23,95	26,35	21,56	129,2	23,22	25,54	20,90	172,1	23,12
6	85,1	16,41	18,05	14,77	95,8	16,36	18,00	14,72	120,9	16,76	18,44	15,08	162,4	16,85

Input Plaxis Force in circle for input Plaxis

T0			T10			T100		
52,2	57,5	47,0	52,1	57,3	46,9	53,3	58,7	48,0
75,9	83,5	68,4	76,2	83,9	68,6	73,9	81,3	66,5
75,5	83,0	67,9	75,3	82,9	67,8	76,4	84,1	68,8
75,5	83,0	67,9	75,3	82,9	67,8	76,4	84,1	68,8
75,9	83,5	68,4	76,2	83,9	68,6	73,9	81,3	66,5
52,2	57,5	47,0	52,1	57,3	46,9	53,3	58,7	48,0

Outpout Plaxis

					Non lin spring					
T10	u_max	u_mid	u_min	Group	U_max	U_mid	U_min	Fmax	Fmid	Fmin
Sup 1	95,5	93,7	90,1	2,4	97,9	96,1	92,5	18,05	16,41	14,77
Sup 2	100,6	95,4	92,3	4,8	105,4	100,2	97,1	26,25	23,86	21,47
Sup 3	100,7	95,4	92,4	4,8	105,5	100,2	97,2	26,08	23,71	21,34

					Non lin spring					
T100	u_max	u_mid	u_min	Group	U_max	U_mid	U_min	Fmax	Fmid	Fmin
Sup 1	120	115,7	114,4	4,2	124,2	119,9	118,6	18,00	16,36	14,72
Sup 2	125,5	122,1	117,7	8,4	133,9	130,5	126,1	26,35	23,95	21,56
Sup 3	124,7	120,6	116,7	8,4	133,1	129	125,1	26,04	23,67	21,30

					Non lin spring					
T1000	u_max	u_mid	u_min	Group	U_max	U_mid	U_min	Fmax	Fmid	Fmin
Sup 1	160,7	156,2	153,5	6	166,7	162,2	159,5	18,44	16,76	15,08
Sup 2	163,1	160,2	158,1	12	175,1	172,2	170,1	25,54	23,22	20,90
Sup 3	165,4	161,3	159,1	12	177,4	173,3	171,1	26,41	24,01	21,61

Resulting differential settlement

Rel. disp.	T0	T10	T100	T1000
Supports	D_u	D_u	D_u	D_u
1&2	5,2	4,8	8,3	9,7
2&3	0,4	0,5	0,4	1,2
3&4	0	0	0	0
4&5	0,4	0,5	0,4	1,2
5&6	5,2	4,8	8,3	9,7

Calc Ad

SCIA results

	T0				T10				T100				T1000	
Supports	Disp [mm]	F [kN]	Upper lim	Lower lim	Disp [mm]	F [kN]	Upper lim	Lower lim	Disp [mm]	F [kN]	Upper lim	Lower lim	Disp [mm]	F [kN]
1	84,9	16,35	17,99	14,72	95,2	16,3	17,93	14,67	120	16,66	18,33	14,99	162,4	16,83
2	90,2	23,82	26,20	21,44	100,2	23,89	26,28	21,50	128,8	23,38	25,72	21,04	172,1	22,92
3	90,5	23,94	26,33	21,55	100,7	24,04	26,44	21,64	130,4	23,94	26,33	21,55	173,9	24,49
4	92,3	24,65	27,12	22,19	102,9	24,70	27,17	22,23	132	24,84	27,32	22,36	175,9	24,99
5	94,2	25,40	27,94	22,86	104,5	24,94	27,43	22,45	132,9	25,23	27,75	22,71	175,7	24,26
6	88,5	17,42	19,16	15,68	96,7	17,69	19,46	15,92	125,4	17,53	19,28	15,78	163,5	18,09

Input Plaxis

Force in circle for input Plaxis

T0			T10			T100		
52,0	57,2	46,8	51,9	57,1	46,7	53,0	58,3	47,7
75,8	83,4	68,2	76,0	83,6	68,4	74,4	81,9	67,0
76,2	83,8	68,6	76,5	84,2	68,9	76,2	83,8	68,6
78,5	86,3	70,6	78,6	86,5	70,8	79,1	87,0	71,2
80,9	88,9	72,8	79,4	87,3	71,4	80,3	88,3	72,3
55,4	61,0	49,9	56,3	61,9	50,7	55,8	61,4	50,2

Outpout Plaxis

					Non lin spring					
T10	u_max	u_mid	u_min	Group	U_max	U_mid	U_min	Fmax	Fmid	Fmin
Sup 1	95,1	92,9	89,4	2,4	97,5	95,3	91,8	17,99	16,35	14,72
Sup 2	100,1	95,3	92,4	4,8	104,9	100,1	97,2	26,20	23,82	21,44
Sup 3	100,3	95,7	92,7	4,8	105,1	100,5	97,5	26,33	23,94	21,55
Sup 4	103	98	94,8	4,8	107,8	102,8	99,6	27,12	24,65	22,19
Sup 5	104,8	100,3	96,7	4,8	109,6	105,1	101,5	27,94	25,40	22,86
Sup 6	99,1	94,1	91,7	2,4	101,5	96,5	94,1	19,16	17,42	15,68

					Non lin spring					
T100	u_max	u_mid	u_min	Group	U_max	U_mid	U_min	Fmax	Fmid	Fmin
Sup 1	119,2	114,8	113,4	4,2	123,4	119	117,6	17,93	16,30	14,67
Sup 2	125,9	121,3	117,3	8,4	134,3	129,7	125,7	26,28	23,89	21,50
Sup 3	125,5	122,2	118,1	8,4	133,9	130,6	126,5	26,44	24,04	21,64
Sup 4	126,5	123,4	120,1	8,4	134,9	131,8	128,5	27,17	24,70	22,23
Sup 5	127,1	124,1	121,0	8,4	135,5	132,5	129,4	27,43	24,94	22,45
Sup 6	127	121,6	117,3	4,2	131,2	125,8	121,5	19,46	17,69	15,92

					Non lin spring					
T1000	u_max	u_mid	u_min	Group	U_max	U_mid	U_min	Fmax	Fmid	Fmin
Sup 1	160,4	155,9	152,9	6	166,4	161,9	158,9	18,33	16,66	14,99
Sup 2	163,1	160,6	158,2	12	175,1	172,6	170,2	25,72	23,38	21,04
Sup 3	164,8	161,0	158,7	12	176,8	173,0	170,7	26,33	23,94	21,55
Sup 4	168,0	163,6	160,7	12	180,0	175,6	172,7	27,32	24,84	22,36
Sup 5	169,6	164,8	161,9	12	181,6	176,8	173,9	27,75	25,23	22,71
Sup 6	166,4	162,2	158,8	6	172,4	168,2	164,8	19,28	17,53	15,78

Resulting differential settlement

Rel. disp.	T0	T10	T100	T1000
Supports	D_u	D_u	D_u	D_u
1&2	5,3	5	8,8	9,7
2&3	0,3	0,5	1,6	1,8
3&4	1,8	2,2	1,6	2
4&5	1,9	1,6	0,9	0,2
5&6	5,7	7,8	7,5	12,2

Rel. disp.	T0	T10	T100	T1000
Supports	D_u	D_u	D_u	D_u
1 & 6	3,6	1,5	5,4	1,1

Calc Ba

SCIA results

	T0				T10				T100				T1000	
Supports	Disp [mm]	F [kN]	Upper lim	Lower lim	Disp [mm]	F [kN]	Upper lim	Lower lim	Disp [mm]	F [kN]	Upper lim	Lower lim	Disp [mm]	F [kN]
1	73,4	17,22	18,94	15,50	80,2	17,02	18,72	15,32	105,7	17,89	19,68	16,10	146,5	17,61
2	74,1	16,77	18,45	15,09	80,9	16,23	17,85	14,61	106,5	16,84	18,52	15,16	147,3	16,47
3	74,2	16,81	18,49	15,13	80,9	17,55	19,31	15,80	106,7	16,07	17,68	14,46	147,4	16,73
4	74,2	16,81	18,49	15,13	80,9	17,55	19,31	15,80	106,7	16,07	17,68	14,46	147,4	16,73
5	74,1	16,77	18,45	15,09	80,9	16,23	17,85	14,61	106,5	16,84	18,52	15,16	147,3	16,47
6	73,4	17,22	18,94	15,50	80,2	17,02	18,72	15,32	105,7	17,89	19,68	16,10	146,5	17,61

Input Plaxis Force in circle for input Plaxis

T0			T10			T100		
54,8	60,3	49,3	54,2	59,6	48,8	56,9	62,6	51,3
53,4	58,7	48,0	51,7	56,8	46,5	53,6	59,0	48,2
53,5	58,9	48,2	55,9	61,4	50,3	51,2	56,3	46,0
53,5	58,9	48,2	55,9	61,4	50,3	51,2	56,3	46,0
53,4	58,7	48,0	51,7	56,8	46,5	53,6	59,0	48,2
54,8	60,3	49,3	54,2	59,6	48,8	56,9	62,6	51,3

Outpout Plaxis

					Non lin spring					
T10	u_max	u_mid	u_min	Group	U_max	U_mid	U_min	Fmax	Fmid	Fmin
Sup 1	81,1	78,4	76,8	2	83,1	80,4	78,8	18,94	17,22	15,50
Sup 2	80,1	77,4	75,9	4	84,1	81,4	79,9	18,45	16,77	15,09
Sup 3	80,2	77,5	76	4	84,2	81,5	80	18,49	16,81	15,13

					Non lin spring					
T100	u_max	u_mid	u_min	Group	U_max	U_mid	U_min	Fmax	Fmid	Fmin
Sup 1	103,7	101	98,9	3,3	107	104,3	102,2	18,72	17,02	15,32
Sup 2	101,8	98,8	97,3	6,6	108,4	105,4	103,9	17,85	16,23	14,61
Sup 3	105	102	99,7	6,6	111,6	108,6	106,3	19,31	17,55	15,80

					Non lin spring					
T1000	u_max	u_mid	u_min	Group	U_max	U_mid	U_min	Fmax	Fmid	Fmin
Sup 1	144,8	142,1	139,5	4,8	149,6	146,9	144,3	19,68	17,89	16,10
Sup 2	140,8	138,2	135,9	9,6	150,4	147,8	145,5	18,52	16,84	15,16
Sup 3	139	136,9	135,4	9,6	148,6	146,5	145	17,68	16,07	14,46

Resulting differential settlement

Rel. disp.	T0	T10	T100	T1000
Supports	D_u	D_u	D_u	D_u
1&2	0,7	0,7	0,8	0,8
2&3	0,1	0	0,2	0,1
3&4	0	0	0	0
4&5	0,1	0	0,2	0,1
5&6	0,7	0,7	0,8	0,8

Calc Bb

SCIA results

	T0				T10				T100				T1000	
Supports	Disp [mm]	F [kN]	Upper lim	Lower lim	Disp [mm]	F [kN]	Upper lim	Lower lim	Disp [mm]	F [kN]	Upper lim	Lower lim	Disp [mm]	F [kN]
1	72,5	16,95	18,65	15,26	80,3	17,25	18,98	15,53	105,1	17,45	19,20	15,71	145,7	17,73
2	73,8	16,95	18,65	15,26	81,6	16,81	18,49	15,13	106,7	16,74	18,41	15,07	147,6	16,45
3	74,5	17,29	19,02	15,56	82,4	17,09	18,80	15,38	107,6	17,01	18,71	15,31	148,7	16,89
4	75,1	17,62	19,38	15,86	83,1	17,52	19,27	15,77	108,4	17,32	19,05	15,59	149,7	17,46
5	75,7	17,92	19,71	16,13	83,7	17,84	19,62	16,06	109,2	17,75	19,53	15,98	150,7	17,57
6	75,5	18,47	20,32	16,62	83,5	18,71	20,58	16,84	109,1	18,94	20,83	17,05	150,8	19,10

Input Plaxis Force in circle for input Plaxis

T0			T10			T100		
54,0	59,3	48,6	54,9	60,4	49,4	55,5	61,1	50,0
54,0	59,3	48,6	53,5	58,9	48,2	53,3	58,6	48,0
55,0	60,5	49,5	54,4	59,8	49,0	54,1	59,6	48,7
56,1	61,7	50,5	55,8	61,3	50,2	55,1	60,6	49,6
57,0	62,7	51,3	56,8	62,5	51,1	56,5	62,2	50,9
58,8	64,7	52,9	59,6	65,5	53,6	60,3	66,3	54,3

Outpout Plaxis

					Non lin spring					
T10	u_max	u_mid	u_min	Group	U_max	U_mid	U_min	Fmax	Fmid	Fmin
Sup 1	80,4	77,8	76,3	2	82,4	79,8	78,3	18,65	16,95	15,26
Sup 2	80,4	77,8	76,3	4	84,4	81,8	80,3	18,65	16,95	15,26
Sup 3	81,1	78,6	77	4	85,1	82,6	81	19,02	17,29	15,56
Sup 4	82	79,2	77,6	4	86	83,2	81,6	19,38	17,62	15,86
Sup 5	82,7	79,8	78,2	4	86,7	83,8	82,2	19,71	17,92	16,13
Sup 6	84,2	81,1	79,5	2	86,2	83,1	81,5	20,32	18,47	16,62

					Non lin spring					
T100	u_max	u_mid	u_min	Group	U_max	U_mid	U_min	Fmax	Fmid	Fmin
Sup 1	104,4	101,5	99,2	3,3	107,7	104,8	102,5	18,98	17,25	15,53
Sup 2	103,5	100,2	98,3	6,6	110,1	106,8	104,9	18,49	16,81	15,13
Sup 3	103,8	101,1	99,1	6,6	110,4	107,7	105,7	18,80	17,09	15,38
Sup 4	105,3	102,1	99,9	6,6	111,9	108,7	106,5	19,27	17,52	15,77
Sup 5	106	102,7	100,6	6,6	112,6	109,3	107,2	19,62	17,84	16,06
Sup 6	109,2	105,3	102,7	3,3	112,5	108,6	106	20,58	18,71	16,84

					Non lin spring					
T1000	u_max	u_mid	u_min	Group	U_max	U_mid	U_min	Fmax	Fmid	Fmin
Sup 1	143,5	140,4	138,3	4,8	148,3	145,2	143,1	19,20	17,45	15,71
Sup 2	141	138,3	136,3	9,6	150,6	147,9	145,9	18,41	16,74	15,07
Sup 3	141,7	139,2	137,2	9,6	151,3	148,8	146,8	18,71	17,01	15,31
Sup 4	142,6	139,9	137,7	9,6	152,2	149,5	147,3	19,05	17,32	15,59
Sup 5	144	141,3	139,2	9,6	153,6	150,9	148,8	19,53	17,75	15,98
Sup 6	148,7	145,7	143	4,8	153,5	150,5	147,8	20,83	18,94	17,05

Resulting differential settlement

Rel. disp.	T0	T10	T100	T1000
Supports	D_u	D_u	D_u	D_u
1&2	1,3	1,3	1,6	1,9
2&3	0,7	0,8	0,9	1,1
3&4	0,6	0,7	0,8	1
4&5	0,6	0,6	0,8	1
5&6	0,2	0,2	0,1	0,1

Tilt	T0	T10	T100	T1000
Supports	D_u	D_u	D_u	D_u
1 & 6	3	3,2	4	5,1

Calc Bc

SCIA results

	T0				T10				T100				T1000	
Supports	Disp [mm]	F [kN]	Upper lim	Lower lim	Disp [mm]	F [kN]	Upper lim	Lower lim	Disp [mm]	F [kN]	Upper lim	Lower lim	Disp [mm]	F [kN]
1	76,7	13,77	15,15	12,39	84,9	13,91	15,30	12,52	110,7	13,93	15,32	12,54	152,8	14,41
2	76,9	18,54	20,39	16,69	85,1	18,45	20,30	16,61	110,9	18,46	20,31	16,61	153,1	18,19
3	76,8	18,50	20,35	16,65	85,1	18,45	20,30	16,61	110,9	18,42	20,26	16,58	153	18,21
4	76,8	18,50	20,35	16,65	85,1	18,45	20,30	16,61	110,9	18,42	20,26	16,58	153	18,21
5	76,9	18,54	20,39	16,69	85,1	18,45	20,30	16,61	110,9	18,46	20,31	16,61	153,1	18,19
6	76,7	13,77	15,15	12,39	84,9	13,91	15,30	12,52	110,7	13,93	15,32	12,54	152,8	14,41

Input Plaxis

Force in circle for input Plaxis

T0			T10			T100		
43,8	48,2	39,4	44,3	48,7	39,8	44,3	48,8	39,9
59,0	64,9	53,1	58,7	64,6	52,9	58,8	64,6	52,9
58,9	64,8	53,0	58,7	64,6	52,9	58,6	64,5	52,8
58,9	64,8	53,0	58,7	64,6	52,9	58,6	64,5	52,8
59,0	64,9	53,1	58,7	64,6	52,9	58,8	64,6	52,9
43,8	48,2	39,4	44,3	48,7	39,8	44,3	48,8	39,9

Outpout Plaxis

					Non lin spring					
T10	u_max	u_mid	u_min	Group	U_max	U_mid	U_min	Fmax	Fmid	Fmin
Sup 1	86,7	82,5	80,1	2	88,7	84,5	82,1	15,15	13,77	12,39
Sup 2	84,4	81,2	79,5	4	88,4	85,2	83,5	20,39	18,54	16,69
Sup 3	84,3	81,1	79,4	4	88,3	85,1	83,4	20,35	18,50	16,65

					Non lin spring					
T100	u_max	u_mid	u_min	Group	U_max	U_mid	U_min	Fmax	Fmid	Fmin
Sup 1	110,6	107,4	104,6	3,3	113,9	110,7	107,9	15,30	13,91	12,52
Sup 2	107,8	104,3	102	6,6	114,4	110,9	108,6	20,30	18,45	16,61
Sup 3	108,2	104,3	101,9	6,6	114,8	110,9	108,5	20,30	18,45	16,61

					Non lin spring					
T1000	u_max	u_mid	u_min	Group	U_max	U_mid	U_min	Fmax	Fmid	Fmin
Sup 1	149,5	147,2	145,5	4,8	154,3	152	150,3	15,32	13,93	12,54
Sup 2	146,4	143,8	141,4	9,6	156	153,4	151	20,31	18,46	16,61
Sup 3	146,3	143,7	141,2	9,6	155,9	153,3	150,8	20,26	18,42	16,58

Resulting differential settlement

Rel. disp.	T0	T10	T100	T1000
Supports	D_u	D_u	D_u	D_u
1&2	0,2	0,2	0,2	0,3
2&3	0,1	0	0	0,1
3&4	0	0	0	0
4&5	0,1	0	0	0,1
5&6	0,2	0,2	0,2	0,3

Calc Bd

SCIA results

	T0				T10				T100				T1000	
Supports	Disp [mm]	F [kN]	Upper lim	Lower lim	Disp [mm]	F [kN]	Upper lim	Lower lim	Disp [mm]	F [kN]	Upper lim	Lower lim	Disp [mm]	F [kN]
1	76,2	13,56	14,92	12,20	84,1	13,71	15,08	12,34	109,5	13,74	15,11	12,37	151,9	13,96
2	77	18,61	20,47	16,75	85,3	18,46	20,31	16,61	110,9	18,4	20,24	16,56	153,2	18,62
3	77,7	18,96	20,86	17,06	86,1	18,9	20,79	17,01	112,1	18,9	20,79	17,01	154,4	18,64
4	78,5	19,36	21,30	17,42	87,1	19,38	21,32	17,44	113,4	19,37	21,31	17,43	155,5	19,07
5	79,3	19,79	21,77	17,81	88,2	19,77	21,75	17,79	114,7	19,87	21,86	17,88	156,8	19,31
6	79,8	14,93	16,42	13,44	88,9	14,99	16,49	13,49	115,7	14,93	16,42	13,44	157,6	15,62

Input Plaxis Force in circle for input Plaxis

T0			T10			T100		
43,2	47,5	38,8	43,6	48,0	39,3	43,7	48,1	39,4
59,2	65,2	53,3	58,8	64,6	52,9	58,6	64,4	52,7
60,4	66,4	54,3	60,2	66,2	54,1	60,2	66,2	54,1
61,6	67,8	55,5	61,7	67,9	55,5	61,7	67,8	55,5
63,0	69,3	56,7	62,9	69,2	56,6	63,2	69,6	56,9
47,5	52,3	42,8	47,7	52,5	42,9	47,5	52,3	42,8

Outpout Plaxis

					Non lin spring					
T10	u_max	u_mid	u_min	Group	U_max	U_mid	U_min	Fmax	Fmid	Fmin
Sup 1	85,6	81,7	79,6	2	87,6	83,7	81,6	14,92	13,56	12,20
Sup 2	84,6	81,4	79,7	4	88,6	85,4	83,7	20,47	18,61	16,75
Sup 3	85,4	82,2	80,5	4	89,4	86,2	84,5	20,86	18,96	17,06
Sup 4	86,6	83,1	81,2	4	90,6	87,1	85,2	21,30	19,36	17,42
Sup 5	87,6	84,2	82,2	4	91,6	88,2	86,2	21,77	19,79	17,81
Sup 6	91,5	86,7	81,7	2	93,5	88,7	83,7	16,42	14,93	13,44

					Non lin spring					
T100	u_max	u_mid	u_min	Group	U_max	U_mid	U_min	Fmax	Fmid	Fmin
Sup 1	111	106,1	103,6	3,3	114,3	109,4	106,9	15,08	13,71	12,34
Sup 2	107,9	104,4	102,1	6,6	114,5	111	108,7	20,31	18,46	16,61
Sup 3	109,2	105,5	103,1	6,6	115,8	112,1	109,7	20,79	18,90	17,01
Sup 4	110,6	106,8	104,2	6,6	117,2	113,4	110,8	21,32	19,38	17,44
Sup 5	112,2	107,9	105,4	6,6	118,8	114,5	112	21,75	19,77	17,79
Sup 6	114,3	112,6	108,7	3,3	117,6	115,9	112	16,49	14,99	13,49

					Non lin spring					
T1000	u_max	u_mid	u_min	Group	U_max	U_mid	U_min	Fmax	Fmid	Fmin
Sup 1	148,8	146,8	144,8	4,8	153,6	151,6	149,6	15,11	13,74	12,37
Sup 2	146,3	143,3	141,1	9,6	155,9	152,9	150,7	20,24	18,40	16,56
Sup 3	148,2	145,1	142,7	9,6	157,8	154,7	152,3	20,79	18,90	17,01
Sup 4	149,6	146,3	144	9,6	159,2	155,9	153,6	21,31	19,37	17,43
Sup 5	151,6	148,3	144,3	9,6	161,2	157,9	153,9	21,86	19,87	17,88
Sup 6	154	151,7	149,9	4,8	158,8	156,5	154,7	16,42	14,93	13,44

Resulting differential settlement

Rel. disp.	T0	T10	T100	T1000
Supports	D_u	D_u	D_u	D_u
1&2	0,8	1,2	1,4	1,3
2&3	0,7	0,8	1,2	1,2
3&4	0,8	1	1,3	1,1
4&5	0,8	1,1	1,3	1,3
5&6	0,5	0,7	1	0,8

Tilt	T0	T10	T100	T1000
Supports	D_u	D_u	D_u	D_u
1 & 6	3,6	4,8	6,2	5,7

Calc Ca

SCIA results

	T0				T10				T100				T1000	
Supports	Disp [mm]	F [kN]	Upper lim	Lower lim	Disp [mm]	F [kN]	Upper lim	Lower lim	Disp [mm]	F [kN]	Upper lim	Lower lim	Disp [mm]	F [kN]
1	83,1	21,71	23,88	19,54	92,4	22,04	24,24	19,84	119,9	22,1	24,31	19,89	164,8	21,38
2	83,3	21,15	23,27	19,04	92,5	20,97	23,07	18,87	120,1	21,05	23,16	18,95	165	21,14
3	83,3	21,16	23,28	19,04	92,5	21,01	23,11	18,91	120,1	20,87	22,96	18,78	165	21,49
4	83,3	21,16	23,28	19,04	92,5	21,01	23,11	18,91	120,1	20,87	22,96	18,78	165	21,49
5	83,3	21,15	23,27	19,04	92,5	20,97	23,07	18,87	120,1	21,05	23,16	18,95	165	21,14
6	83,1	21,71	23,88	19,54	92,4	22,04	24,24	19,84	119,9	22,10	24,31	19,89	164,8	21,38

Input Plaxis Force in circle for input Plaxis

T0

69,1	76,0	62,2
67,32	74,1	60,6
67,35	74,1	60,6
67,35	74,1	60,6
67,32	74,1	60,6
69,1	76,0	62,2

T10

70,2	77,2	63,1
66,7	73,4	60,1
66,9	73,6	60,2
66,9	73,6	60,2
66,7	73,4	60,1
70,2	77,2	63,1

T100

70,3	77,4	63,3
67,0	73,7	60,3
66,4	73,1	59,8
66,4	73,1	59,8
67,0	73,7	60,3
70,3	77,4	63,3

Outpout Plaxis

					Non lin spring					
T10	u_max	u_mid	u_min	Group	U_max	U_mid	U_min	Fmax	Fmid	Fmin
Sup 1	93,5	89,3	86,8	2,4	95,9	91,7	89,2	23,88	21,71	19,54
Sup 2	91,9	87,9	85,5	4,8	96,7	92,7	90,3	23,27	21,15	19,04
Sup 3	91,9	87,9	85,5	4,8	96,7	92,7	90,3	23,28	21,16	19,04

					Non lin spring					
T100	u_max	u_mid	u_min	Group	U_max	U_mid	U_min	Fmax	Fmid	Fmin
Sup 1	119,7	115,6	112	4,2	123,9	119,8	116,2	24,24	22,04	19,84
Sup 2	116,3	111,5	108,6	8,4	124,7	119,9	117	23,07	20,97	18,87
Sup 3	117	111,9	108,9	8,4	125,4	120,3	117,3	23,11	21,01	18,91

					Non lin spring					
T1000	u_max	u_mid	u_min	Group	U_max	U_mid	U_min	Fmax	Fmid	Fmin
Sup 1	159,7	157,2	154,2	6	165,7	163,2	160,2	24,31	22,10	19,89
Sup 2	156,5	152,8	150	12	168,5	164,8	162	23,16	21,05	18,95
Sup 3	155,3	152	149,3	12	167,3	164	161,3	22,96	20,87	18,78

Resulting differential settlement

Rel. disp.	T0	T10	T100	T1000
Supports	D_u	D_u	D_u	D_u
1&2	0,2	0,1	0,2	0,2
2&3	0	0	0	0
3&4	0	0	0	0
4&5	0	0	0	0
5&6	0,2	0,1	0,2	0,2

Calc Cb

SCIA results

	T0				T10				T100				T1000	
Supports	Disp [mm]	F [kN]	Upper lim	Lower lim	Disp [mm]	F [kN]	Upper lim	Lower lim	Disp [mm]	F [kN]	Upper lim	Lower lim	Disp [mm]	F [kN]
1	82,7	21,54	23,69	19,39	91,7	21,79	23,97	19,61	119,5	21,86	24,05	19,67	163,6	22,7
2	83,6	21,29	23,42	19,16	92,7	21,17	23,29	19,05	120,7	21,16	23,28	19,04	164,7	20,94
3	84,4	21,6	23,76	19,44	93,7	21,41	23,55	19,27	121,7	21,53	23,68	19,38	165,6	20,89
4	85,2	21,91	24,10	19,72	94,6	21,80	23,98	19,62	122,7	21,66	23,83	19,49	166,6	21,16
5	86,0	22,22	24,44	20,00	95,4	22,23	24,45	20,01	123,6	21,82	24,00	19,64	167,4	21,40
6	86,6	23,08	25,39	20,77	96,1	23,26	25,59	20,93	124,4	23,60	25,96	21,24	168,1	24,53

Input Plaxis Force in circle for input Plaxis

T0			T10			T100		
68,6	75,4	61,7	69,4	76,3	62,4	69,6	76,5	62,6
67,8	74,5	61,0	67,4	74,1	60,6	67,4	74,1	60,6
68,8	75,6	61,9	68,2	75,0	61,3	68,5	75,4	61,7
69,7	76,7	62,8	69,4	76,3	62,5	68,9	75,8	62,1
70,7	77,8	63,7	70,8	77,8	63,7	69,5	76,4	62,5
73,5	80,8	66,1	74,0	81,4	66,6	75,1	82,6	67,6

Outpout Plaxis

					Non lin spring					
T10	u_max	u_mid	u_min	Group	U_max	U_mid	U_min	Fmax	Fmid	Fmin
Sup 1	93,2	88,8	86,4	2,4	95,6	91,2	88,8	23,69	21,54	19,39
Sup 2	92,5	88,1	85,7	4,8	97,3	92,9	90,5	23,42	21,29	19,16
Sup 3	93,4	89,1	86,5	4,8	98,2	93,9	91,3	23,76	21,60	19,44
Sup 4	94,4	89,9	87,2	4,8	99,2	94,7	92	24,10	21,91	19,72
Sup 5	95,1	90,6	87,9	4,8	99,9	95,4	92,7	24,44	22,22	20,00
Sup 6	98,7	93,3	90,3	2,4	101,1	95,7	92,7	25,39	23,08	20,77

					Non lin spring					
T100	u_max	u_mid	u_min	Group	U_max	U_mid	U_min	Fmax	Fmid	Fmin
Sup 1	119,3	115,2	111,2	4,2	123,5	119,4	115,4	23,97	21,79	19,61
Sup 2	117,4	112,3	109,3	8,4	125,8	120,7	117,7	23,29	21,17	19,05
Sup 3	118,3	113	109,9	8,4	126,7	121,4	118,3	23,55	21,41	19,27
Sup 4	119,5	114,5	111,2	8,4	127,9	122,9	119,6	23,98	21,80	19,62
Sup 5	120,8	115,9	112,3	8,4	129,2	124,3	120,7	24,45	22,23	20,01
Sup 6	123,9	119,6	115,7	4,2	128,1	123,8	119,9	25,59	23,26	20,93

					Non lin spring					
T1000	u_max	u_mid	u_min	Group	U_max	U_mid	U_min	Fmax	Fmid	Fmin
Sup 1	159,2	156,6	153	6	165,2	162,6	159	24,05	21,86	19,67
Sup 2	156,4	153	150,2	12	168,4	165	162	23,28	21,16	19,04
Sup 3	158,1	154,5	151,6	12	170,1	166,5	163,6	23,68	21,53	19,38
Sup 4	158,8	155,3	152,1	12	170,8	167,3	164,1	23,83	21,66	19,49
Sup 5	159,5	156	153,1	12	171,5	168	165,1	24,00	21,82	19,64
Sup 6	164,2	160,8	158,3	6	170,2	166,8	164,3	25,96	23,60	21,24

Resulting differential settlement

Rel. disp.	T0	T10	T100	T1000
Supports	D_u	D_u	D_u	D_u
1&2	0,9	1	1,2	1,1
2&3	0,8	1	1	0,9
3&4	0,8	0,9	1	1
4&5	0,8	0,8	0,9	0,8
5&6	0,6	0,7	0,8	0,7

Rel. disp.	T0	T10	T100	T1000
Supports	D_u	D_u	D_u	D_u
1 & 6	3,9	4,4	4,9	4,5

Calc Cc

SCIA results

	T0				T10				T100				T1000	
Supports	Disp [mm]	F [kN]	Upper lim	Lower lim	Disp [mm]	F [kN]	Upper lim	Lower lim	Disp [mm]	F [kN]	Upper lim	Lower lim	Disp [mm]	F [kN]
1	88,7	17,48	19,23	15,73	98,4	17,69	19,46	15,92	126,5	18,23	20,05	16,41	171,1	18,67
2	88,7	23,27	25,60	20,94	98,5	23,16	25,48	20,84	126,6	22,89	25,18	20,60	171,2	22,67
3	88,7	23,27	25,60	20,94	98,5	23,16	25,48	20,84	126,6	22,89	25,18	20,60	171,2	22,68
4	88,7	23,27	25,60	20,94	98,5	23,16	25,48	20,84	126,6	22,89	25,18	20,60	171,2	22,68
5	88,7	23,27	25,60	20,94	98,5	23,16	25,48	20,84	126,6	22,89	25,18	20,60	171,2	22,67
6	88,7	17,48	19,23	15,73	98,4	17,69	19,46	15,92	126,5	18,23	20,05	16,41	171,1	18,67

Input Plaxis

Force in circle for input Plaxis

T0			T10			T100		
55,6	61,2	50,1	56,3	61,9	50,7	58,0	63,8	52,2
74,1	81,5	66,7	73,7	81,1	66,3	72,9	80,1	65,6
74,1	81,5	66,7	73,7	81,1	66,3	72,9	80,1	65,6
74,1	81,5	66,7	73,7	81,1	66,3	72,9	80,1	65,6
74,1	81,5	66,7	73,7	81,1	66,3	72,9	80,1	65,6
55,6	61,2	50,1	56,3	61,9	50,7	58,0	63,8	52,2

Outpout Plaxis

					Non lin spring					
T10	u_max	u_mid	u_min	Group	U_max	U_mid	U_min	Fmax	Fmid	Fmin
Sup 1	99,6	95,5	94	2,4	102	97,9	96,4	19,23	17,48	15,73
Sup 2	98,6	93,8	90,7	4,8	103,4	98,6	95,5	25,60	23,27	20,94
Sup 3	98,6	93,8	90,7	4,8	103,4	98,6	95,5	25,60	23,27	20,94

					Non lin spring					
T100	u_max	u_mid	u_min	Group	U_max	U_mid	U_min	Fmax	Fmid	Fmin
Sup 1	125,6	120,9	117,5	4,2	129,8	125,1	121,7	19,46	17,69	15,92
Sup 2	124,3	118,6	115,2	8,4	132,7	127	123,6	25,48	23,16	20,84
Sup 3	124,3	118,6	115,2	8,4	132,7	127	123,6	25,48	23,16	20,84

					Non lin spring					
T1000	u_max	u_mid	u_min	Group	U_max	U_mid	U_min	Fmax	Fmid	Fmin
Sup 1	169	163,9	160,6	6	175	169,9	166,6	20,05	18,23	16,41
Sup 2	161,8	159,5	156,5	12	173,8	171,5	168,5	25,18	22,89	20,60
Sup 3	161,8	159,5	156,5	12	173,8	171,5	168,5	25,18	22,89	20,60

Resulting differential settlement

Rel. disp.	T0	T10	T100	T1000
Supports	D_u	D_u	D_u	D_u
1&2	0	0,1	0,1	0,1
2&3	0	0	0	0
3&4	0	0	0	0
4&5	0	0	0	0
5&6	0	0,1	0,1	0,1

Calc Cd

SCIA results

	T0				T10				T100				T1000	
Supports	Disp [mm]	F [kN]	Upper lim	Lower lim	Disp [mm]	F [kN]	Upper lim	Lower lim	Disp [mm]	F [kN]	Upper lim	Lower lim	Disp [mm]	F [kN]
1	88,0	17,27	19,00	15,54	97,6	17,8	19,58	16,02	126,3	17,67	19,44	15,90	170,2	18,19
2	88,9	23,36	25,70	21,02	98,8	23,12	25,43	20,81	127,4	23,06	25,37	20,75	171,3	23,07
3	89,9	23,73	26,10	21,36	99,8	23,54	25,89	21,19	128,4	23,59	25,95	21,23	172,4	22,61
4	90,9	24,11	26,52	21,70	100,9	23,34	25,67	21,01	129,4	24,22	26,64	21,80	173,4	23,92
5	91,9	24,48	26,93	22,03	102,0	24,89	27,38	22,40	130,4	23,92	26,31	21,53	174,4	24,81
6	92,7	18,68	20,55	16,81	103,0	18,94	20,83	17,05	131,4	19,19	21,11	17,27	175,4	19,04

Input Plaxis

Force in circle for input Plaxis

T0			T10			T100		
55,0	60,5	49,5	56,7	62,3	51,0	56,2	61,9	50,6
74,4	81,8	66,9	73,6	81,0	66,2	73,4	80,7	66,1
75,5	83,1	68,0	74,9	82,4	67,4	75,1	82,6	67,6
76,7	84,4	69,1	74,3	81,7	66,9	77,1	84,8	69,4
77,9	85,7	70,1	79,2	87,2	71,3	76,1	83,8	68,5
59,5	65,4	53,5	60,3	66,3	54,3	61,1	67,2	55,0

Outpout Plaxis

					Non lin spring					
T10	u_max	u_mid	u_min	Group	U_max	U_mid	U_min	Fmax	Fmid	Fmin
Sup 1	98,5	93,8	91,1	2,4	100,9	96,2	93,5	19,00	17,27	15,54
Sup 2	98,8	94,3	91	4,8	103,6	99,1	95,8	25,70	23,36	21,02
Sup 3	101,1	95,3	92	4,8	105,9	100,1	96,8	26,10	23,73	21,36
Sup 4	101,7	96,1	93,4	4,8	106,5	100,9	98,2	26,52	24,11	21,70
Sup 5	102,5	97,4	94,3	4,8	107,3	102,2	99,1	26,93	24,48	22,03
Sup 6	104,8	99,9	96,7	2,4	107,2	102,3	99,1	20,55	18,68	16,81

					Non lin spring					
T100	u_max	u_mid	u_min	Group	U_max	U_mid	U_min	Fmax	Fmid	Fmin
Sup 1	127,4	122,5	117,7	4,2	131,6	126,7	121,9	19,58	17,80	16,02
Sup 2	123,7	119,1	115,5	8,4	132,1	127,5	123,9	25,43	23,12	20,81
Sup 3	125,3	119,9	116,4	8,4	133,7	128,3	124,8	25,89	23,54	21,19
Sup 4	124,2	119,1	116,2	8,4	132,6	127,5	124,6	25,67	23,34	21,01
Sup 5	127	123,2	120,2	8,4	135,4	131,6	128,6	27,38	24,89	22,40
Sup 6	132,2	126,4	122,5	4,2	136,4	130,6	126,7	20,83	18,94	17,05

					Non lin spring					
T1000	u_max	u_mid	u_min	Group	U_max	U_mid	U_min	Fmax	Fmid	Fmin
Sup 1	167,1	163	159,8	6	173,1	169	165,8	19,44	17,67	15,90
Sup 2	162,2	159,3	157,0	12	174,2	171,3	169	25,37	23,06	20,75
Sup 3	164	161,4	158,9	12	176	173,4	170,9	25,95	23,59	21,23
Sup 4	165,6	161,7	159,3	12	177,6	173,7	171,3	26,64	24,22	21,80
Sup 5	164,5	161,2	159,1	12	176,5	173,2	171,1	26,31	23,92	21,53
Sup 6	175	169,7	165,9	6	181	175,7	171,9	21,11	19,19	17,27

Resulting differential settlement

Rel. disp.	T0	T10	T100	T1000
Supports	D_u	D_u	D_u	D_u
1&2	0,9	1,2	1,1	1,1
2&3	1	1	1	1,1
3&4	1	1,1	1	1
4&5	1	1,1	1	1
5&6	0,8	1	1	1

Rel. disp.	T0	T10	T100	T1000
Supports	D_u	D_u	D_u	D_u
1 & 6	4,7	5,4	5,1	5,2